Endoprosthetic Growth Module Mechanism for the Skeletally Immature

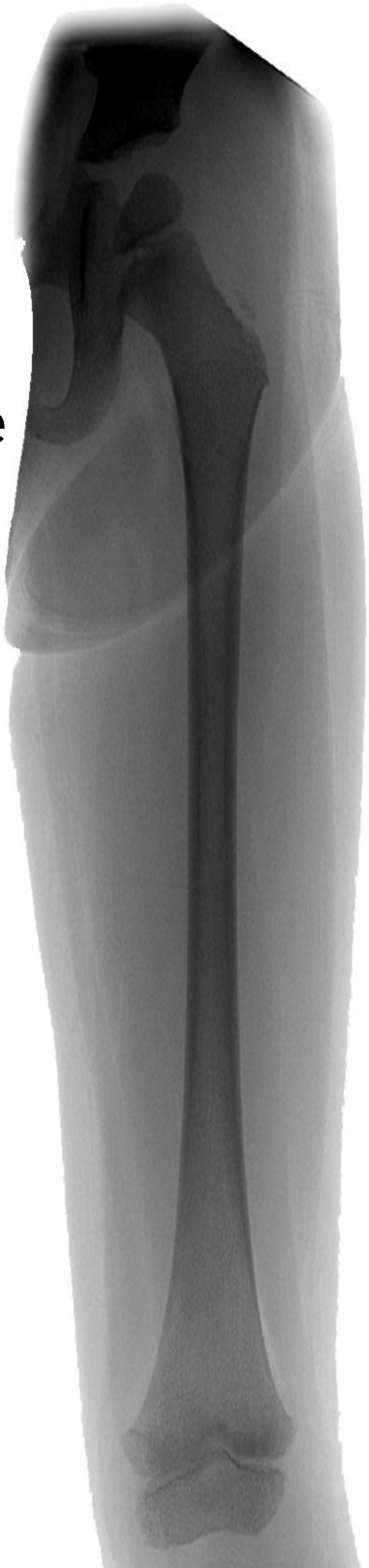

Author: Adam Thane Parsons

(PRSADA001 / 1264906)

Date: 29th August 2011

Plagiarism Declaration

I know the meaning of plagiarism and declare that all the work in the document, save for that which is properly acknowledged, is my own.

Adam Thane Parsons (PRSADA001 / 1264906)

Acknowledgements

Thanks to Dr. George Vicatos, for inspiring a passion in biomedical engineering, and for his support and advice throughout the course of this dissertation.

Thanks to Mr. Samuel Ginsberg, for his advice and contribution to the design and development of the electronic systems of the extendible endoprosthesis.

Table of Contents

List of Figures

List of Tables

Glossary of Terms

Term	Definition
Antero-posterior	Relating to or directed from front to back
Diaphysis	Mid section of a Long bone between metaphyses
Distal	Situated away from the centre of the body (opposite proximal)
Endoprosthesis	An artificial body part (prosthesis) housed entirely within the body
Epiphysis	End part of a Long bone
Femoral	Of or relating to the femur
Femur	Long bone in the upper leg, between the hip and knee
Humeral	Of or relating to the humerus
Humerus	Long bone in the upper arm, between the shoulder and elbow
Lateral	Situated on one side or other of the body or of an organ, especially in the region furthest from the median plane (opposite medial)

Medial	Situated near the median plane of the body or the midline of an organ (opposite lateral)
Medio-lateral	
Metaphysis	End part of a Long bone, between epiphysis and diaphysis
Orthoroentgenogram/Scanogram	A radiographic technique used for showing true dimensions by moving a narrow orthogonal beam of X-rays along the length of the structure being measured.
Osteosarcoma / Osteogenic Sarcoma	A cancerous, malignant bone tumour
Proximal	Situated nearer to the centre of the body (opposite distal)
Resection	Surgical removal of tissue or part of an organ
Tibia	Lone bone in the lower leg, between the knee and the ankle
Tibial	Of or relating to the tibia

List of Abbreviations

Abbreviation	Definition
AP	Antero-posterior
ML	Medio-lateral
MRI	Magnetic Resonance Imaging
Ti6Al4V	Medical Grade Titanium (6% Aluminium, 4% Vanadium)
UHMWPE	Ultra High Molecular Weight Polyethylene
Op-amp	Operational Amplifier

1. Introduction

Limb salvage surgery for the treatment of ***osteosarcoma*** in the skeletally immature necessitates the development of an endoprosthetic replacement, capable of extending at a rate comparable to that of natural growth without surgical intervention.

Osteosarcoma occurs predominantly in the extremities, involving either the ***distal*** or ***proximal epiphyses*** of a Long bone and the adjacent joint. While osteosarcoma can develop at any age, it is more frequently initiated by and associated with the adolescent growth spurt in skeletally immature individuals. In order to prevent the spread of the cancer to other regions of the body, surgical ***resection*** of the tumour is required. This removal of a section of the Long bone (distal or proximal) and its adjacent joint compromises the function of the limb involved, which historically necessitated amputation of the limb above the tumour site. Advances in chemotherapy, surgical techniques and biomedical engineering have allowed for the development of limb salvage surgery as an alternative to amputation. Limb salvage surgery is achieved through the replacement of surgically removed bones and joints with endoprostheses. In the case of skeletally immature patients, a further problem presents as the removed proximal / distal tumour involves the removal of the epiphyseal plate, resulting in diminished growth capacity of the bone and ultimately limb length inequality. This limb length inequality must be prevented / recovered to avoid gait disturbances and resultant back pain.

Over the past 30 years, a variety of different extendible endoprostheses have been developed, with the goal of overcoming limb length inequality as well as improving the patient's quality of life. Earlier devices, while able to prevent limb length inequality required repeated invasive surgery in order to achieve extension. Repeated surgeries incur considerable financial costs and expose the patient to significant risk of infection. As a result, subsequent devices have sought to overcome such risks, developing non-invasive means of extension, which in turn reduces the duration and need for hospital visits. Stanmore Implants Worldwide has contributed greatly to the progressive development of extendible endoprostheses, more recently developing a completely non-invasive extendible

endoprosthesis (Stanmore Mark V JTS). While the Mark V overcomes the risks associated with repeated surgeries, it requires physician facilitated periodic extension which results in infrequent large extensions to recover limb length inequality.

Although currently available extendible endoprostheses have overcome the need for repeated surgical extension procedures, they require physician facilitated extensions, which results in increased costs as well as infrequent large extensions that strain soft tissues surrounding the device. In addition, currently available devices commonly contain ferromagnetic materials which have a detrimental effect on MRI image quality, excluding it as a means of follow-up assessment. Ideally, a device containing no ferromagnetic materials would improve follow-up assessment of the tumour site through MRI compatibility. As such, there is a need to develop a non-ferromagnetic device capable of carrying out frequent minor extensions comparable to natural growth. Such a device would reduce the costs associated with hospital visits and physician facilitated extension procedures, as well as permitting accurate monitoring of the cancer site through MRI.

This dissertation details the design of an extendible endoprosthesis overcoming some of the issues mentioned above. The scope is limited to the design and development of such an extendible endoprosthesis and its control. While it is expected that this device would attach to both a joint replacement at one end as well as the remaining length of the Long bone at the other, the design of the interfaces is not covered in this dissertation. For this reason, the device will also be referred to as an endoprosthetic growth module mechanism.

In order to convey the need for extendible endoprostheses, this dissertation begins with a background in order to give an understanding of the nature and location of bone cancer together with its diagnosis and subsequent treatment, as well as the problems that ensue. Extendible endoprosthetic replacements have proven to be an effective means of treating osteosarcoma in skeletally immature patients and, as such, a description of historical and current devices is provided, indicating the areas for improvement. After assessment of these designs, the requirements for the design of a new extendible endoprosthesis are considered, following which the design and development of the device is detailed. In order

to prove the design concept, the procedures and results of several tests are presented, including distraction force, gamma compatibility and MRI compatibility.

2. Background

2.1. The Long Bone

The skeletal system provides a means of support and protection for the various organs housed within the human body. Of the several types of bone that contribute to the skeletal system, only Long bones are of particular relevance to this dissertation and the development of an extendible endoprosthesis for limb salvage surgery in cases of osteosarcoma. These Long bones provide support and structure to the limbs, offering moment arms to attaching muscles, enabling motion and environmental interaction. Long bones are distinguished through the observation of dimensions, defined as possessing dimensions in which the length exceeds the diameter (Tortora & Grabowski 2003). The Long bone is the dominant type present in the extremities, with examples including the ***Humerus*** (upper arm), the ***Femur*** (upper leg), and the ***Tibia*** (lower leg).

A typical Long bone can be divided into several distinct regions, contributing to the growth or structure of the bone itself. These regions are indicated in Figure 2.

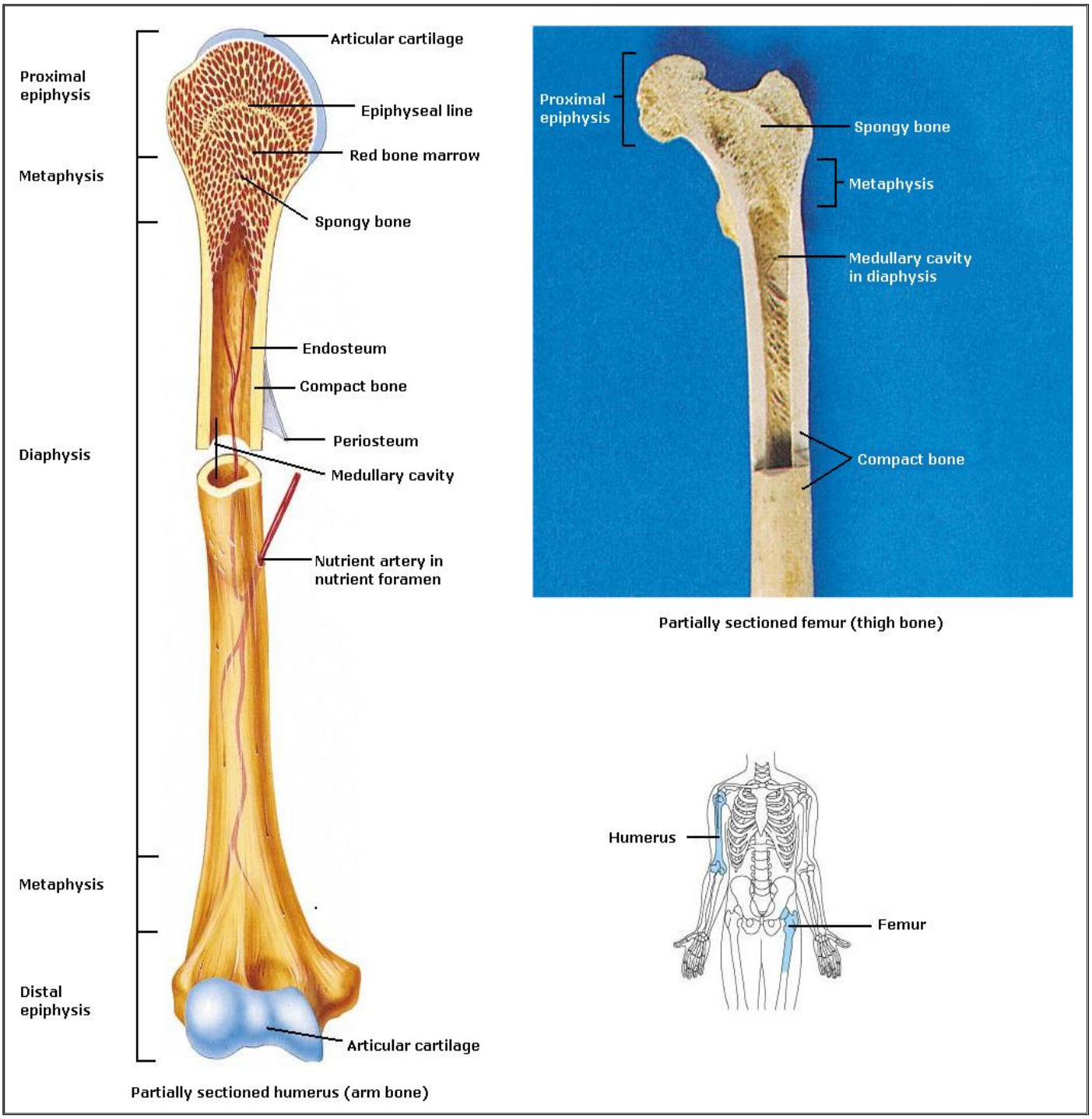

Figure 1: Parts of a long bone (Tortora & Grabowski 2003)

2.2. Growth

Biological growth and ageing necessitates the generation of new cells, which occurs through cellular division. This process occurs more rapidly in the early stages of an individual's life, up and until the realisation of adulthood, after which cellular division takes place merely as a means of replacing worn-out or dying cells, as well as facilitating repairs to injuries (What is Cancer - Childhood Cancers n.d.). In the case of longitudinal growth of a Long bone, this growth is facilitated by and occurs at the epiphyseal plate, located between the ***epiphysis*** and ***metaphysis*** at both distal and proximal ends of the bone (Figure 2). Cells located in the epiphyseal plate multiply and differentiate, resulting in the progressive lengthening of the ***diaphysis***. Closure of this epiphyseal plate and hence cessation of growth typically occurs at an age of 14.2 and 15.4 years for females and males respectively (Tupman, G S 1962).

Through investigation of a sample size of 100 children (50 females & 50 males), Anderson *et al (1963)* obtained valuable data for predicting the growth of Long bones in the lower extremities. Measurements were carried out at least once a year for the eight years prior to cessation of growth (Anderson, Green & Messner 1963). Dimensions of the femur and tibia were established through ***orthoroentgenograms*** (commonly known as ***scanograms***), with both the proximal and distal epiphyses included in the measurement (Anderson, Green & Messner 1963).

The following two graphs (Figure 3 and Figure 4) are based on the source data collected by *Anderson et al (1963)* (Appendix A-1). Both show the comparison between male and female dimensions against chronological age up to the point of skeletal maturity, Figure 3 (***Femoral***), Figure 4 (***Tibial***).

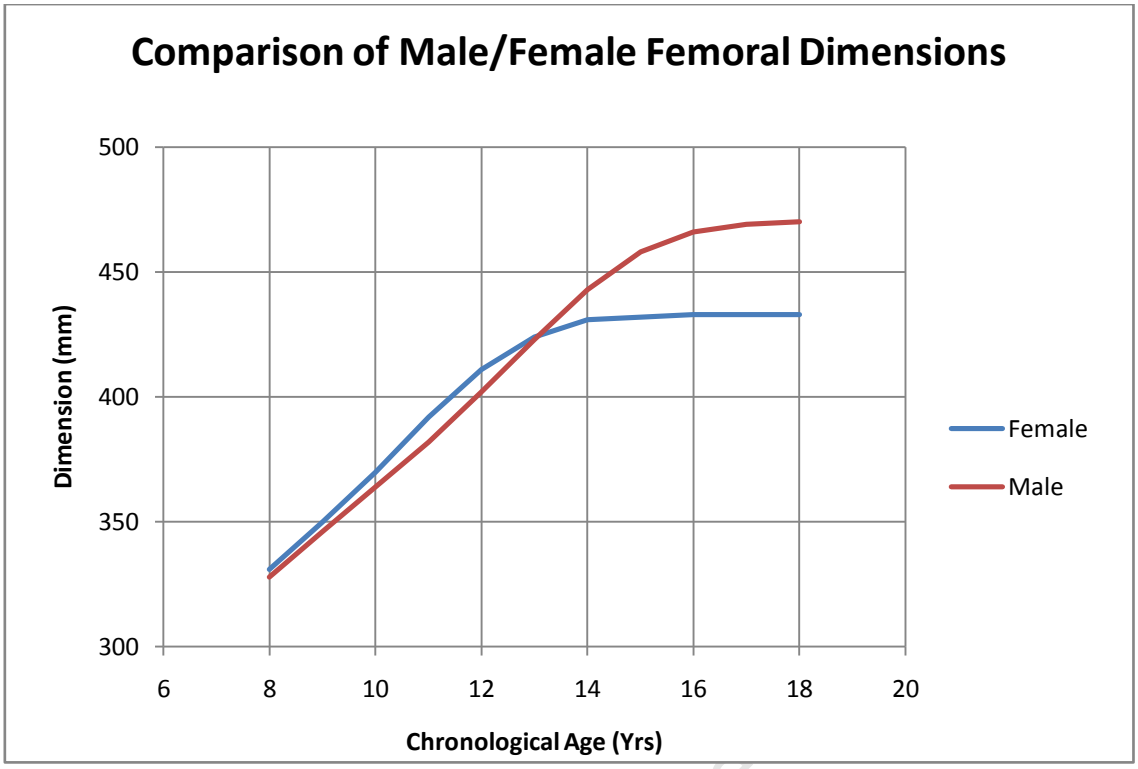

Figure 3: Comparison of male/female femoral dimensions (Source Data (Anderson, Green & Messner 1963))

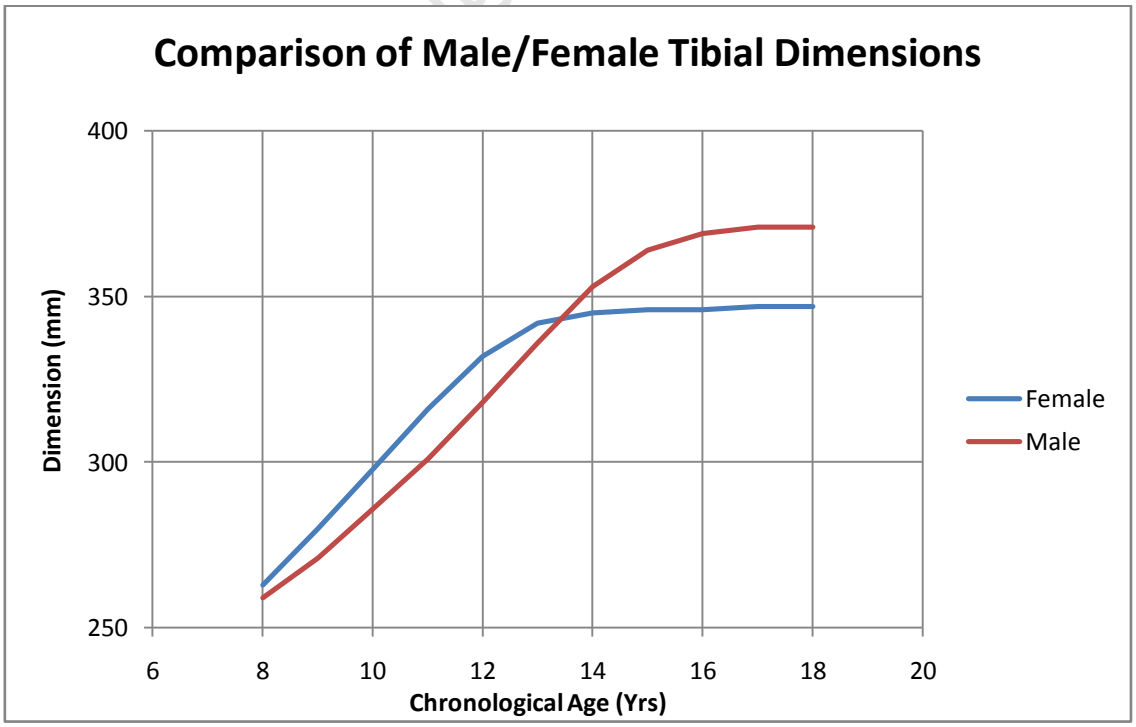

Figure 4: Comparison of male/female tibial dimensions (Source Data (Anderson, Green & Messner 1963))

Additionally, *Anderson et al (1963)* investigated the rate at which this growth occurs. This rate of growth for the femur and tibia in both males and females (Appendix A-2) is indicated in Figure 5 and Figure 6.

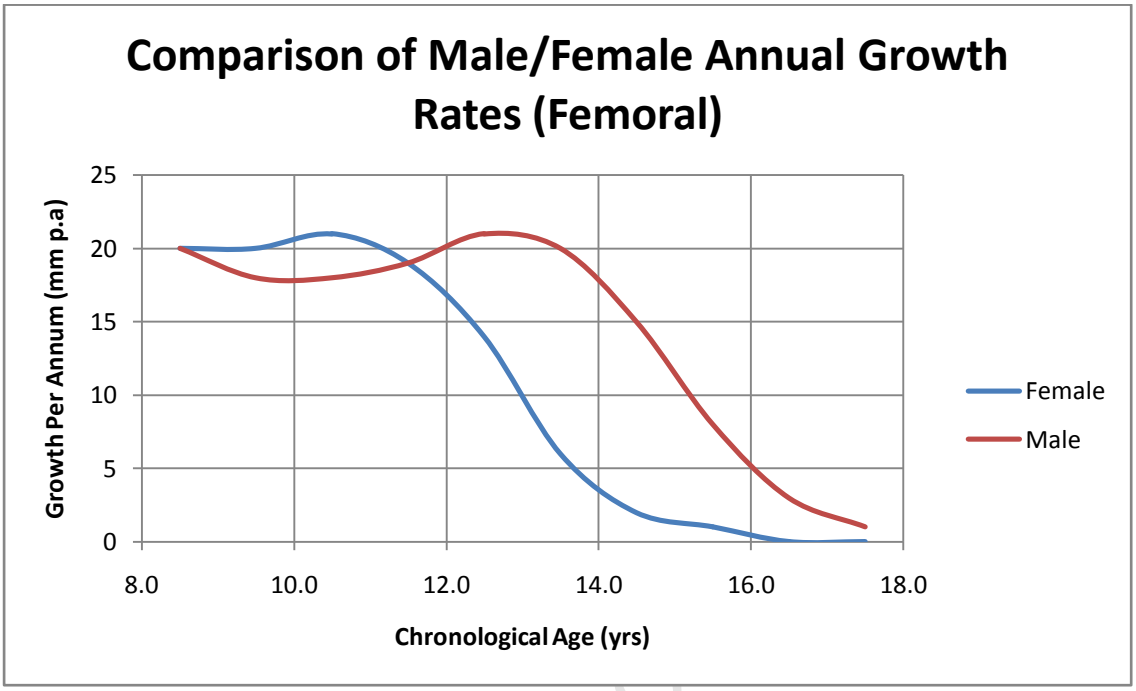

Figure 5: Comparison of male/female annual growth rates (Femoral)

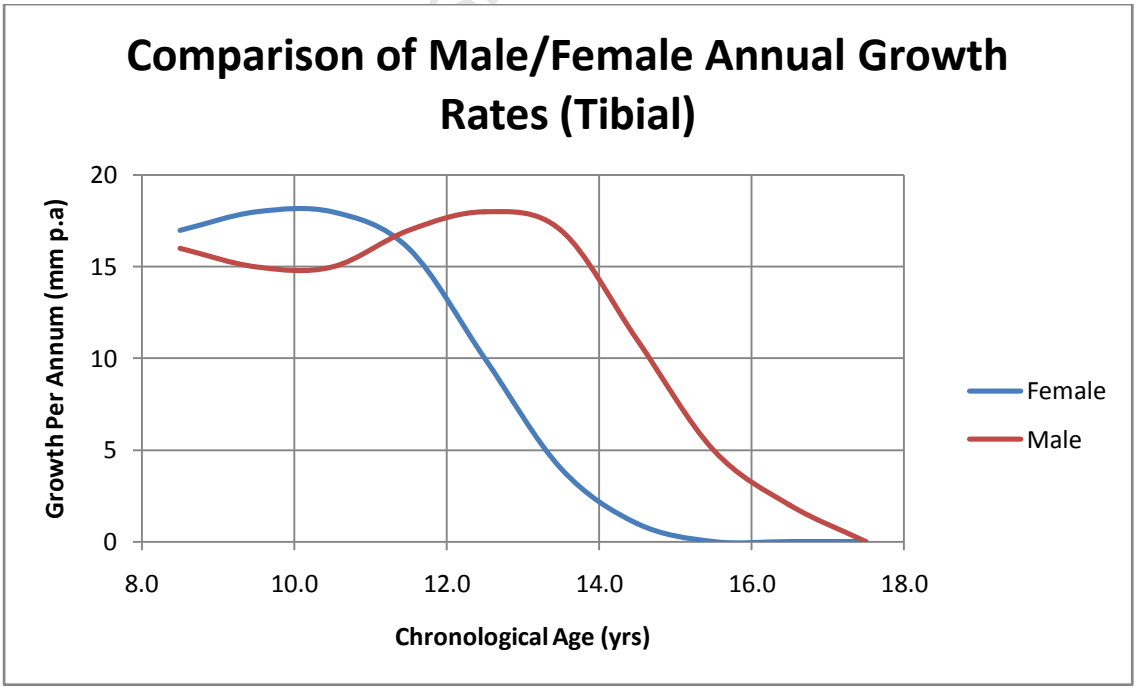

Figure 6: Comparison of male/female annual growth rates (Tibial)

2.3. Cancer

The controlled process of growth and reparation of cells can get out of control, typically resulting in the development of cancer (What Is Cancer? 2009). The cancerous cells differ in that the DNA is damaged and cannot be repaired, making these cells superfluous (What Is Cancer? 2009). Replication of these cells continues and as these cells outlive healthy ones (What is Cancer - Childhood Cancers n.d.), it results in the development of excess tissue, referred to as tumours or neoplasms, which can be cancerous, fatal or harmless (Tortora & Grabowski 2003). A cancerous neoplasm is called a malignant tumour or malignancy, characterised by the ability to undergo metastasis and spread cancerous cells to other parts of the body (What is Osteosarcoma? 2009) (Tortora & Grabowski 2003). As the tumour size increases it begins to compete with healthy tissue for blood supply, to the detriment of the normal tissue which decreases in size and dies (Tortora & Grabowski 2003). In order to prevent the spread of the damaged cells (cancer), treatment is necessary, often through chemotherapy and/or surgical intervention (resection).

Malignant tumours originating within the connective tissue of the human body are referred to as sarcomas, occurring in muscle, bone, fat, as well as soft tissue (Board 2008). More specifically, cancer occurring within bone is referred to as Osteosarcoma (or ***Osteogenic Sarcoma*** (What is Osteosarcoma? 2009)). Osteosarcoma is most frequently found in the immature bones of children and adolescents, typically arising in the ends of Long bones (Lewis 2005), due to the high concentration of replicating cells, resulting in the destruction and weakening of bone tissue (Board 2008). While osteosarcoma can originate in any bone of the body, the most common sites for development are outlined in Table 1 (What is Osteosarcoma? 2009)(Board 2008)(Mehlman & Cripe 2008)(Schindler et al. 1997)(Dominkus et al. 2001).

Table 1: Osteosarcoma prevalence and location

Bone	Osteosarcoma Prevalence	Location
Femur	42 %	25 % Proximal 75 % Distal
Tibia	19 %	80 % Proximal 20 % Distal
Humerus	10 %	90 % Proximal 10 % Distal

Statistically, the occurrence of osteosarcoma is slightly higher in males (5.2 million p.a) than in females (4.5 million p.a) (Mehlman & Cripe 2008). While it is extremely rare in young children (0.5 per million per year in children < 5), incidence increases with age, dramatically so in adolescence corresponding to the adolescent growth spurt (Mehlman & Cripe 2008). Specific frequency relating to the occurrence of osteosarcoma in children has been captured by *Mehlman et al (2008)*; shown in Figure 7 below.

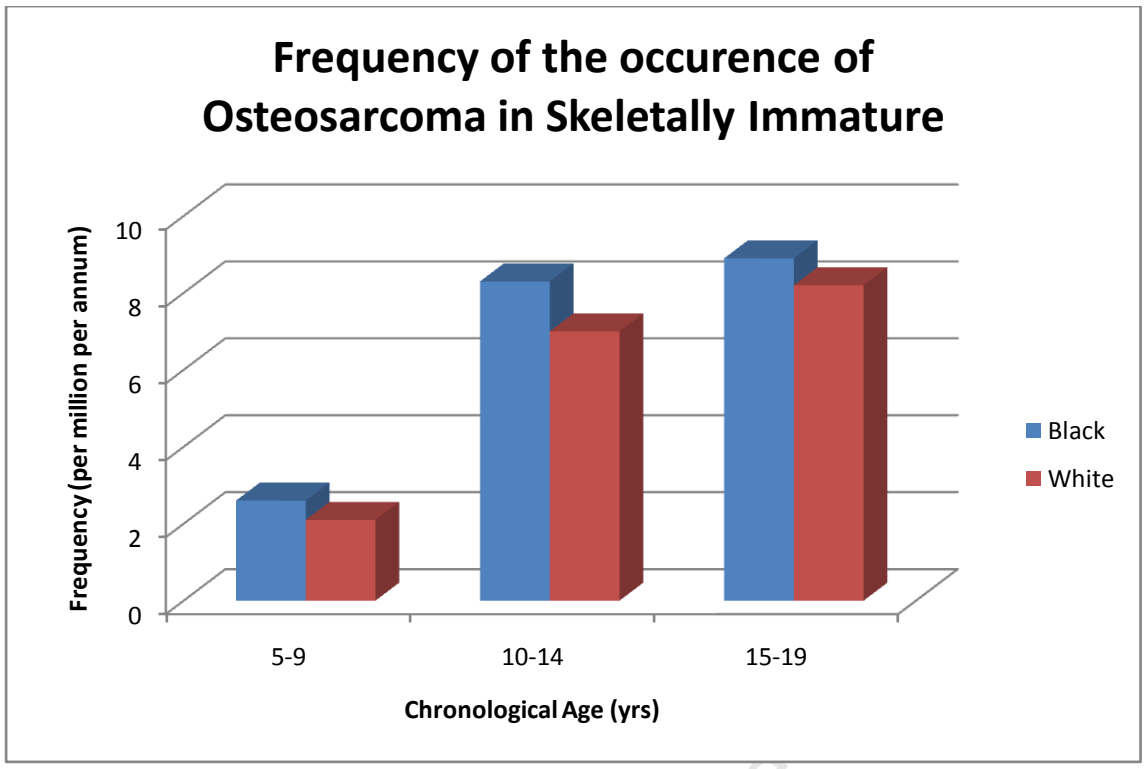

Figure 7: Osteosarcoma frequency

While the frequency of occurrence differs somewhat between racial groups, it is of no relevance to the development of an endoprosthetic growth module mechanism.

2.4. Detection and Diagnosis

Crucial to the effective treatment of cancer is its early detection. While cancer is often difficult to detect, imaging techniques have proven invaluable to the early detection thereof. Imaging techniques employed are not only necessary for detection, but also vital to the determination of the precise location and stage of the cancer, fundamental to the mode of treatment. In addition, imaging facilitates the assessment of a particular treatment's efficacy as well as the monitoring of recurrence. (Cancer Imaging n.d.)(Board 2009) A variety of imaging techniques are employed for the detection and monitoring of cancer, outlined below.

2.4.1. Radiography

X-rays are the most common method employed in medical imaging. Two-dimensional images are produced as a result of the varying absorption rates of different bodily tissues. Different materials may be brought into focus by varying the intensity of the X-ray (Cancer Imaging n.d.). Images of bony or dense structures appear clear, while those of soft tissues or organs are of much lower quality (Tortora & Grabowski 2003). Observed abnormalities can only indicate the possibility of cancer.

2.4.2. Computed Tomography (CT)

Formerly known as Computerized Axial Tomography (CAT scan), CT scans employ computer-controlled X-rays to generate images. The distinct advantage of CT is the ability to generate visualisations of soft tissues and organs with significantly more detail than conventional radiography. In addition, multiple CT images may be assembled to produce three-dimensional views. (Tortora & Grabowski 2003)

2.4.3. Magnetic Resonance Imaging (MRI)

Magnetic resonance imaging (MRI), through the use of magnetic fields and radio frequency pulses, produces very detailed two or three-dimensional computer images of organs, soft tissues, bone and various other internal body structures (Tortora & Grabowski 2003). Through the ability to accurately differentiate between abnormal (diseased) and normal tissue, MRI provides a means of improved assessment of body parts and diseases compared

to alternative imaging techniques such as X-ray, ultrasound and computed tomography (CT) scans (MRI of the Body (Chest, Abdomen, Pelvis) n.d.). The accurate imaging provided by MRI allows physicians to diagnose and monitor tumours within the body. MRI is a relatively safe means of imaging the body, however implanted ferromagnetic medical devices may malfunction or cause problems during an MRI exam (MRI of the Body (Chest, Abdomen, Pelvis) n.d.), affecting the magnetic field and either distorting the images or shifting position.

2.4.4. Sonography

Sonography is used to observe the size, location, and actions of organs as well as blood flow through vessels. High-frequency sound waves reflected by body tissues are converted into an image (Tortora & Grabowski 2003). Sonography is a very safe, non-invasive and painless diagnostic tool and is typically used to differentiate solid- and fluid-filled growths within the body.

2.5. Treatment

Prior to the advent of chemotherapy in the 1970s, the dominant mode of treatment for malignant bone tumours often resulted in amputation (What is Osteosarcoma? 2009) (Lewis 1986). Subsequent developments in the medical field have seen improvements in chemotherapy as well as diagnostic techniques. This has resulted in higher survival rates of the majority of children with osteosarcoma of the Long bones, which in turn has necessitated the development of limb salvage treatments yielding better quality of life than that of amputation (Delepine et al. 1998)(Schindler et al. 1997) (Schindler et al. 1998). No difference has been observed between the survival rates of limb salvage surgery and amputation, even with the higher rate of local recurrence in cases of limb salvage (Grimer, Taminiau & Cannon 2002) (Schindler et al. 1997).

Amputation has a variety of alternate treatment options, including autograft, allograft, bone distraction, rotationplasty, and endoprosthetic replacements (Grimer 2005), all of which show positive functional results (Delepine et al. 1998). Limb salvage techniques typically carried out in older child osteosarcoma patients such as autograft, allograft and bone distraction are not suitable where there is a high likelihood of considerable limb length discrepancies (Neel et al. 2003). As such, treatment options differ where skeletal immaturity of the patient is a factor, due to the majority of tumours being located around the epiphyses and that resection often results in limb length discrepancy. Surgical options to recover or prevent limb length discrepancy include shortening the contralateral limb, over lengthening of a prosthesis at the time of implantation, contralateral epiphysiodesis or the use of extendable prostheses allowing dynamic leg length equalisation over time (Dominkus et al. 2001) (Letson et al. 2003). Treatment of child osteosarcoma presents a surgical challenge to permit the patient to grow/age as normally as possible (Grimer 2005), favouring extendible endoprostheses over alternate options.

2.5.1. Amputation

The limb is removed above the site of osteosarcoma, including a wide margin and reducing the likelihood of recurrence. Following healing of the surgical site, the patient is fitted with a conventional prosthesis. The cosmetic result of an amputation for distal osteosarcoma is shown in Figure 8 below. In the majority of cases, amputation results in the removal of the knee, resulting in poor functioning and gait disturbances with the fitted prosthesis.

Figure 8: Amputation for distal osteosarcoma of the right leg and subsequent prosthesis (Kotz et al. 2002)

2.5.2. Rotationplasty

Rotationplasty presents advantages over amputation, including improved function through knee joint substitution, and the absence of phantom pain that is common to amputations (Grimer 2005). In the 1970s, Salzer and Kahn began applying rotationplasty as an alternative to amputation in the treatment of malignant bone tumours around the knee. Having first been described by Borgreve (1930) for the treatment of ankylosis of the knee joint, rotationplasty was subsequently adopted by Van Ness (1950) for cases of congenital defects of the femur (Wicart et al. 2002).

Rotationplasty can be used in the treatment of proximal and distal osteosarcoma of the femur as well as that of the proximal tibia, following the removal of the tumour and associated joint. In the case of distal femoral osteosarcoma, the remaining healthy distal tibia together with the foot is rotated 180^{o} and attached to the residual proximal section of the femur, fusing the tibia and femur together to act as a new femur. In treatment of proximal osteosarcoma, the remaining healthy leg is rotated 180^{o} with the knee joint replacing the position and function of the hip joint, while the tibia serves as the new femur. In both cases, the 180^{o} rotation is necessary to allow the ankle to serve as a knee replacement. Rotationplasty treatment of proximal tibial osteosarcoma is carried out in the same way as that for distal femoral osteosarcoma.

Following successful treatment, the patient is then able to make use of a below-knee amputation prosthesis, and has improved function compared to amputees. An example of the cosmetic result following rotationplasty for treatment of distal femoral osteosarcoma is shown in Figure 9, as well as the subsequent prosthesis.

Figure 9: Rotationplasty in the treatment of distal femoral osteosarcoma and subsequent prosthesis (Kotz et al. 2002)

2.5.3. Endoprosthesis

The use of extendible endoprosthetic replacements for skeletally immature patients with bone tumours has become an acceptable and safe method of limb salvage, exhibiting local recurrence rates of between 5 and 10 %, comparable to that of amputation surgery (Schindler et al. 1997) (Cool et al. 1997) (Unwin & Walker 1996). Additionally, the use of extendible endoprostheses facilitates patient emotional acceptance, overcoming the undesirable and severe cosmetic results of amputation and / or rotationplasty and their subsequent orthotics (Letson et al. 2003) (Unwin & Walker 1996).

The goal of expandable endoprosthetic reconstruction is to provide limb salvage surgery in children with malignant primary tumours of bone, while ensuring little to no limb length inequality. Allowing for the maintenance of leg length equality while the patient is growing as well as preserving the limb is a distinct advantage compared with alternative methods of treatment (Unwin & Walker 1996).

Figure 10 below shows the surgical implantation of an extendible endoprosthesis, as well as the subsequent cosmetic result.

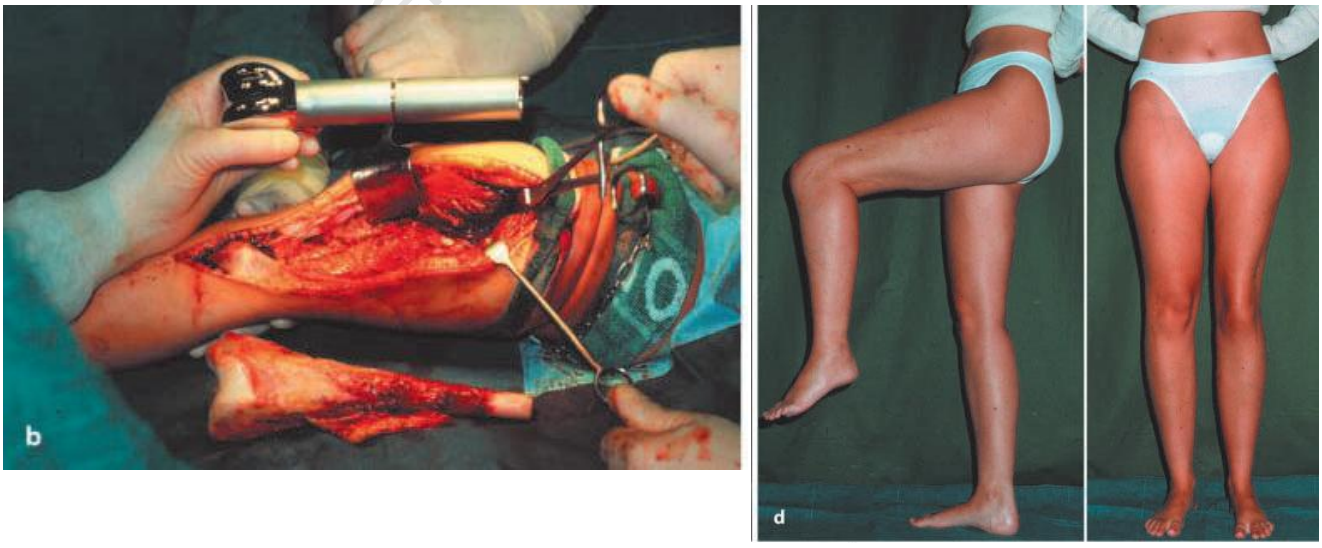

Figure 10: Limb sparing reconstruction with HMRS extendable endoprosthesis, implantation (Left) and condition after 9 extension procedures (Right) (Kotz et al. 2002)

3. Literature Review

3.1. Historical Development

Limb salvage surgery following tumour resection is the preferred treatment in cases of osteosarcoma in skeletally immature patients. Osteosarcoma is typically located in either the distal or proximal region of the Long bone (Figure 2), with resection resulting in the removal of one or both epiphyseal plates of the bone. The removal of one or both epiphyses results in diminished growth capacity of the bone, which in the case of the tibia and femur, leads to limb length inequality. This inequality affects the gait cycle and biomechanical loading of the body, resulting in damage to body joints such as the hip and spine (Letson et al. 2003). Extendible endoprostheses were developed in order to overcome the length inequality between the affected limb and the contralateral healthy limb through periodic adjustments to the extendible endoprosthesis, matching the length of the contralateral unaffected limb (Unwin & Walker 1996).

A large variety of extendible endoprostheses have been developed, revised and improved on over the past 30 years. The motivation for development has been the improvement of patient quality of life through the reduction in revision surgeries for prosthesis extension which increases both the risk of infection (Unwin & Walker 1996), and financial implications. This design progression has resulted in three distinct categories of extendible endoprostheses, outlined in Table 2.

Table 2: Categories of extendible endoprostheses

Type	Description	Advantages	Disadvantages	Examples
Modular	Extension achieved and controlled through insertion of specifically sized modular segments.	- Solution to limb length inequality resulting from reduced growth capacity.	- Requires regular highly invasive surgery. - Regular and repeated invasive surgery poses significant risk of infection. - Major financial implications due to repeated surgeries.	- Kotz Modular Femoral and Tibial Reconstruction (KMFTR) - Howmedica Modular Reconstruction System (HMRS) - Stanmore Mark II & III
Minimally-invasive	Extension achieved and controlled through advancing a drive screw mechanism or similar.	- Solution to limb length inequality resulting from reduced growth capacity. - Improved surgical extension procedures, requiring minimally-invasive surgery.	- Surgery is required to produce an extension of the device. - Risk to patient from regular and repeated surgery. - Major financial implications due to repeated surgeries.	- Lewis Expandable Adjustable Prosthesis (LEAP) - Stanmore Mark IV
Non-Invasive	Extension achieved and controlled externally to the patient.	- Solution to limb length inequality resulting from reduced growth capacity. - Extension achieved externally; no surgery required - No hospitalisation required.	- No notable disadvantages to the concept of non-invasive extendible endoprostheses	- Phenix - Stanmore Juvenile Tumour System (JTS) - Repiphysis

Unwin et al (1996) investigated the use of extendible endoprostheses in the treatment of Long bone osteosarcoma. The occurrence of osteosarcoma and its location was highlighted in Section 2.3, however extendible endoprostheses are not used in all cases of Long bone osteosarcoma. Table 3 below shows the frequency with which these devices are used and their location, with the majority of extendible endoprostheses being used in the distal femur.

Table 3: Use of extendible endoprostheses

Location of Extendible Endoprosthesis		Frequency (%)
Femur	Proximal	8.9
	Distal	62.5
	Proximal & Distal	1.8
Tibia	Proximal	16.7
Humerus	Proximal	4.8
	Distal	1.2
	Proximal & Distal	4.2

While the earlier modular designs facilitated limb salvage, avoiding amputation, the regular extension procedures required invasive surgery. One of the most devastating and serious complications in replacement surgery is that of deep infection which increases with the number of surgical procedures (Delepine et al. 1998) (Schindler et al. 1998). This disadvantage of the early designs encouraged the development of extendible endoprostheses which achieve extension through minimally-invasive procedures and, more recently, devices that do not require surgery therefore vastly improving patient quality of life.

Stanmore Implants Worldwide is an orthopaedic company founded in 1949 and based in Stanmore, Middlesex, England. The company designs and manufactures both custom and standardised orthopaedic implants (focusing on the restoration of limb and joint functions). Stanmore has contributed considerably to the development of extendible endoprostheses, having developed the first such device in 1976 (the Mark I) and continued to revise and improve the design of extendible endoprostheses up to present day (Unwin & Walker 1996). Following the Mark I, Stanmore has revised and developed a further four generations of extendible endoprosthesis mechanisms, introducing a ball bearing mechanism in 1982 (Mark II) which was followed by the 'C' collar type in 1988 (Mark III) (Unwin & Walker 1996). Stanmore revisited and modified the mechanism of the early design by Scales and Sneath, introducing a minimally-invasive extendible endoprosthesis in 1991 (Mark IV) (Unwin & Walker 1996). Further development by Stanmore resulted in the introduction of the Mark V, a non-invasive extendible prosthesis in 2006 (Gupta et al. 2006)(Gupta et al. 2006). While many other manufactures have also contributed to the development, the designs are similar to those of Stanmore and, as such, a review of the designs developed by Stanmore provides a comprehensive overview of the design progression in the field of extendible endoprostheses.

3.2. Mark II (1982)

The Mark II extendible endoprosthesis consists of titanium alloy components, a hollow inner shaft and piston housed within an outer shaft. Extension is realised through the introduction of ball bearings into the hollow inner shaft, forcing a telescopic piston to extend, resulting in advancing the inner shaft's protrusion from the outer.

Tungsten Carbide ball bearings (ø 6.35 mm) are inserted into the threaded angled entry port and forced into the hollow inner shaft by a threaded introducer (Unwin & Walker 1996); insertion of each, results in the medical grade titanium alloy piston (Ti6Al4V) extending by 6.35 mm (Schindler et al. 1997). Later versions incorporating the ball bearing mechanism were modified to include a decreased angle in the entry port, and bilateral anti-rotation keys (Schindler et al. 1997), preventing rotation of the inner shaft relative to the outer. Additional modifications included the machining of two grooves, permitting the use of a distraction tool to assist the extension process (Unwin & Walker 1996).

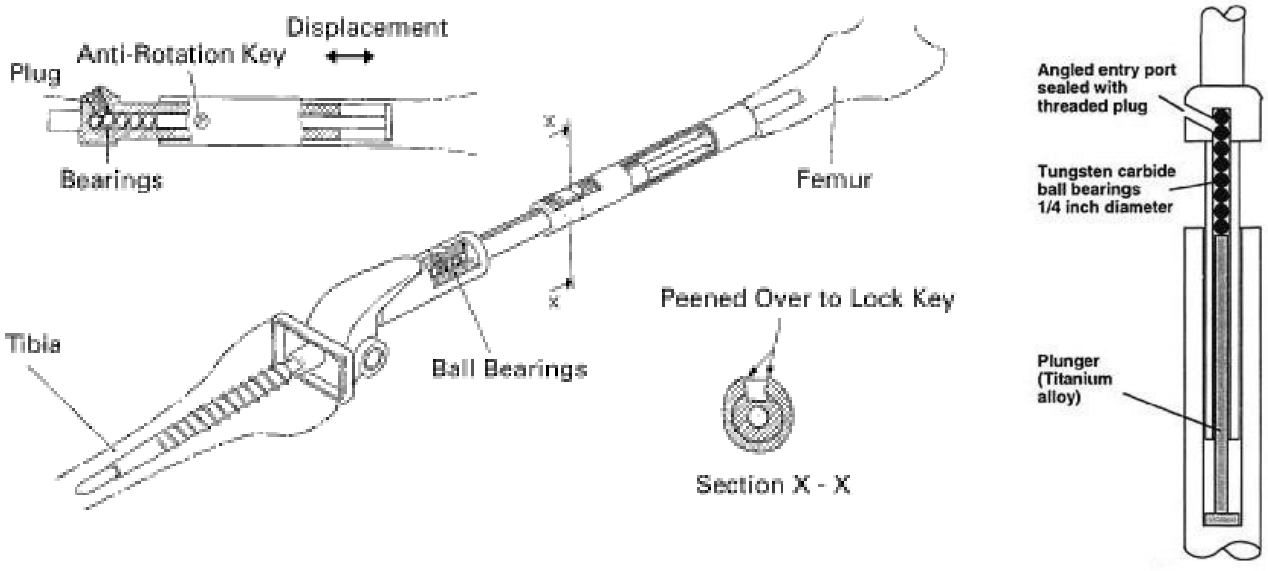

Figure 11: Mark II device (Unwin & Walker 1996) (Schindler et al. 1997)

Experience with the device was gained through implantation at various locations, predominantly distal femur, followed by proximal femur and tibia, as well as distal and proximal humerus (Unwin & Walker 1996). Numerous complications arose from the use of the Stanmore Mark II device. The invasive procedure necessary to expose the expansion mechanism and allow insertion of ball bearings resulted in a risk of infection. At the same time, this risk was significantly increased through the repeated surgery required for maintenance of limb length equality (Unwin & Walker 1996). The use of ball bearings limits the minimum expansion, and any further expansion, to graduated increments of 6.35 mm, resulting in overextension at the time of surgery (Unwin & Walker 1996). Although overextension would be negated over time through the continued growth of the contralateral limb, initial fixed flexion deformities of the knee were observed (Unwin & Walker 1996). In addition to the physiological complications, the mechanism itself also presented difficulties with jamming of the mechanism that occurred frequently due to fractured segments of the ball bearing, resulting from high point contact loading (Unwin & Walker 1996). Such jamming of the telescopic mechanism necessitated modifications to accommodate a distraction tool, reducing the loads on the bearings at the time of lengthening. However, this modification did not overcome the frequent mechanical failure due to ball bearing fracture within the mechanism (Unwin & Walker 1996)(Schindler et al. 1998). Such common mechanical failure finally resulted in the device being superseded by the simpler Mark III design (Schindler et al. 1997)(Schindler et al. 1998).

3.3. Mark III (1988)

The Mark III device comprises of titanium alloy components, namely a piston contained within a hollow shaft. Extension is achieved through the successive addition of ring spacers placed on the telescopic shaft of the piston (Schindler et al. 1998), facilitating and maintaining increased piston extension.

A distraction tool facilitates the extension of the mechanism. The jaws of the distraction tool are inserted into the two grooves on the endoprosthesis, the intramedullary stem and the hollow shaft housing the piston. The distraction tool forces the piston to extend from within the hollow shaft. The achieved extension of the mechanism is maintained by the insertion of titanium alloy (Ti6Al4V) 'C' clips of variable length (typically 6 mm) on the telescopic shaft of the piston (Schindler et al. 1998)(Unwin & Walker 1996)(Schindler et al. 1997). On each 'C' clip are lugs which mesh with a corresponding recess, preventing rotation of the clip relative to the shaft.

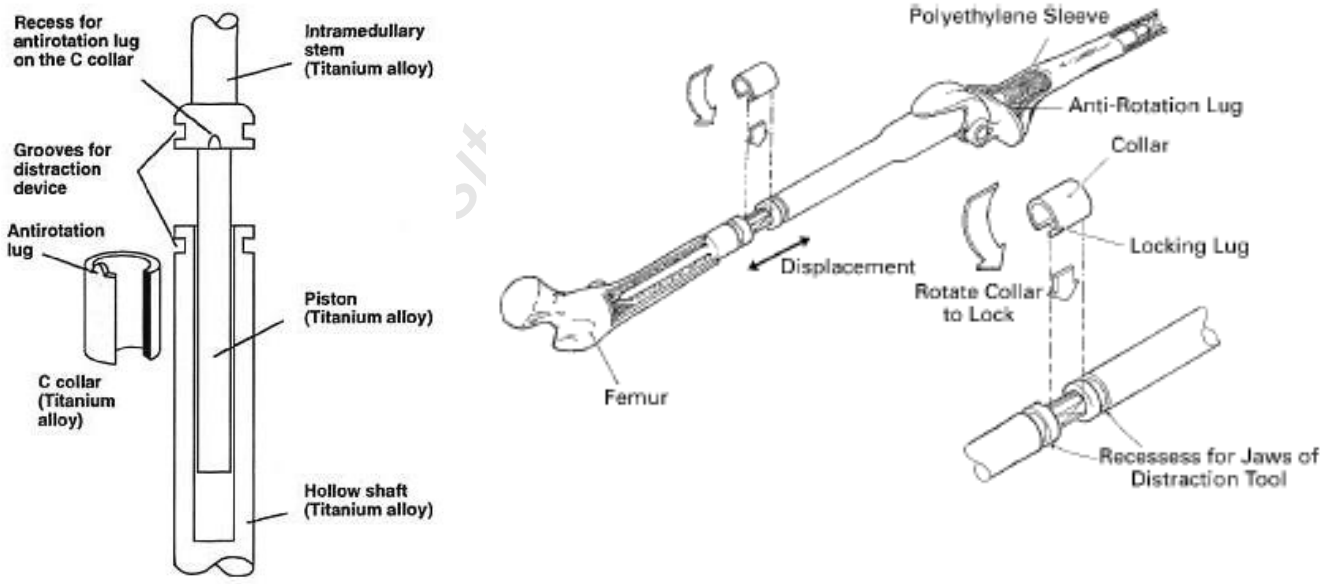

Figure 12: Mark III modular extension device (Unwin & Walker 1996) (Schindler et al. 1997)

A significant disadvantage of the Mark III device was the invasive procedure necessary for extension of the endoprosthesis. The use of a distraction tool required a large incision to

expose the grooves on the mechanism as well as permit extension, while through each successive extension procedure, the relative displacement of the grooves increased. This necessitated progressively larger incisions for following expansion procedures (Schindler et al. 1997). In addition, the lengthening could only be carried out in set graduations of 6 mm and, like its predecessor the Mark II, such inflexible extension increments resulted in over lengthening, over loading surrounding tissue and caused fixed flexion deformities of the knee. This device was similarly superseded by an extension mechanism, the Mark IV, in an effort to minimise the degree of tissue impingement required for active extension (Unwin & Walker 1996).

3.4. Mark IV (1991); Revision of Mark I

The Stanmore Mark IV endoprosthesis consists of a CoCrMo extension module incorporated into a hollow titanium alloy (Ti6Al4V) sleeve. The extension module is comprised of a telescopic worm wheel screw gearing mechanism, operated with a screw driver. 'Extension modules of the Stanmore Mark IV prosthesis are available in three diameters (15, 20 and 30 mm), with the smallest allowing the production of a minimal shaft diameter of 20 mm' (Schindler et al. 1998). Overall extension limited to approximately 12 cm, depending on the original length of the prosthesis. (Schindler et al. 1998)

Extension is achieved through a minimally-invasive procedure, exposing the hexagonal slot for the drive. Operation of the drive with a screwdriver results in the piston extending from the hollow shaft, allowing for precise lengthening of the prosthesis (Unwin & Walker 1996).

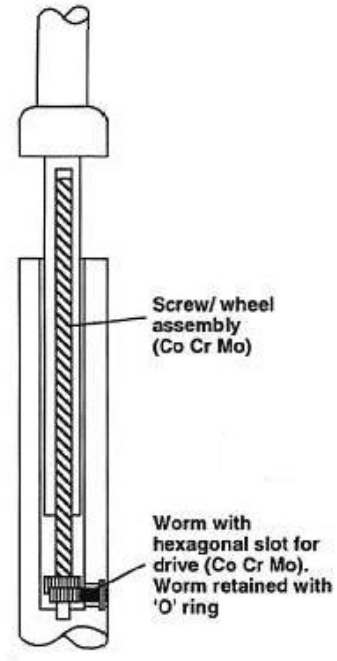

Figure 13: Worm drive mechanism (Mark I & IV) (Unwin & Walker 1996)

In studying the use of the Stanmore Mark IV minimally-invasive endoprosthesis, *Unwin et al (1998)* report no complications with the device, recognising the significant reduction in the length of hospital stays after lengthening procedures (Unwin & Walker 1996).

The Mark IV minimally-invasive endoprosthesis saw a return of the original design employed by the Mark I developed by Scales and Sneath as part of Stanmore in 1976, the Mark I (Unwin & Walker 1996).

3.5. Mark V JTS

JTS drive unit was developed to provide a means of controlling extension of an endoprosthesis non-invasively. This drive unit produces a controlled expansion of the prosthesis without a need of for surgery (Stamore Implants n.d.).

Similarly, by employing a power screw mechanism to jack apart two shafts, the Stanmore Mark V JTS endoprosthesis achieves limb lengthening non-invasively, driven by a rare earth NdFeB alloy disc magnet, operating through a gearbox (Gupta et al. 2006). The gearbox itself is composed of stainless steel coated in titanium nitride and lubricated with liquid paraffin (Stamore Implants n.d.). The shafts of the device are manufactured from titanium (Stamore Implants n.d.). The Stanmore Mark V JTS is available in different length options: 50, 70 and 90 mm, providing a maximum extension length of 60 mm (Gupta et al. 2006). Dimensions of the JTS dictate that the minimum length of resection sufficient to accommodate the prosthesis is 170 mm (Gupta et al. 2006). The Stanmore JTS Extendible Endoprosthesis is shown in Figure 15 below. JTS drive specifications are detailed in Appendix C-3.

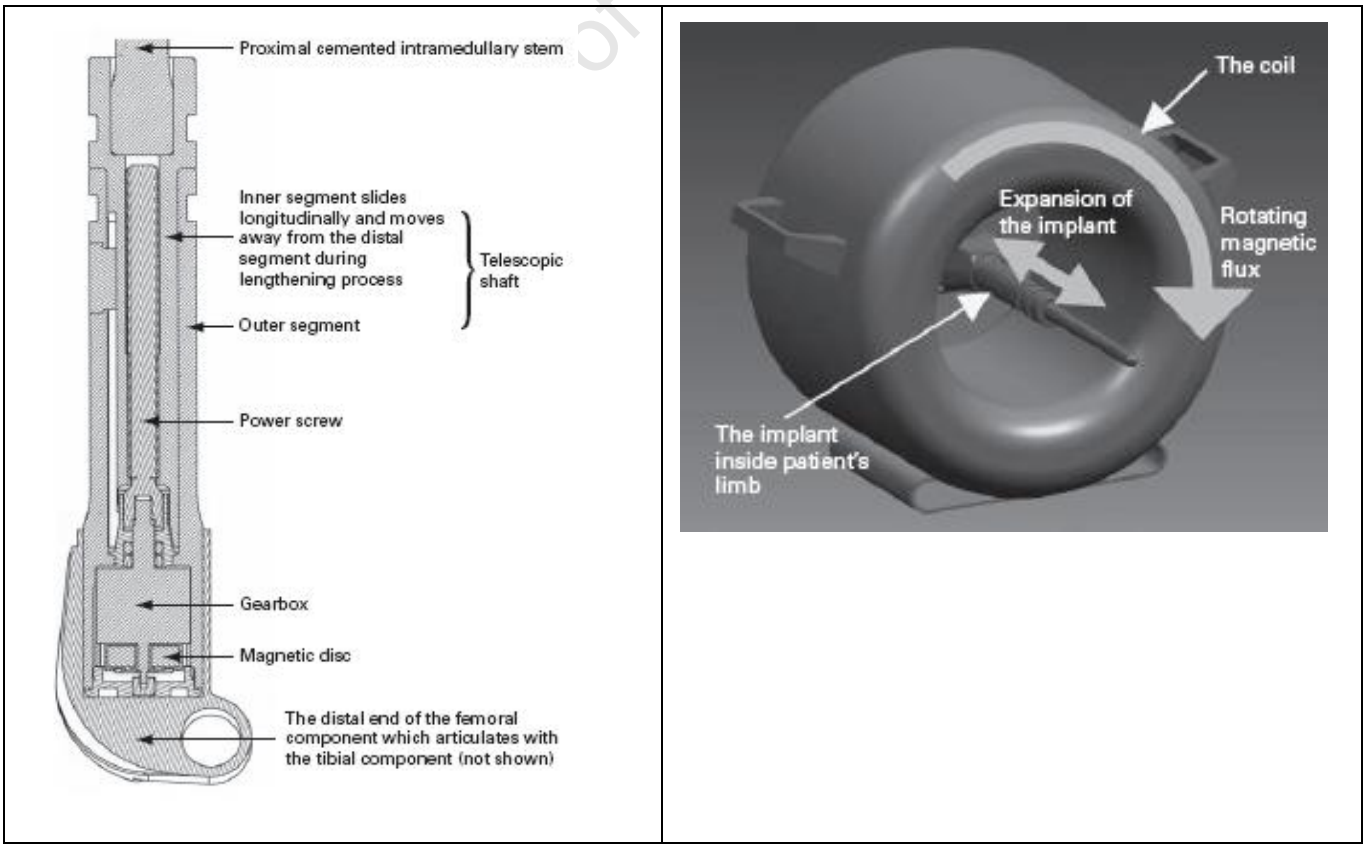

Figure 14: Stanmore Mark V JTS (Gupta et al. 2006)

A lengthening procedure involves the use of an external drive unit, generating a rotating magnetic field. The rotating magnetic field induces synchronous rotation of the magnetic disc contained within the endoprosthesis, providing the gearbox with an input torque which is magnified to drive the power screw mechanism (Gupta et al. 2006). The resulting extension of the device is achieved non-invasively.

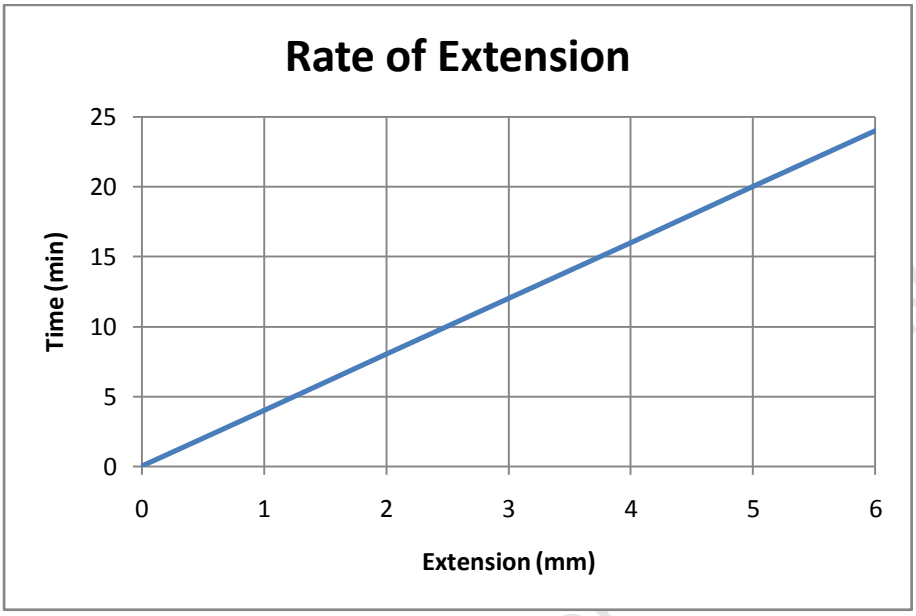

Figure 15: Stanmore JTS extension rate (Stamore Implants n.d.)

The JTS device has significant advantages over previous designs, particularly the non-invasive nature of the device, allowing for extension procedures to be carried out in an out-patient setting. In addition, the endoprosthesis provides controlled and measurable lengthening. During extension there is no noticeable feeling of any vibrations, heat or stretching of tissues for small amounts of extension (Stamore Implants n.d.).

The external drive unit (magnetic coil) is a cumbersome and expensive piece of equipment and, as such, requires that extension of the patients' limb is carried out in a hospital setting. The need for a physician to carry out extension procedures means that extensions can only be carried out sporadically, every six months in the case of the Mark V. These characteristics present as disadvantages of this device.

4. Design Requirements

4.1. Summary of Design Requirements

A variety of aspects have been considered in order to improve and overcome some of the disadvantages of the extendible endoprostheses currently available, specifically the incompatibility with MRI and the inability to monitor and carry out frequent minor extensions. These aspects are crucial to the design and functioning of the endoprosthesis, and are described in further detail in the following sections.

Table 4: Summary of design requirements

Category	Details		
	Specification	Value	Units
Dimensions	Diameter	28	mm
	Overall Length (Max)	200	mm
	Extension Capacity (Max)	100	mm
Distraction	Linear Force (Min)	500	N
	Antero-Posterior Moment	9.5	BWcm[1]
	Medio-Lateral Moment	6.7	BWcm[1]
	Torsion	1.3	BWcm[1]
Material	Endoprosthesis	Ti6Al4V	-
	Seals	UHMWPE[2]	-
	Motor	As supplied	
	Gearbox	As supplied	
Operation	Non-invasive	-	-
Life Span		5 yrs	

[1]BW – Body Weight

[2]UHMWPE – Ultra High Molecular Weight Polyethylene

4.2. Dimensions

Fundamental to the design of an extendible endoprosthetic *femoral* replacement are the dimensions of the femur and, more specifically, the typical resection dimensions that the device intends to replace. As in the case of a normal femur, the endoprosthesis must not impinge on the surrounding muscle and tissue.

The relevant dimensions are the diameter, length and capacity for extension. The minimum diameter of the femur is located mid-way along the diaphysis, approximately ϕ 28.1 mm, while the average overall length of the femur is approximately 433 mm and 470 mm for females and males respectively (Section 2.2). However, in the case of limb salvage surgery, the dimension of the resected section of the femur is more specific to the design of an endoprosthesis if it is to serve as a replacement. Typically, the removal of osteosarcoma together with reasonable margins to avoid recurrence, results in an average resection length of 115 mm (ranging 80-200 mm) either proximally or distally (Kapukaya et al. 2000).

While the overall dimensions of the endoprosthesis must be limited to a diameter of ϕ 28 mm and an overall length of < 200 mm, the device must also be capable of providing a reasonable amount of extension. Reasonable extension, in this case, is deemed to be of sufficient amount to allow for a significant time span between revision surgeries, limiting risks and financial costs associated with surgery. Based on the data collected by *Anderson et al (1963)* (Appendix A-1), the remaining growth for both the femur and tibia has been plotted for consecutive chronological ages (Figure 16 and Figure 17 respectively).

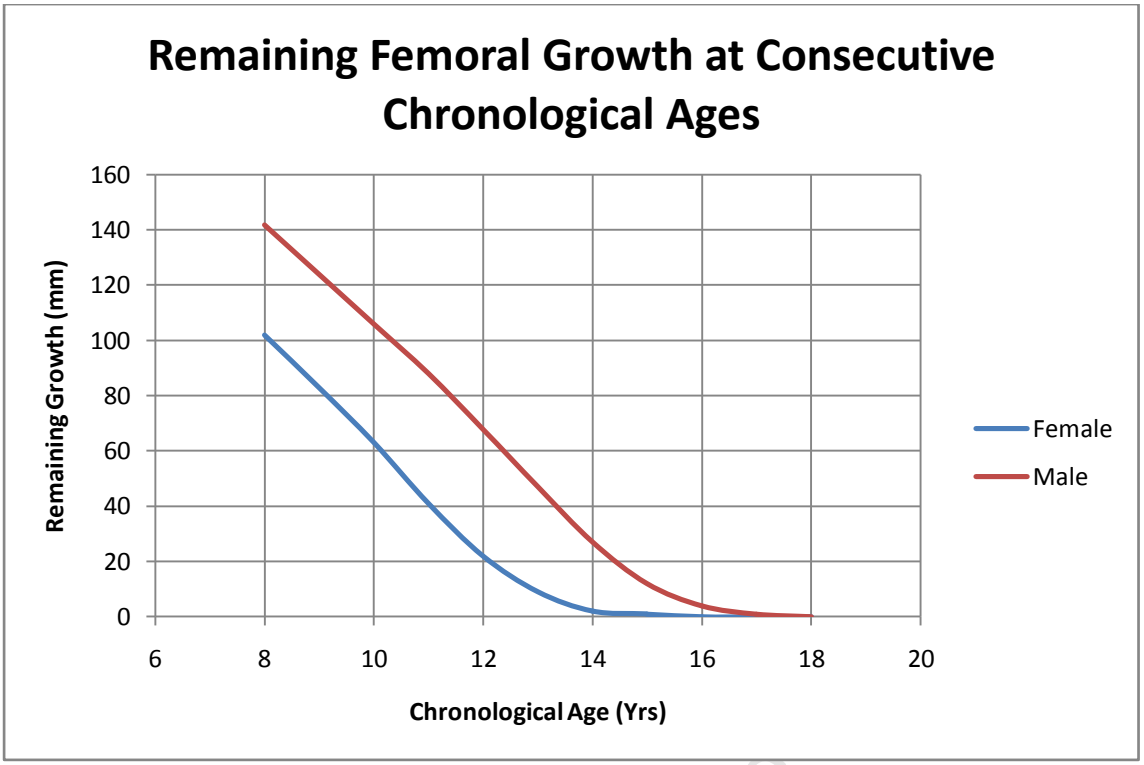

Figure 16: Remaining femoral growth at consecutive chronological ages

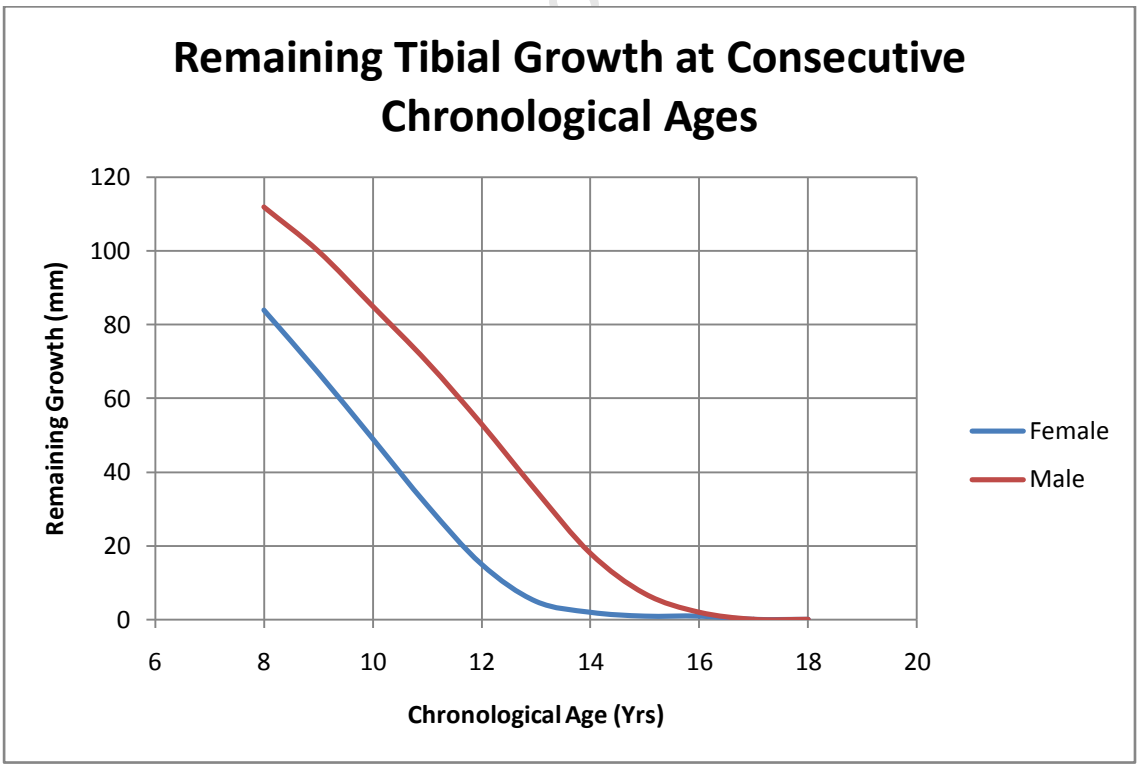

Figure 17: Remaining tibial growth at consecutive chronological ages

The remaining growth indicated in Figure 16 and Figure 17 account for that in both the proximal and distal epiphyses, however the growth rates of epiphyses differ slightly. The remaining distal femoral and proximal tibial growth for both males and females are shown in Figure 18 and Figure 19 respectively.

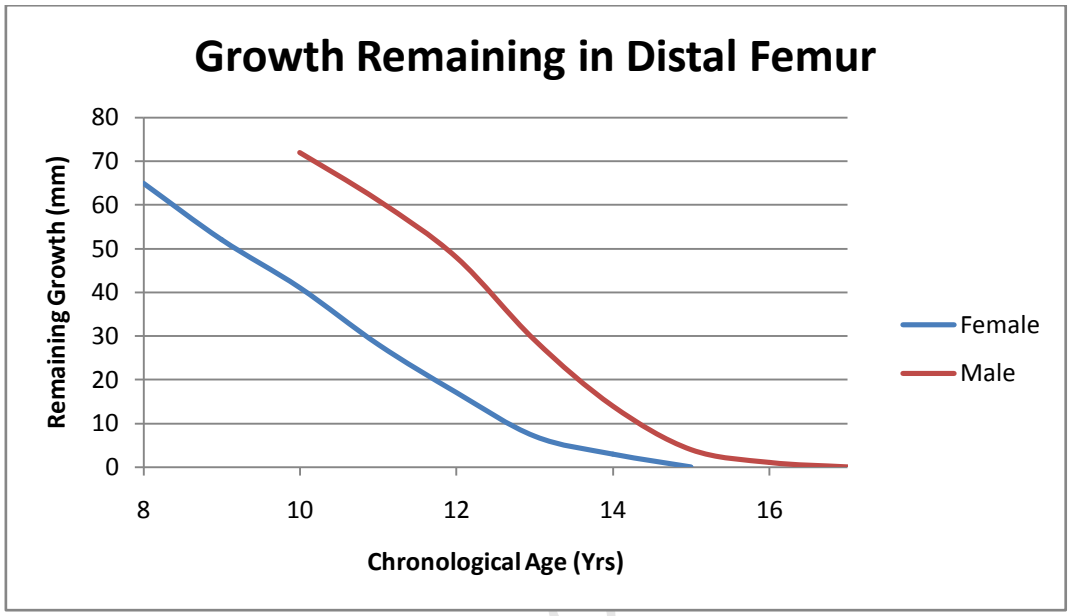

Figure 18: Distal femoral growth remaining

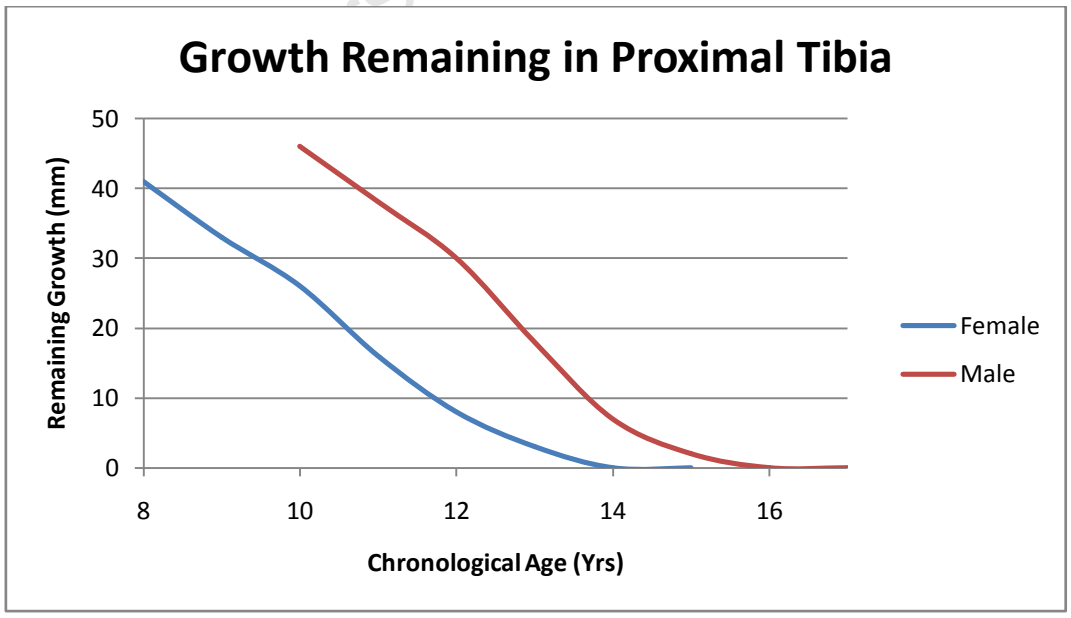

Figure 19: Proximal tibial growth remaining

Osteosarcoma can develop at any chronological age, however the occurrence increases with age up to maturity (Section 2.3). It is not possible to predict at what age the extendible replacement would be required and thus should ideally provide for the maximum possible growth remaining, approximately 70 mm (10 yr old Male distal femur) (Appendix A-1).

4.3. Biomaterials

Biomaterials are defined as 'any substance (other than a drug) or combination of substances synthetic or natural in origin, which can be used for any period of time as a whole or part of a system which treats, augments or replaces tissue, organ or function of the body' (Snyder & Helmus n.d.). Such materials are required for the design of an endoprosthesis so as not to induce an inflammatory response in the patient which could lead to tissue necrosis (Teoh 2007).

In establishing the required biomaterials, certain aspects of the material must be considered, including biocompatibility, practicality, imaging compatibility and sterilisation compatibility.

4.3.1. Biocompatibility and Practicality

Metals

Used in applications requiring rigid and high strength support, common alloys include austenitic stainless steels, cobalt-chrome alloys including molybdenum based alloys, tantalum and titanium. These materials are relatively easy to machine.

Polymers

A wide variety of biopolymers are used in a similarly wide range of applications. The more commonly used polymers include but are not limited to silicone, poly-ethylene and tetraflouroethylene. Use of biopolymers within the desired endoprosthesis is limited to seals and cable insulation.

Silicone elastomers have proven to be chemically stable, however it does form molecular bonds with lipids which, in the long term, results in the material becoming rigid and brittle (Szpalski, Gunzberg & Mayer 2002). The properties of silicone make it a useful material for electrical applications such as wire insulation (Kutz 2009). Additionally, silicone remains unaffected by gamma sterilisation in excess of 108 rads (Thermometrics, Precision

Temperature Sensors n.d.). Although considered biologically inert, rare allergic reactions to silicone have been reported (Oprea et al. 2009), causing adverse inflammatory responses, including tissue degradation (Bigata et al. 2001).

Ultra-high molecular weight polyethylene (UHMWPE), having been used in orthopaedics since 1962, is a distinctive material due to its notable properties including chemical inertness, lubricity, impact resistance, abrasion resistance and radiation tolerance (1000 kGy) (Kurtz 2004) (Nordian n.d.), making it a favourable choice of polymer for device sealing.

Typically used in electrical insulation applications, mechanical properties of Ethylene-TetrafluoroEthylene (ETFE) include flexibility, chemical inertness, impact resistance and abrasion resistance (Thermometrics, Precision Temperature Sensors n.d.). ETFE has an excellent radiation tolerance of 1000 kGy (Nordian n.d.) and, as such, is the most suitable biopolymer for cable insulation.

4.3.2. Imaging Compatibility

Ferromagnetic materials are known to have adverse effects on MRI, resulting in distorted images. While structural components of the endoprosthesis are to be fabricated from biocompatible and non-ferromagnetic materials, the materials encased within the device, although not biocompatible, must contain limited amounts of ferromagnetic materials to avoid imaging complications.

4.3.3. Sterilisation Compatibility

Any implant must be sterilised to prevent introducing bacteria into the body. A variety of sterilisation techniques exist including steam, ETO and Gamma (Teoh 2007). As such, the extendible endoprosthesis must be compatible with at least one mode of sterilisation, permitting thorough sterilisation without any detriment to materials and / or electronics within the device.

Steam Autoclaving

The original method of sterilising biomedical implants was that of steam sterilisation or autoclaving. The device to be implanted is exposed to pressurised steam at 120 ^{o}C for approximately 15 to 30 minutes, after acquiring the correct temperature (Davis 2003). Caution is necessary with this method given the high temperatures as some polymers and adhesives may undergo softening or melting (Davis 2003). In order to effectively sterilise, the steam must be exposed to all surfaces of all components.

Ethylene Oxide

A low-temperature means of sterilisation compatible with a large range of materials. Components are exposed to either pure or diluted EtO at 30 to 50 ^{o}C for 2 to 48 hrs (Davis 2003). The toxicity of EtO presents as a disadvantage for use as a sterilisation method (Davis 2003). In order to effectively sterilise, the EtO gas must come into contact with all surfaces of all components, as in the case of autoclaving.

Gamma Ray

Ionizing radiation of gamma rays from a source of cobalt-60 isotope provides a method for the sterilisation of implants. Cobalt-60 radiation is an advantageous method as it is rapid and reliable and, in addition, radiation is not absorbed by components (i.e. materials are not radioactive following sterilisation) (Davis 2003). When a level of between 25 and 40 kGy has been absorbed by the implant, it is deemed to be sterilized and free of bacteria (Davis 2003). As the gamma rays are able to penetrate the material of the components, it is not necessary for all surfaces of all components to be exposed as in the case of steam and ETO sterilisation. All polymers are affected by radiation, some more than others with many effects considered negligible. Polymers incompatible with radiation include Polyacetal, Polypropylene and Teflon (Nordian n.d.). UHMWPE exhibits an increase in strength due to cross-linking, and is radiation stable with a tolerance level of 1000 kGy.

4.4. Loads

The forces and loads to be experienced by an endoprosthetic replacement present a significant design consideration. If the implant is to serve a purpose and best restore normal bodily function, it must be able to withstand the stresses introduced by typical activities. Typical loading on the femur involves axial stresses in supporting body mass. Activities such as walking, stair ascent and descent, and jogging result in additional axial loads, bending moments and torsional moments on the femur, all of which the device must be capable of withstanding in order to cater for limb salvage surgery and preservation of function. Axial loading also occurs during extension due to the resistance of muscles and tissue. The expected forces imparted to the extendible endoprosthesis can be divided into two categories, namely distraction and functional forces, detailed below. It is possible to consider these two types of forces separately as extension of the Long bone is intended to be carried out in a relaxed position, which excludes the influence of functional forces and vice versa.

Essential to the design of the endoprosthesis is the resistance to failure. The intended location of the device means that revision/replacement poses significant risk and difficulties, and failure of any component within the device prior to scheduled revision surgery is unacceptable. Allowing for the achievement of reasonable extension, it is expected that the device would be implanted for approximately 5 years. In this time, the endoprosthesis must resist both static and fatigue failure due to normal loading of the femur as well as loads due to distraction (extension).

4.4.1. Distraction Loads

In an effort to realise the resistance to expansion, *Meswania et al (1998)* studied the in-vivo distraction forces on an extendible endoprosthetic replacement, investigating 34 extendible endoprostheses implanted in patients aged 4 to 18 years, yielding a total of 76 extension measurements (Meswania et al. 1998). The study was carried out on a modular type of endoprosthesis in both the femur and tibia, as these required regular invasive surgery for extension which allowed easy access to the device to measure distraction forces. The

distraction tool was modified to include a Wheatstone Bridge arrangement of strain gauges to allow for measurement of the pure distraction force (Meswania et al. 1998). This study provided insight into the distraction forces compared with extension in the femur which has the greatest resistance to extension due to the greater muscle mass compared with other Long bones.

Distraction forces were recorded at 1 mm extension increment up to 9 mm, over an extension interval of 10 s for both the femur and tibia (Meswania et al. 1998). Additionally, to investigate the effects of creep recovery of the soft tissues, further recordings were carried out at 30 s intervals (Meswania et al. 1998).

The results for femoral distraction are shown in Figure 20 below.

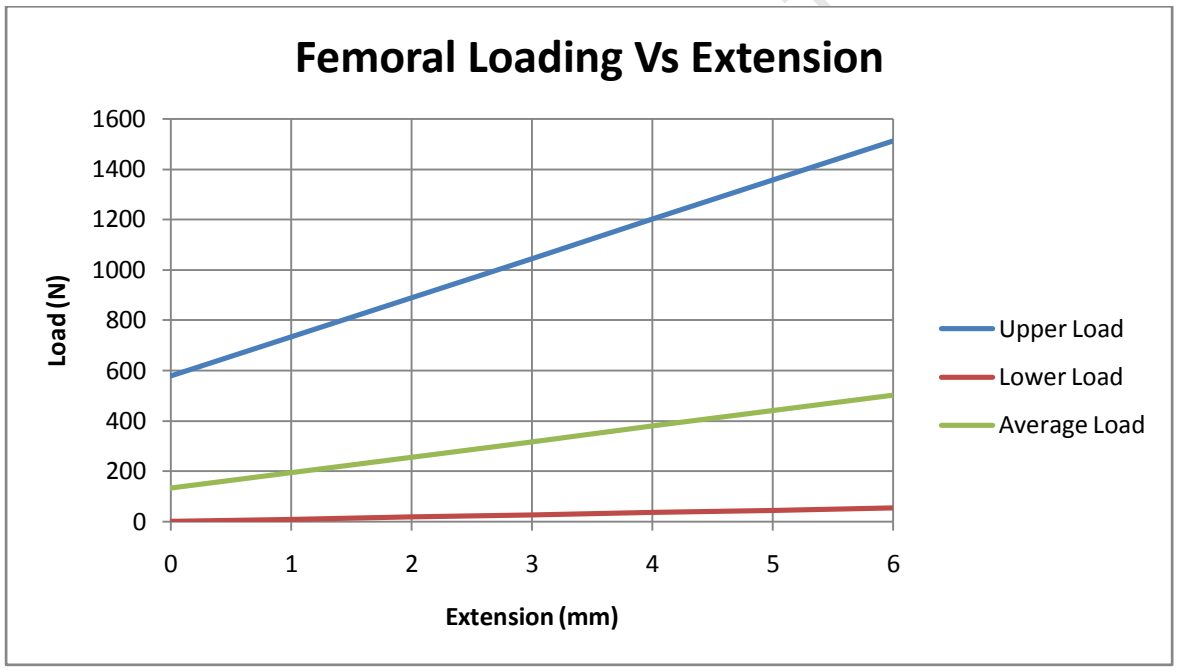

Figure 20: Distraction loading of femur vs. extension

The initial soft tissue and muscle loading on the femoral modular endoprosthesis varied from 1 – 578 N, with an average of 135 N (Meswania et al. 1998). Continued investigation of loading at greater values of extension enabled *Meswania et al (1998)* to establish a linear relationship between load and extension. The variation in load at 6 mm extension was significantly larger than that of the initial loading, ranging from 33 – 1513 N, an average of

502 N (Meswania et al. 1998). Regression analyses applied to the curves yielded an initial load of 122 N increasing to 516 N at 6 mm (Meswania et al. 1998).

Figure 21 below shows the results of tibial distraction.

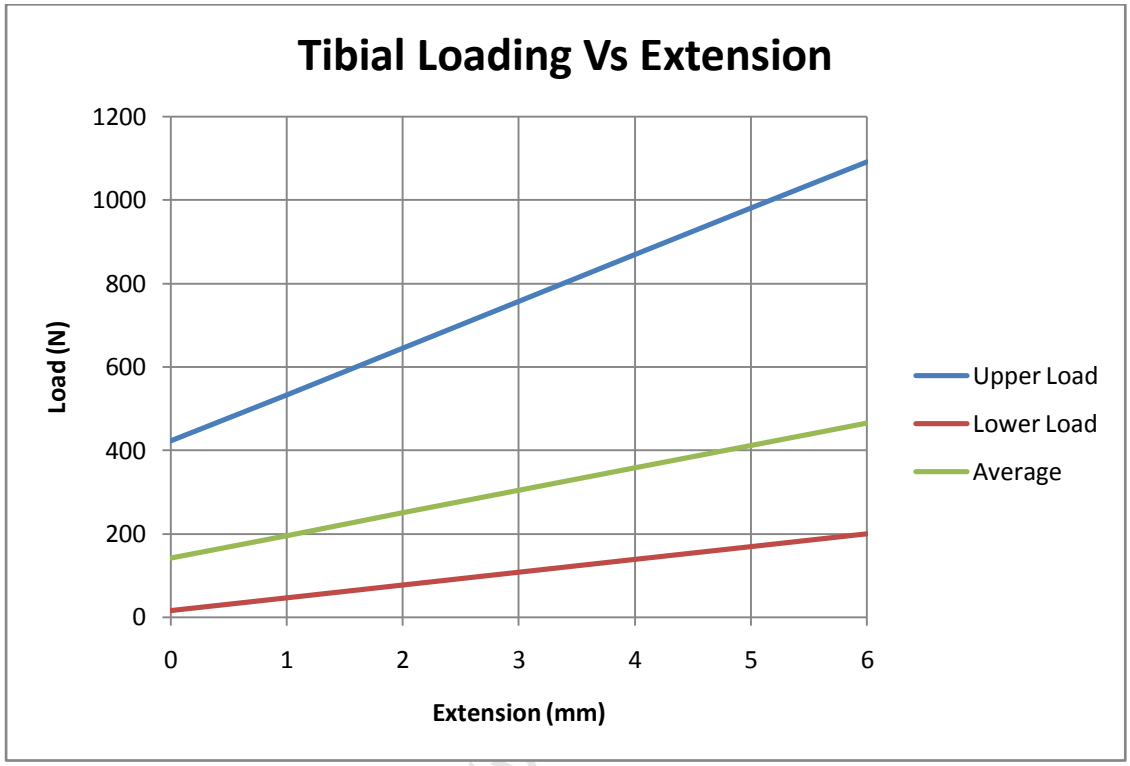

Figure 21: Distraction loading of tibia vs. extension

Initial loading of the tibial endoprosthesis ranged from 16 N to 422 N (mean 142 N), which increased to an average of 466 N at an extension of 6 mm (range 200 – 1092 N).

In both femoral and tibial distraction measurements, upper and lower loads occur due to varying amounts of scar tissue and muscle mass of the 34 patients studied (Meswania et al. 1998).

Meswania et al (1998) also investigated the influence of tissue relaxation on the distraction loads. While previous data presented shows distraction loads for extension increments at 10 s intervals, Figure 22 below shows the effects of increasing the time interval between extensions to 30 s, compared to that of 10 s intervals. The force difference is negligible at extensions below 3 mm but increases with larger extensions due to tissue stiffening (Meswania et al. 1998).

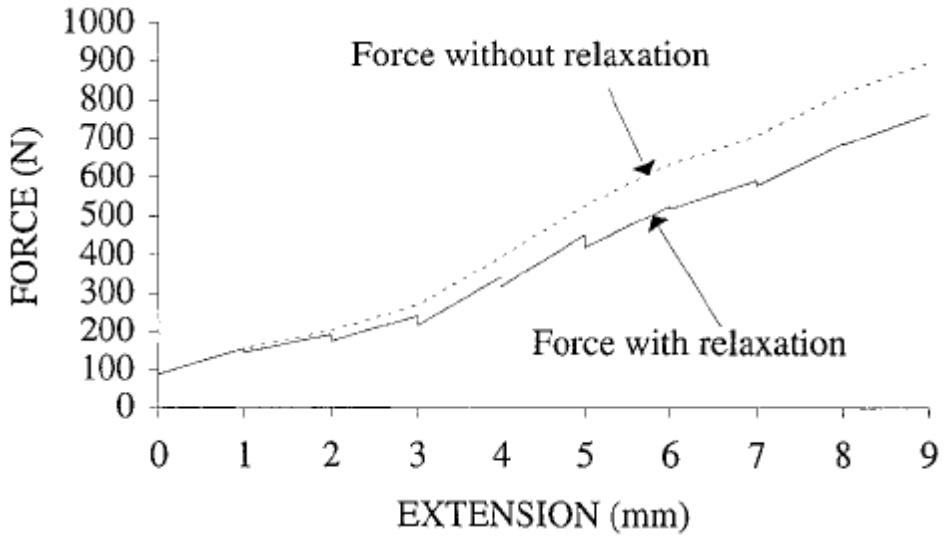

Figure 22: Tissue relaxation after 30s pause after each 1 mm extension (Meswania et al. 1998)

From Figure 22 it can be seen that small extensions require significantly lower distraction forces, further improved by tissue relaxation between extensions. It would be advantageous for the design to cater for such conditions, providing extension at a rate comparable to natural growth, achieving minor extensions frequently in contrast to large periodic extensions. While the study presented by *Meswania et al (1998)* provides a reasonable prediction of average distraction forces, the influence of scar tissue resulting from massive surgery can affect the distraction force required.

Although the device is intended to carry out frequent minor extensions, it should also cater for the possibility of large periodic extensions, generating the average 500 N required for 6 mm extension.

4.4.2. Functional Loads

Of all the Long bones, the femur experiences the greatest functional loading and, as such, is most relevant to the design capabilities of an extendible endoprosthetic replacement. Designed for femoral loads, the device would be more than adequate for replacing other Long bones.

The loading on the femur has been mathematically modelled by a variety of authors, including but not limited to *Duda et al (1997)*, and *Frey Law & Shields (2004)*. While these calculated data are advantageous in its/their application to any number of subjects, many of the assumptions regarding muscle action, joint contact points, and other factors introduce uncertainty. In contrast, in-vivo telemetry studies generate valid measurements of forces in implants (Taylor & Walker 2001).

Using strain gauges mounted on distal *femoral* replacements in two patients (shown in Figure 23) and tracking the patients for 2.5 years following implantation, *Taylor et al (2001)* documented the in-vivo loads (axial, bending and torsional) experienced by the femur under various activities (Appendix A-4): walking, stair ascent and descent, and jogging.

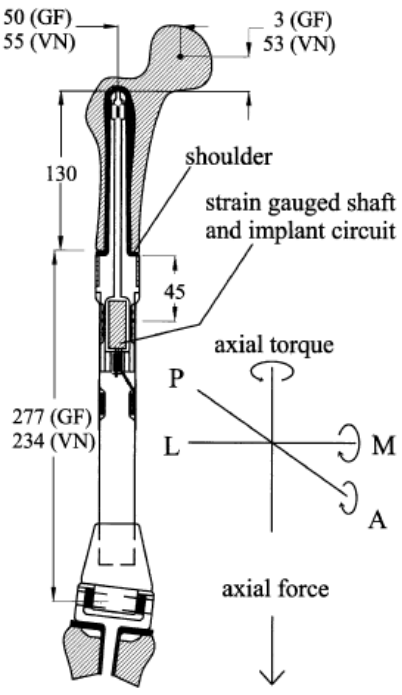

Figure 23: Instrumented femoral replacement

The variation in forces and moments observed by *Taylor et al (2001)* are shown in Figure 24 below for two gait cycles. Three distinct axial loading peaks occur through a gait cycle, the first (0.9-1.1 BW) immediately before heel strike, the second (1.9 BW) and third (2.4 BW) during middle and late stance. The peak AP and ML moments are 6.7 BWcm and 4.4 BWcm respectively. Axial torque peaks at 0.8 BWcm.

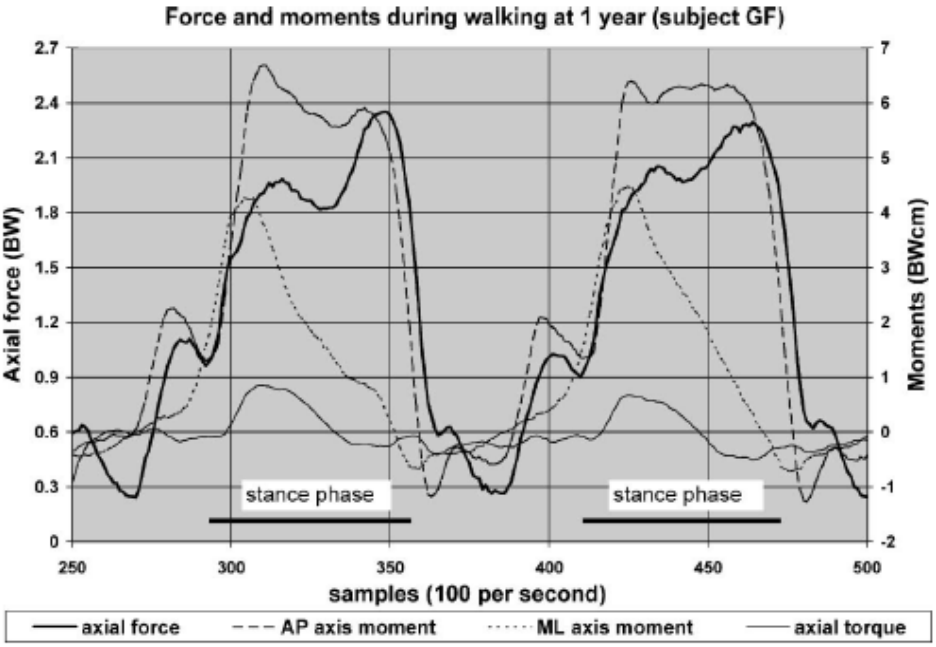

Fig. 2. Two typical cycles of level walking at 1.1 m/s for GF at 1 year follow-up. The A-P axis moment is positive in varus (loadline offset medial to prosthesis axis). The M-L axis moment is positive in hip flexion or knee extension (loadline offset anterior to prosthesis axis). The axial torque is positive in outward direction of the knee w.r.t. the hip (eversion of the foot).

Figure 24: Forces and moments during gait cycle

These data indicate the typical loading to be expected on the femur during walking, stair ascent and descent, and jogging. However, various other common daily activities such as climbing stairs result in considerably higher loading on the femur. The peak axial force, net moments (combined anterior-posterior (AP) and ***medial***-lateral (ML) Moments), as well as torsional moments during these activities, are shown in Figure 25, Figure 26 and Figure 27 (based on the *femoral* replacement telemetry data captured by *Taylor et al (2001)*).

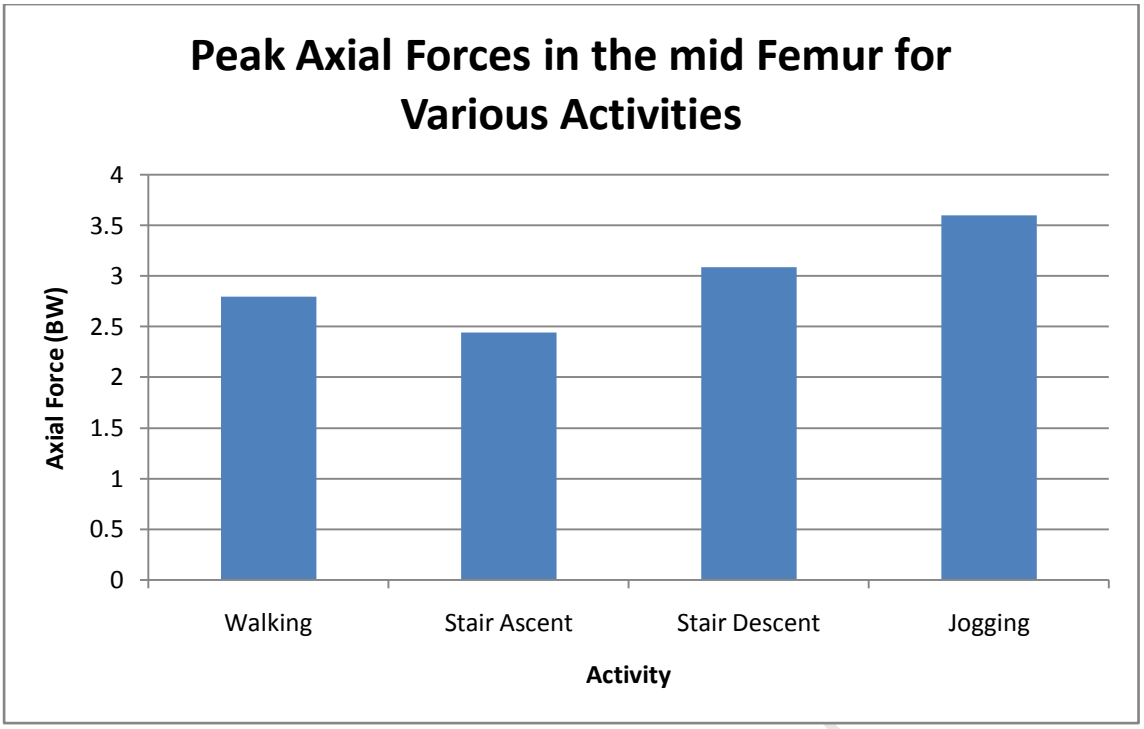

Figure 25: Peak axial forces in the femur during various activities

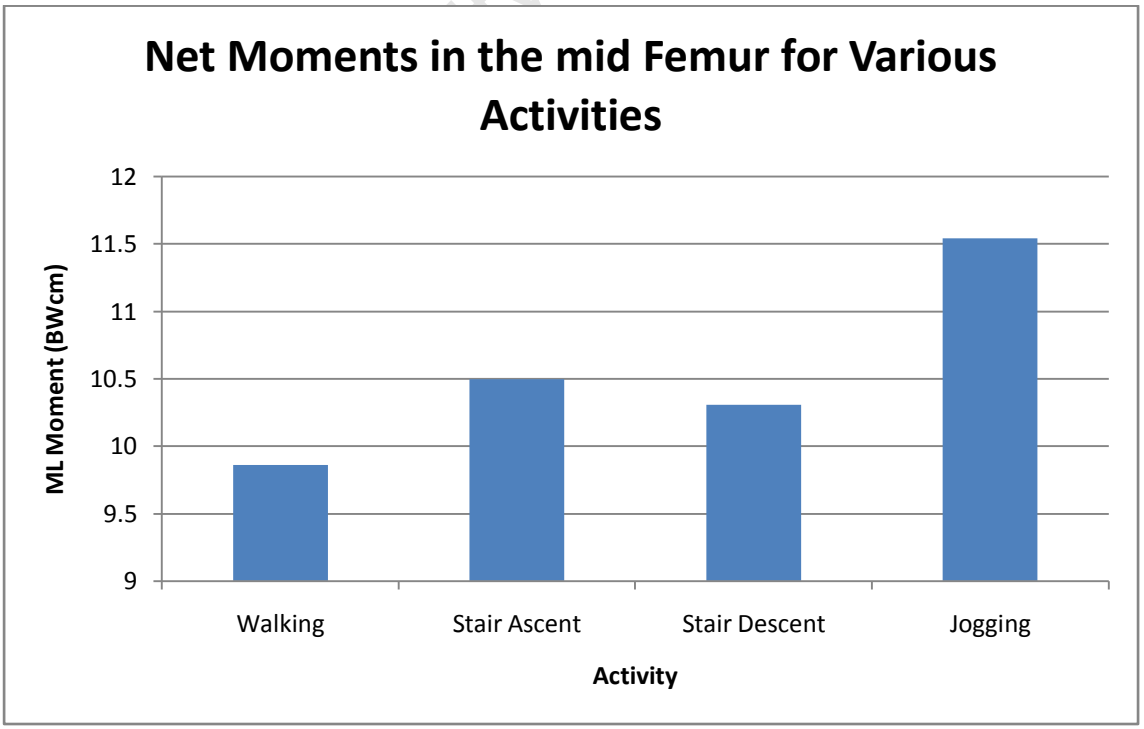

Figure 26: Net moment in the femur during various activities

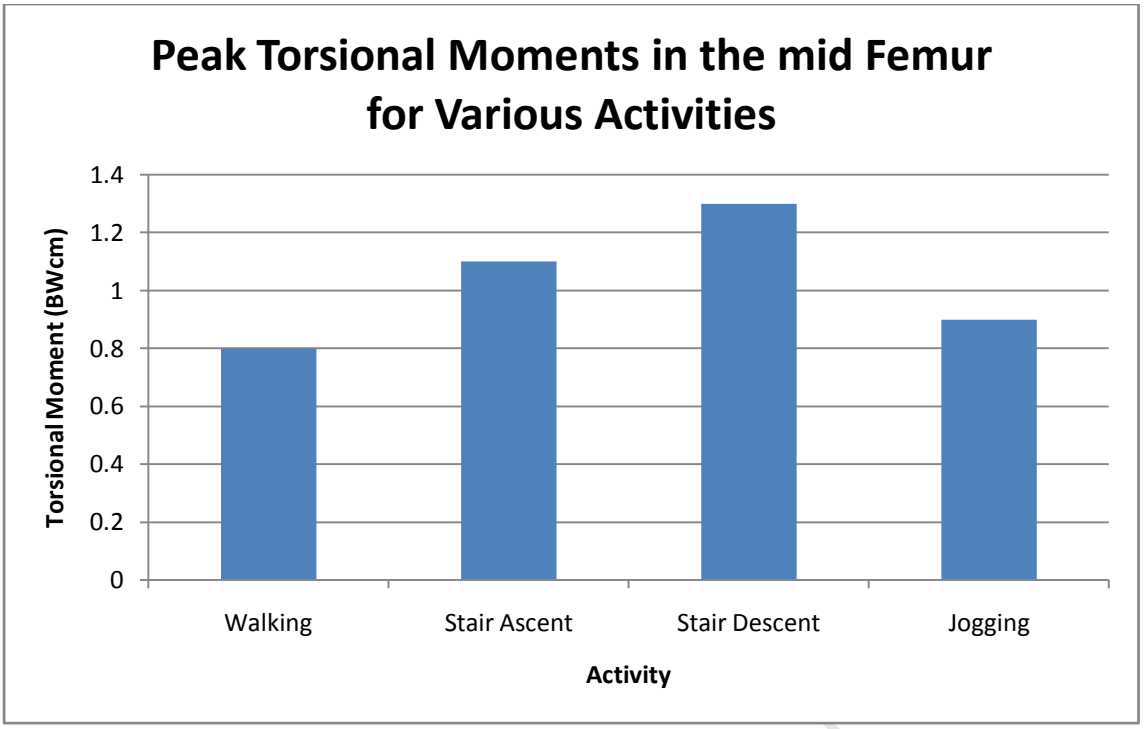

Figure 27: Peak torsional moments in the femur during various activities

From the charts above, it can be seen that jogging results in peaks in the *femoral* axial force of 3.09 BW as well as the net moment, 11.5 BWcm. Ascending stairs similarly causes *femoral* load peaks in the torsional moment of 1.3 BWcm.

4.5. Drive

A variety of different drive mechanisms have been and are employed in previous and current devices, including ratchet mechanisms driven by screw drivers or tibial rotation, magnetic coupling, as well as electro-mechanical mechanisms using small electric motors. All of the aforementioned drive mechanisms require gearing of some sort to develop the significant linear force required to carry out an extension. While ratchet systems are simplistic, they either require minimally-invasive surgery to perform extensions or cannot be controlled accurately (as in the case of tibial rotation). Ideally, in order to minimise patient discomfort, extensions must be carried out non-invasively. This necessitates the use of an electrical or magnetic drive system, both of which are employed in currently available devices. The nature of operation of these drives is that they require ferromagnetic material, which is detrimental to imaging techniques crucial to the accurate diagnosis of cancer, such as MRI. It is therefore necessary to search for an alternative to ferromagnetic materials, while still being able to perform extensions remotely and non-invasively. The recently developed rotary piezo motor provides for such a scenario. These motors are capable of developing high torques while containing no ferromagnetic material and are an ideal choice for the drive mechanism. However, in contrast to magnetic coupling, the use of a motor requires a power source.

4.6. Power

The intended location of the device limits the options available as a means of powering the piezo motor within the device. While battery power is an option, it requires a considerable amount of space, of which there is minimal. Furthermore, given the frequency of operation and the intended life span of the device, a sufficiently small battery is unlikely to store enough power for operation. It is therefore necessary to obtain power from a source external to the body/patient. This further presents an issue in that an electrical link between the motor and the power source is needed. It would be unwise to pass an electrical cable through the skin and deep into the body tissue as the risk of infection is great. Inductive coupling across the skin would overcome this barrier and, making use of a power source external to the body/patient such as the wall outlet, means there is essentially an unlimited supply and the inefficiencies of wireless power transfer are of no concern. The wireless power transfer would be achieved through a primary coil placed externally against the skin, while the secondary receiving coil is placed subcutaneously. When the axes of the coils are aligned, power is transferred from the primary coil to the secondary, generating an alternating current in the secondary coil. The frequency of the inductive coupling must not result in cellular damage or thermal effects. The electromagnetic spectrum and the effect of the various frequencies on body tissues are shown in Figure 28. The internally placed piezo motor requires a direct current and, as such, the alternating current generating in the secondary receiving coil must be rectified. In addition to powering the motor to develop extension of the device, a means of control is required to regulate and monitor the amount of extension developed at any stage. A conceptual flow diagram of the proposed circuitry is shown in Figure 29.

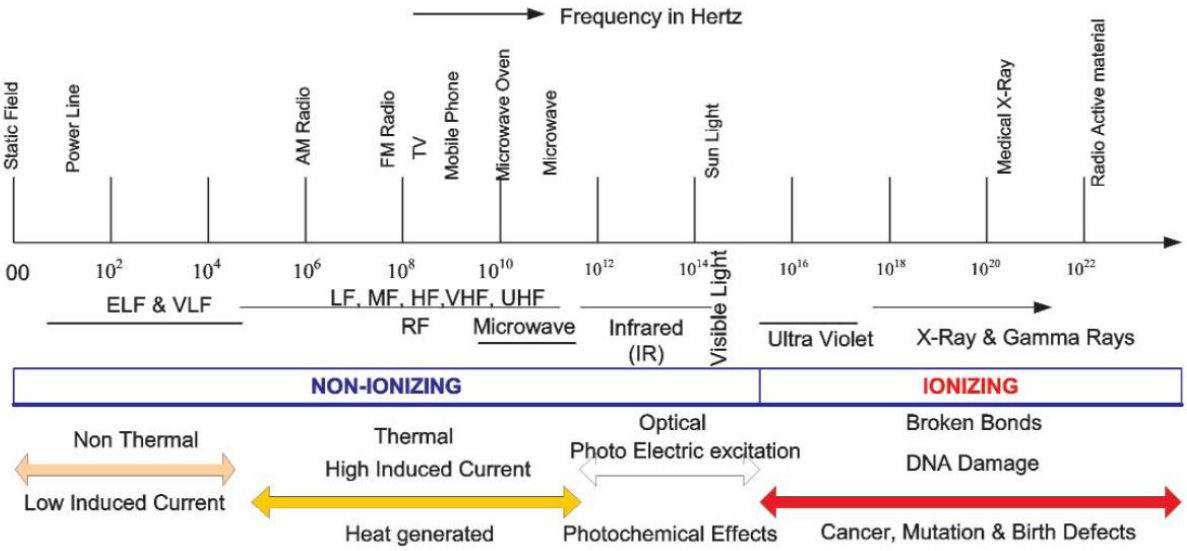

Figure 28: Electromagnetic spectrum with reference to biological effects (Zamanian & Hardiman 2005)

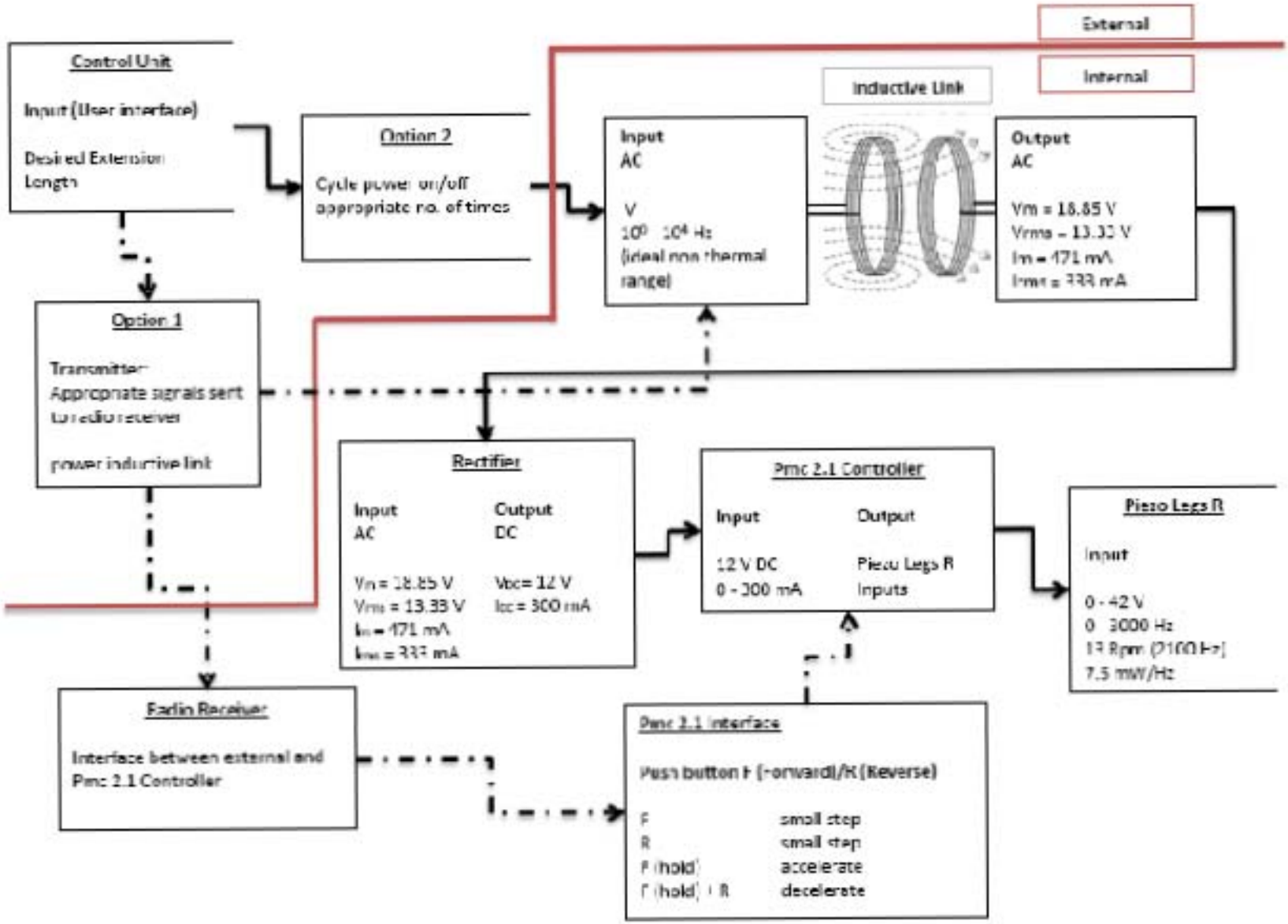

Figure 29: Proposed drive powering and control components

4.7. Feedback and Control

The endoprosthesis is intended to match the growth of the contralateral limb, preventing limb length discrepancy. The growth rate of a normal healthy femur (the contralateral femur) varies considerably with skeletal age (Section 2.2) therefore any extension of the endoprosthesis must be controlled to match the growth of the healthy contralateral limb. The magnitude of extension can be controlled by the time over which the device provides a constant extension rate, as well as allowing feedback from the device itself to precisely monitor the rotation of the motor.

In order to best match the normal growth of the femur, frequent minor extensions are required (daily extensions). It is unrealistic for the patient to be expected to make frequent visits to the physician in order to achieve this 'natural growth' and, as such, it is necessary for the patient to perform these operations from home, requiring the control to be as simple and self-explanatory as possible.

The controller would be required to act as the extension prescription. A computer program facilitates physician interaction with the controller (Section 5.2.3). The physician having pre-programmed the controller with the required overall extension desired over a period (e.g. six months), the controller would calculate the daily extension required to achieve the overall extension for the period. Safety measures would also be required on the controller to limit patient interference as much as possible, including ensuring accurate extension of the device, limiting/preventing over extension, as well as preventing operation of the controller with a different endoprosthesis. A flow diagram of the device control logic is shown in Figure 31.

Allowing feedback from sensors within the extendible endoprosthesis could also provide valuable data, providing further data on in-vivo distraction forces, as well as functional loading. The circuit components necessary for the control and data capture of the device are biologically incompatible and as such must be completely sealed from the surrounding body tissue and fluids.

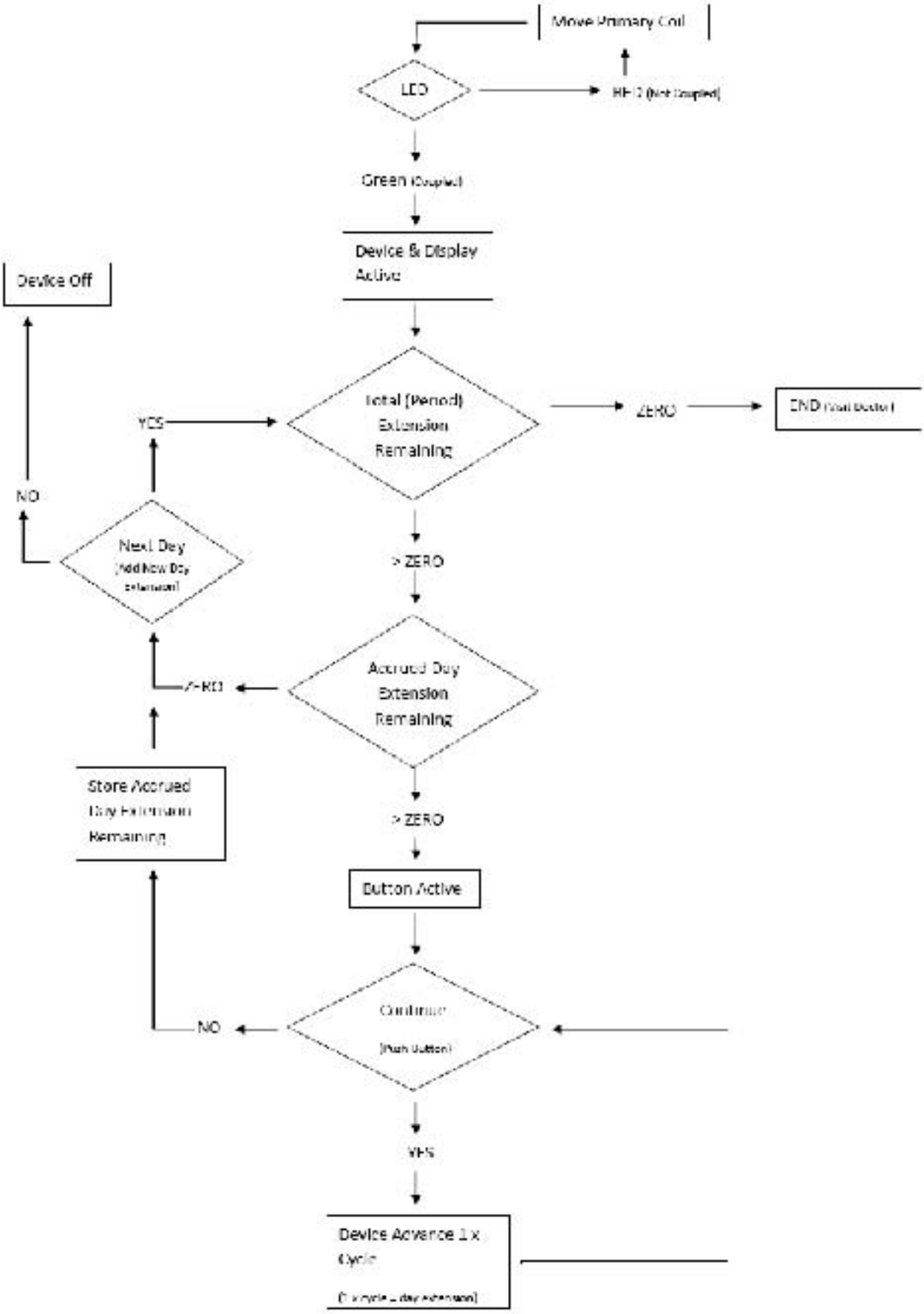

Figure 30: Flow Diagram of Device Control logic

4.8. Extension

It is clear from the study of in-vivo distraction forces by *Meswania et al (1998)* (Section 4.4.1) that minor extensions coupled with tissue relaxation results in significantly lower tissue tension and stiffening. Ideally, the rate of extension of the endoprosthesis should be reduced to mimic the natural rate of growth as realistically as possible. Such a progressive and slow rate of extension would result in no damage to tissues through distraction.

In the case of current devices, extension procedures are carried out periodically with relatively large extensions, 6 mm at six month intervals (Stanmore Mark V). Ideally, in an effort to reduce the resulting strain on muscles and tissues, growth should be matched to that of a normal femur, carrying out minute extensions at high frequency (daily). This extension would be achieved in a similar fashion to previous and current devices available using a screw mechanism; rotational motion converted into linear translation.

Based on the data collected by *Anderson et al (1963)* (Section 2.2), the approximate daily growth rates, and therefore the ideal extension rates for the femur and tibia, have been calculated, shown in Figure 32 and Figure 33 respectively. Growth rates shown are the approximate distal or proximal growth rates and are based on the growth rate of the combined epiphyses. It can be seen that the maximum growth rate required is approximately 30 µm per day.

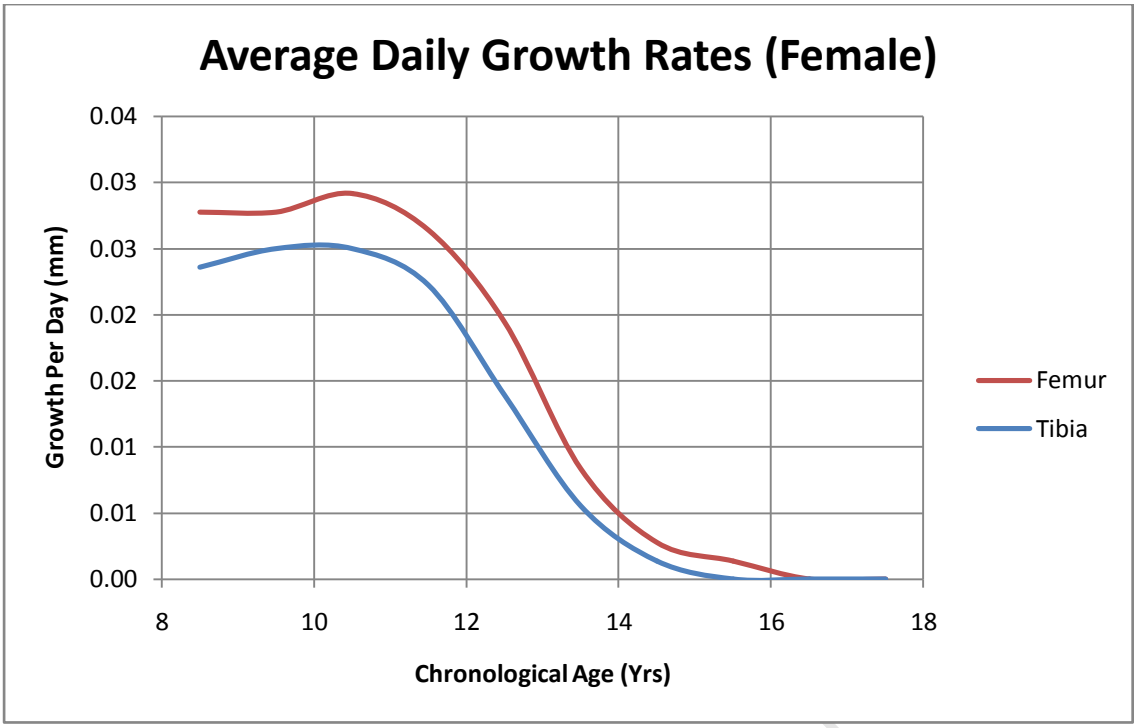

Figure 32: Comparison of male/female daily growth rates (Femoral)

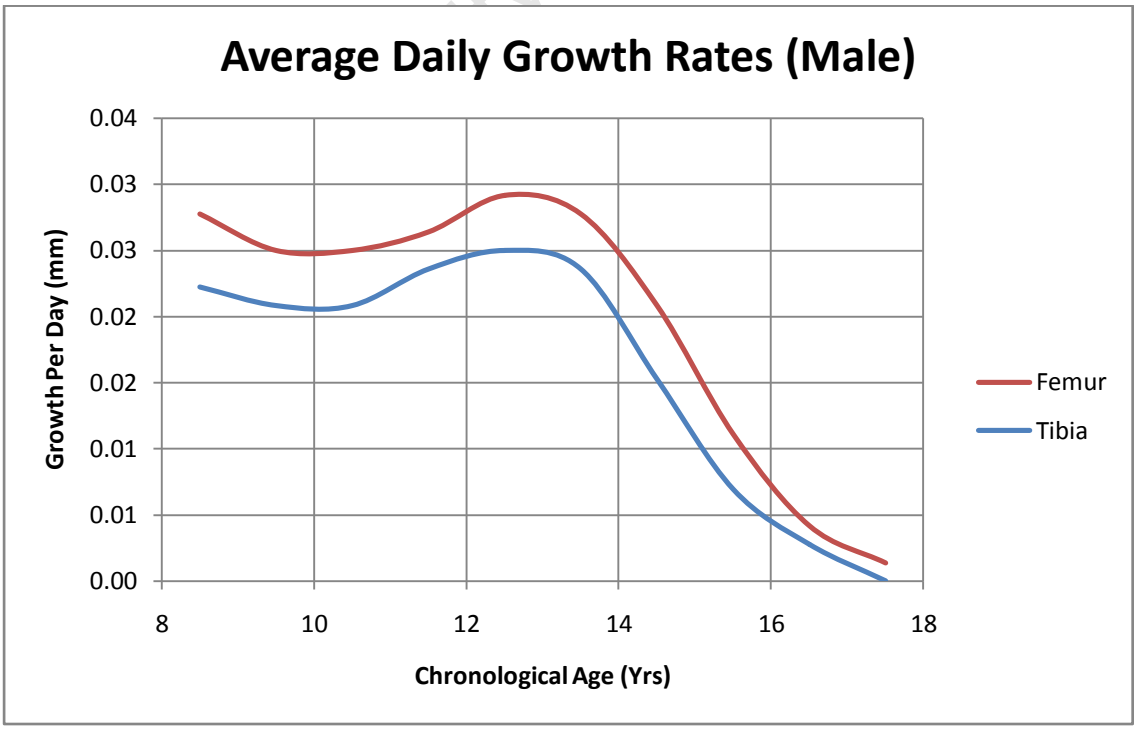

Figure 33: Comparison of male/female daily growth rates (Tibial)

4.9. Sealing

The intended location of the endoprosthesis will result in the device being continuously bathed in bodily fluids. At this stage of the design, both the motor and gearbox are not of custom design and, as such, are likely to contain biologically incompatible materials that cannot come into contact with the surrounding tissues and bodily fluids. In addition, the components used in the electronic control circuitry make use of materials that are similarly incompatible with the body. As such, all components of the device must be completely sealed to prevent ingress of body fluids.

5. Prototype Development

5.1. Summary of Device Specifications

Table 5: Summary of device specifications

Category	Details		
	Specification	Value	Units
Dimensions	Diameter	28.1	mm
	Length	< 170	mm
Distraction Load	Linear Force (max)	800	N
Functional Load	Axial	3.09	BW
	Antero-Posterior Moment	9.5	BWcm
	Medio-Lateral Moment	6.7	BWcm
	Torsion	1.3	BWcm
Material	Endoprosthesis	Ti6Al4V	-
	Seals	UHMWPE	-
	Motor	As supplied	
	Gearbox	As supplied	
Operation	Non-Invasive, wireless power and control	-	-
Life Span		5 yrs	
Extension	Possible Extension	70	mm
Ingress Protection	IP	68	

5.2. Extension

The extension mechanism is required to:

- Convert rotational motion to linear, and develop a longitudinal change in the dimensions of the endoprosthesis
- Act as a structural component of the endoprosthesis enduring distraction and functional loading
- Develop the linear force required for extension of the limb

Developing extension through the use of a power screw allows for conversion of rotational motion to linear, additionally gearing the forces. The required telescopic extension of the endoprosthesis is to be achieved through rotation of an externally threaded shaft (drive shaft) contained within a matching internally threaded tube (extension shaft) whose rotation is prevented by set screws located in a further tube surrounding the power screw (cover shaft), thus converting the rotational power of the drive shaft into linear movement of the extension shaft. The power screw mechanism is shown in Figure 34, and is to be fabricated from medical grade titanium (Ti6Al4V). The end of the extension shaft (highlighted in Figure 34) is required to accommodate a threaded piston shaft used during the experimental phase of the device development. This indicated region of the prosthesis will be revised to accommodate components required for bone interface (which is outside the scope of this dissertation).

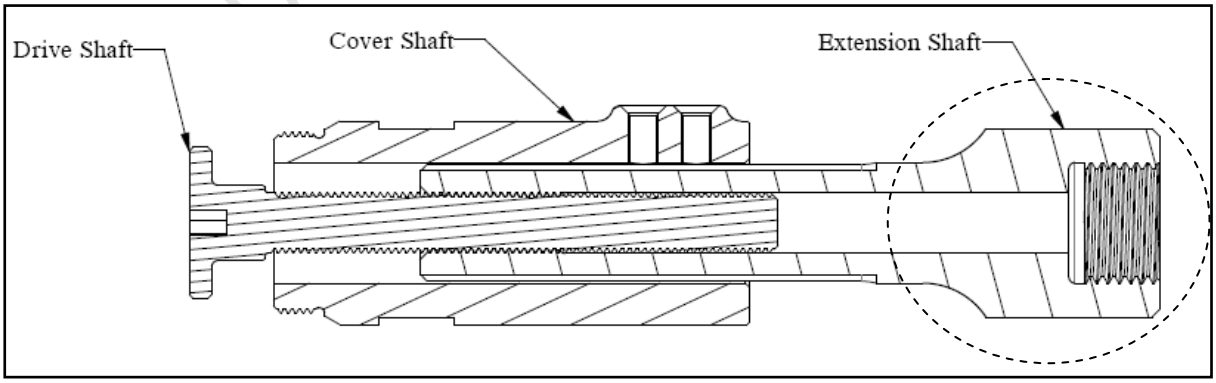

Figure 34: Power screw mechanism

The power screw is required to endure the stresses resulting from both distraction and functional loading (Section 4.4.1 and 4.4.2 respectively), while occupying the least amount of space (Section 4.2). The distraction and functional forces are not intended to occur simultaneously as the patient is intended to be in a relaxed position during extension procedures. In both loading scenarios, the forces used in modelling the stresses in the device are based on those experienced by the femur, greatest of all the Long bones. A design capable of withstanding such loading would therefore be more than adequate for replacement of the tibia and / or humerus.

The threads considered include:

Table 6: Drive shaft considered threads

Thread*	Nominal Diameter (mm)	Thread Pitch (mm)	Mean Diameter (mm)	Minor Diameter (mm)	Lead (mm)
M6	6	1	5.5	5	1
M8	8	1	7.5	7	1
M10	10	1.25	9.375	8.75	1.25
M12	12	1.25	11.375	10.75	1.25

*All threads considered are self locking, Appendix E-1

The linear force required to overcome the resistance of muscle and tissue, and develop extension has been described in Section 4.4.1 for extensions ranging from 1-6 mm. The average required distraction forces at 0 mm and 6 mm extensions are indicated on the graph in Figure 35 together with the power screw input torque and corresponding linear force output for all threads in Table 6. The torque required, as indicated on the graph,

includes that required to overcome friction of the drive shaft collar that facilitates axial location (indicated in Figure 34).

The output linear force of the power screw was calculated according to the following formulae (Shigley, Mischke & Budynas n.d.), detailed in Appendix E-2 and E-3.

$$Input\ Torque = T_R + T_c$$

$$T_R = \left(\frac{F d_m}{2}\right)\left(\frac{l + \pi f d_m}{\pi d_m - f l}\right)$$

$$T_c = \frac{F f_c d_c}{2}$$

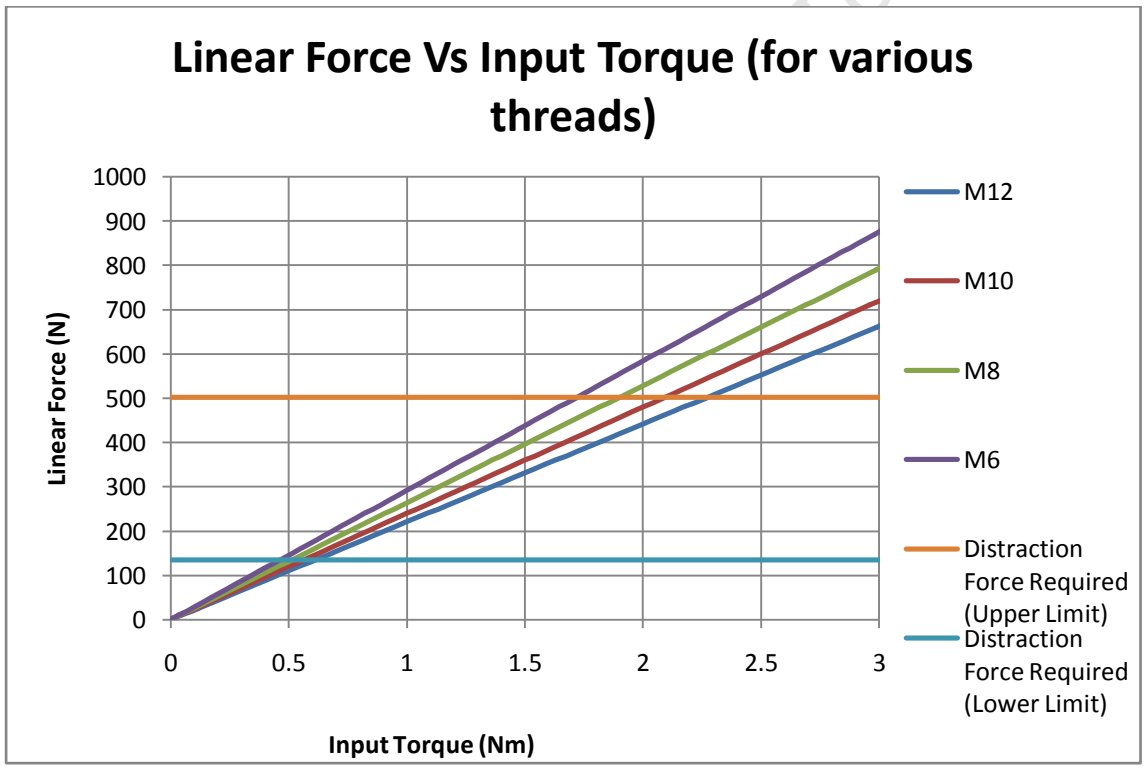

Figure 35: Power screw linear force vs. input torque for various threads

All threads considered are capable of overcoming collar friction and generating the linear force necessary for a 6 mm extension with an input torque <2.5 Nm. Based on the data presented in the graph, the M6x1 thread is the most suitable, offering the greatest mechanical advantage as well as smallest diameter. However, in addition to extending the

endoprosthesis, the threaded drive shaft must be sufficiently sized to avoid the possibility of fatigue.

In the process of extending the femur, the resistance from muscles and soft tissues increases with the magnitude of extension. This, coupled with the stress due to the torque required for extension, results in complex stresses on the threads, which must be resisted. Similarly, thread stresses arise due to the axial forces experienced during various activities such as walking, jogging etc (max 3.5 BW). Figure 36 indicates the thread root stress developed as a result of axial loading, taking into account the torque required to develop the same axial force and overcome the friction of the drive shaft collar.

The thread root stress was calculated according to the following formula (Shigley, Mischke & Budynas n.d.), detailed in Appendix E-4.

$$\sigma' = \frac{1}{\sqrt{2}}\left((\sigma_x - \sigma_y)^2 + (\sigma_y - \sigma_z)^2 + (\sigma_z - \sigma_x)^2 + 6(\tau_{xy}^2 + \tau_{yz}^2 + \tau_{zx}^2)\right)^{1/2}$$

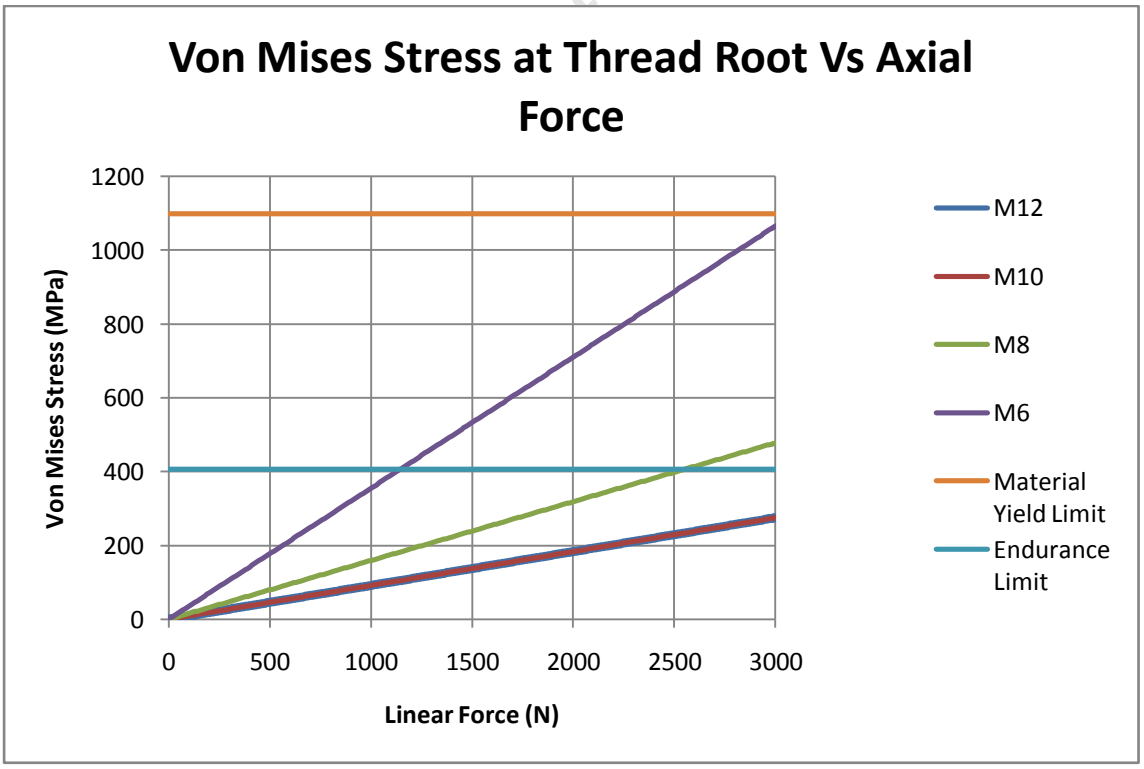

Figure 36: Thread root stress vs. axial force

The peak axial force experienced during distraction (avg 500 N, max 1500 N (Section 4.4.1)) is considerably lower than the maximum expected during functional activities such as jogging (max 2400 N for a 70 kg individual). It can be seen from the graph above that with an axial load of 2400 N, the resulting M6x1 thread stresses are in excess of the material endurance limit and, as such, susceptible to fatigue failure. The same axial force applied to an M8x1 thread results in a thread stress of approximately 380 MPa, below the material endurance limit. As such an M8x1 thread is the most suitable for the endoprosthesis, providing sufficient mechanical advantage for extension and withstanding the maximum expected axial load without fatigue, based on reasonable activity (participation in active sports is rare for patients with endoprostheses (Grimer 2005)).

The designed M8x1 threaded drive shaft, cover shaft and extension shaft are shown in Appendix D-1-10, D-1-12 and D-1-13 respectively. A brass prototype of the extension mechanism was developed to test concept prior to machining titanium.

5.3. Drive Unit

The drive unit is required to:

- Develop the necessary torque required to overcome the distraction loads of soft tissue and generate an extension of 6 mm (approximately 2 Nm for M8x1 thread, Section 5.1)

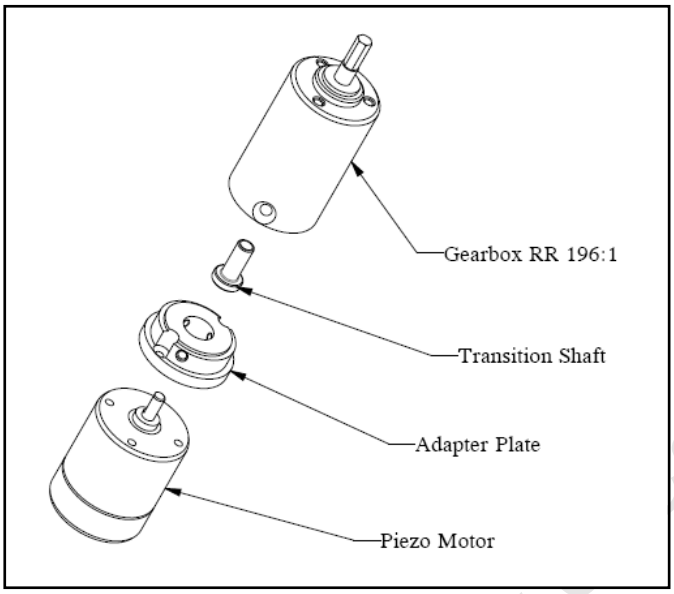

Figure 37: Drive unit (Exploded View)

5.3.1. Motor

In order to ultimately achieve an endoprosthesis compatible with MRI, the motor used in the device must not contain ferromagnetic materials. Piezo motors are an ideal choice to ensure MRI compatibility, containing no ferromagnetic material. Rotation is achieved by sequentially activating radially spaced piezo crystals, in contrast to the magnetic field interaction of more commonly used stepper motors.

The choice of motor is further limited by the space available for the endoprosthesis. Of the various piezo motors investigated, two are suitably sized to meet the dimension

requirements of the device (ϕ 28.1 mm, Section 4.2). The relevant properties of the two motors are shown in Table 7.

Table 7: Piezo motor options

	Dimensions (mm)	Stall Torque (mNm)	Holding Torque (mNm)
DTI Piezo Motor #PMLL-18R	Φ20 x 28	22	40
Piezo Motor Piezo Legs R01S-12	Φ23 x 27	80	90

It can be seen from the table above that difference in dimensions is negligible compared to that of the stall/holding torque. In light of this, the Piezo Legs motor is the ideal choice for use in the extendible endoprosthesis.

The characteristics of the Piezo Legs R01S-12 motor supplied by Piezo Motor Gmbh are shown below (Figure 38), specifications shown in Appendix C-2.

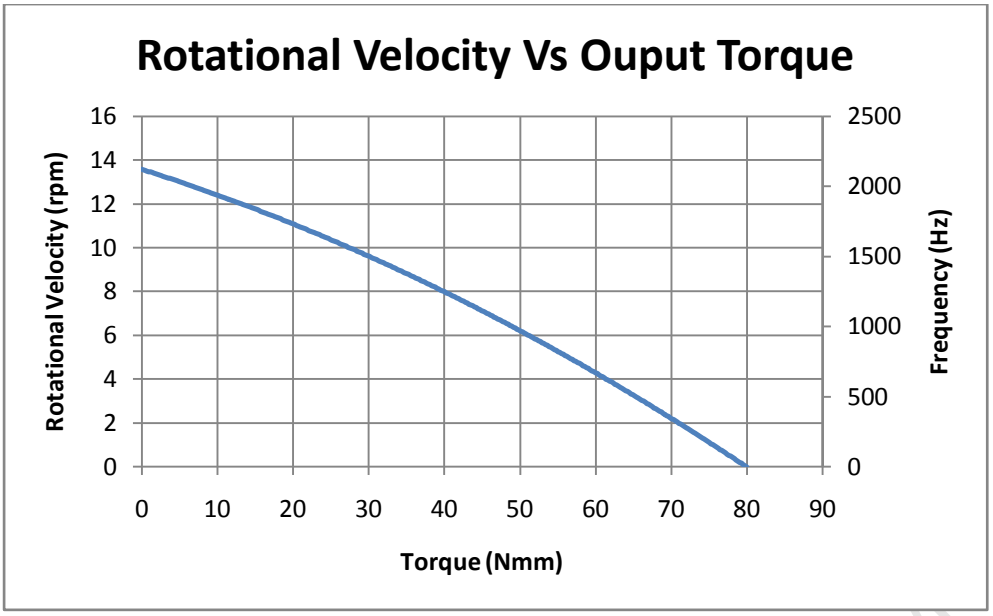

Figure 38: Piezo legs rotary motor characteristics

The drive shaft requires an input torque of >2 Nm to perform an extension of 6 mm (Section 5.1). The operating torque of the piezo motor alone is insufficient to develop the necessary axial force required for extension, requiring further increasing the torque.

5.3.2. Gearbox

In order to increase the output torque of the drive unit, the output torque of the motor must be geared. Again, dimensions are a constraint on the gearbox. Wittenstein Cybermotor Gmbh manufactures suitable sized and rated gearboxes for the task, a three-stage planetary gearbox GCP 022, available in Reduction Ratios (RR) of 64:1, 112:1 and 196:1 and rated to maximum torque of 3 Nm (Appendix C-1). All RR options make use of the three stages and as such the dimensions of the gearbox are unaffected (Appendix D-1-6). The gearbox output torque versus input torque is shown in Figure 39.

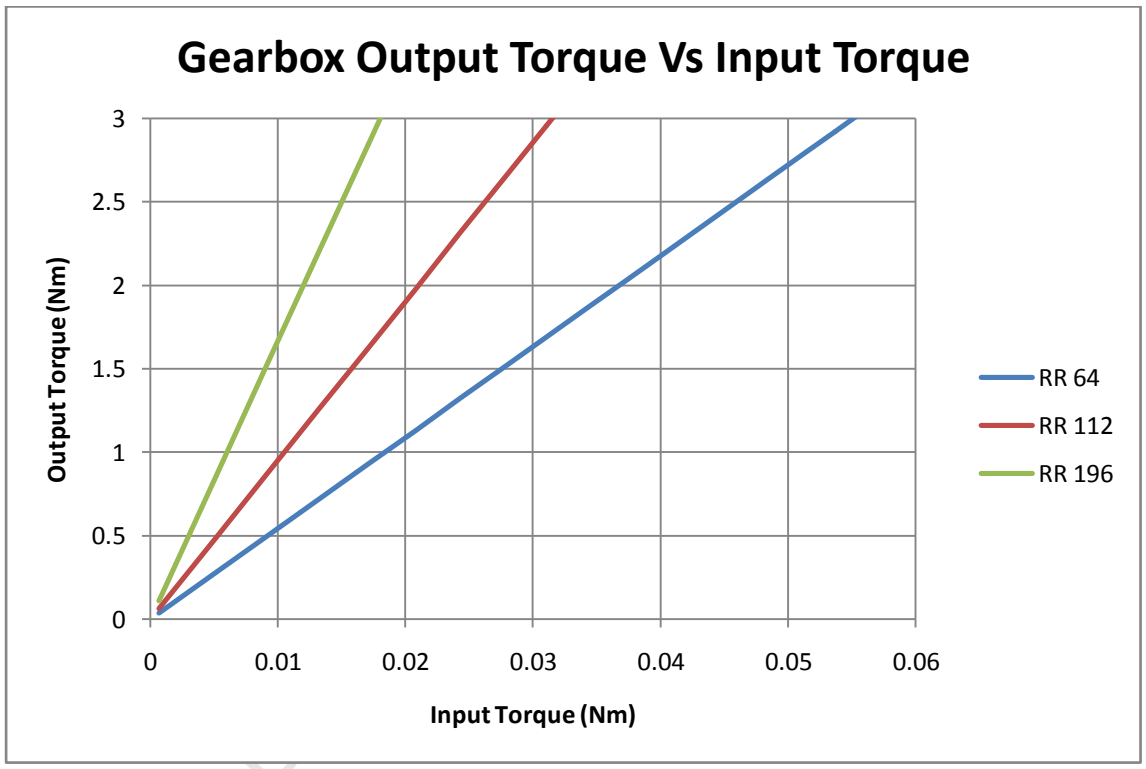

Figure 39: Gearbox output torque vs. input torque

Any of the three gearboxes shown in the Figure 39 is capable of generating the rated maximum torque of 3 Nm when coupled with the piezo motor output torque of up to 80 Nmm (0.08 Nm). An input torque of 3 Nm to the screw mechanism yields an extension force of approximately 800 N (Figure 35).

Figure 40 shows the extension rate of the endoprosthesis based on a drive unit consisting of the piezo motor and the RR196 gearbox.

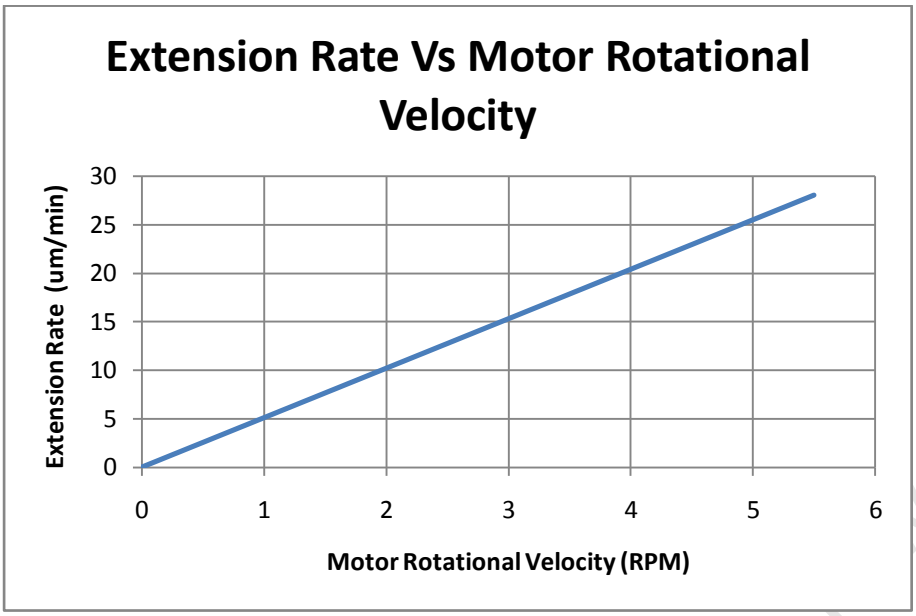

Figure 40: Extension rate vs. Piezo motor rotation velocity

5.3.3. Transition Shaft

As supplied, the piezo motor and gearbox connections were incompatible. The output of the piezo motor was a smooth shaft of smaller diameter than the gearbox input hole, and as such, a transition piece was required.

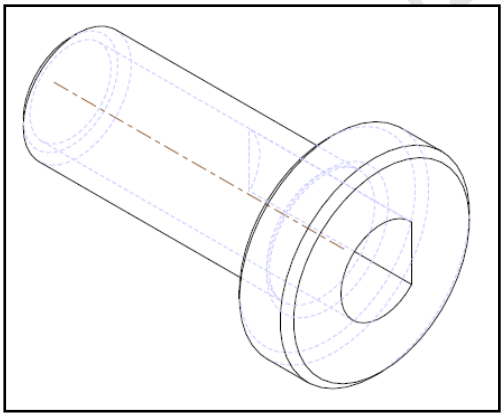

Figure 41: Transition shaft

The transition shaft (Appendix D-1-5) shown in Figure 41 was developed to facilitate connection and torque transfer between the motor and gearbox. In order to ensure efficient transfer of torque and prevent slip, a single flat was machined on the output shaft of the

piezo motor (Appendix D-1-3). Connection between the transition shaft and motor is facilitated by a corresponding internal single flat. Connection to the gearbox is achieved by an interference fit between the transition shaft and gearbox input smooth hole.

5.3.4. Drive Unit Casing

The drive unit casing (Appendix D-1-7) shown below in Figure 42 is required to house and isolate the drive unit (Figure 37) from the surrounding body fluid and tissues.

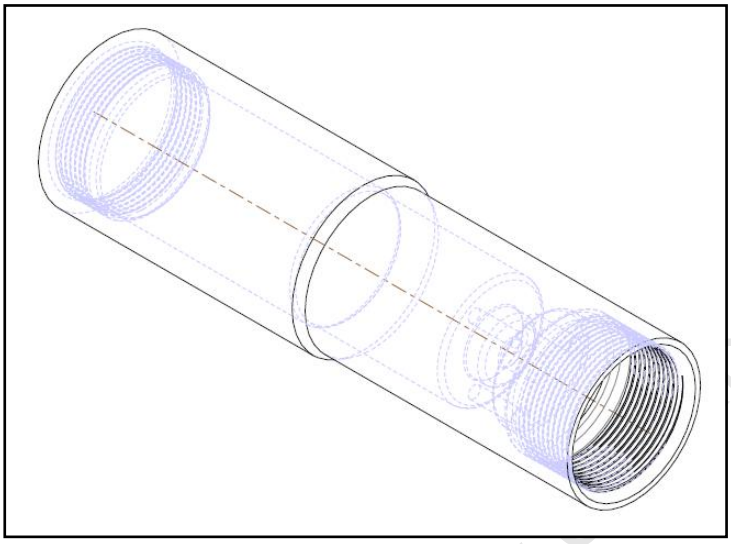

Figure 42: Drive unit casing

5.1. Functional Stress Analysis

The endoprosthesis is required to withstand the typical stresses experienced by a femur during normal activities, including walking, ascending and descending stairs as well as jogging.

The irregular shape of the endoprosthetic device results in different developed stress for the same loading and requires that it be separated into sections in which the material stresses can be calculated; 12 different sections shown in Figure 43, and cross-sectional areas in Figure 44. The distraction and functional loads are considered separately as extension procedures are to be carried out in the absence of functional loads.

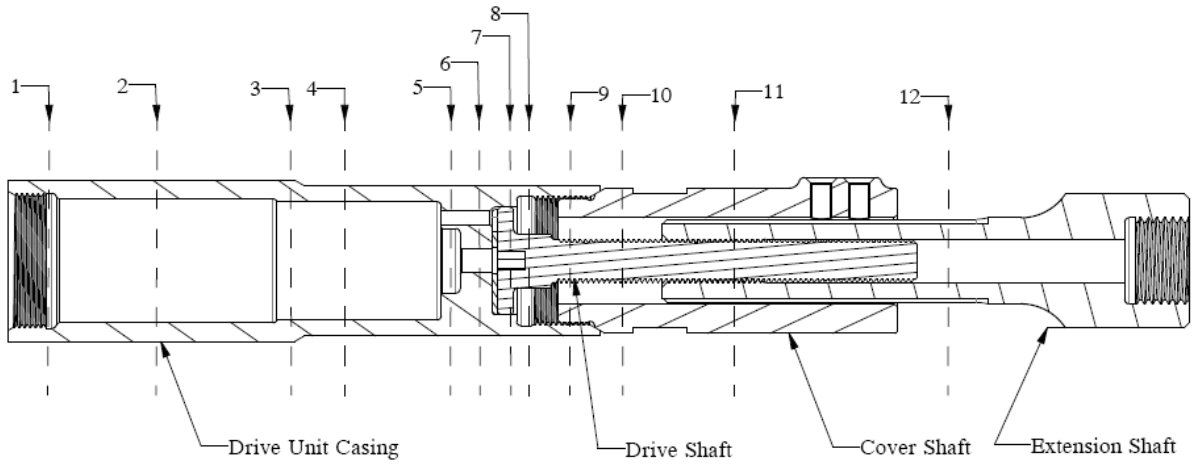

Figure 43: Indication of section locations

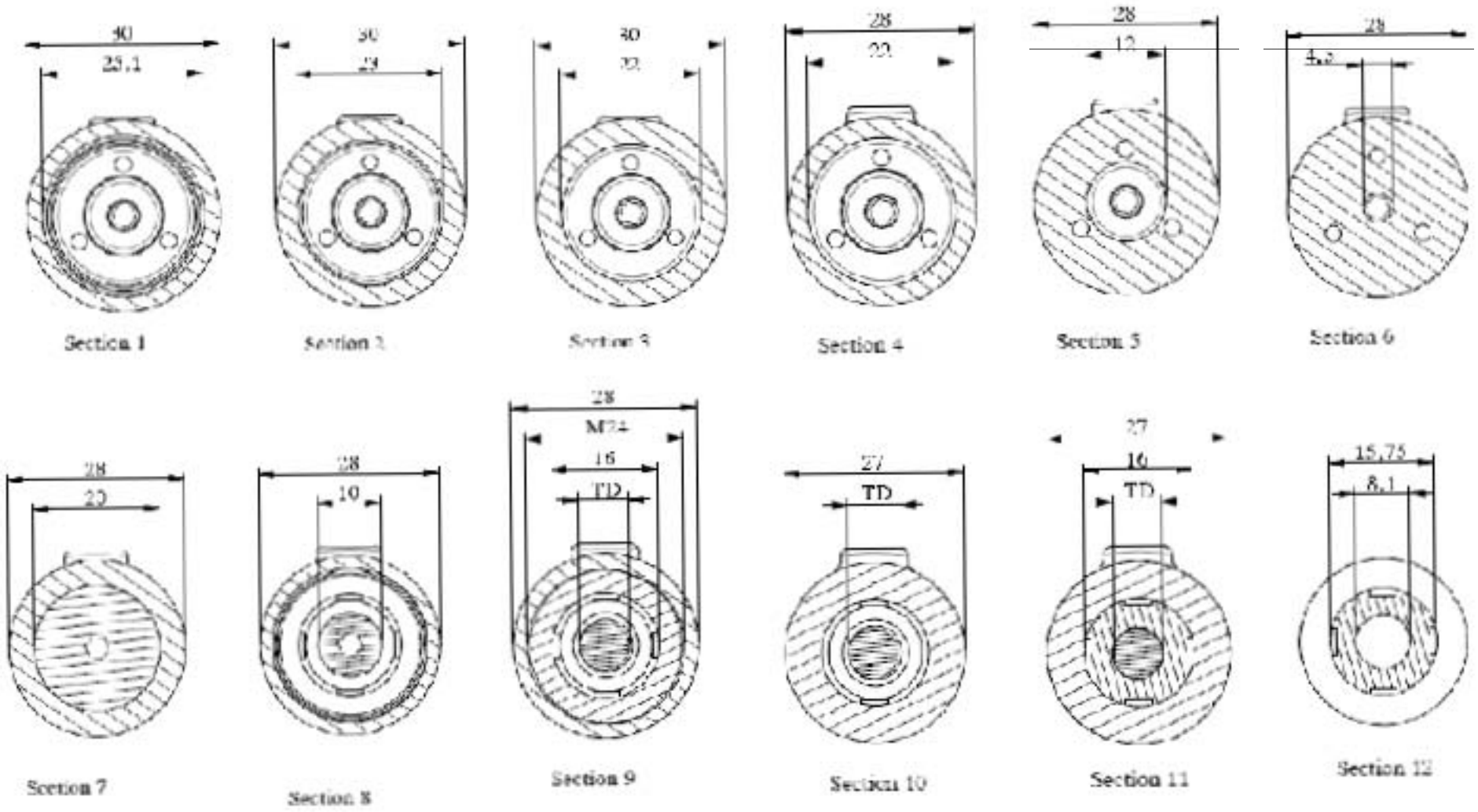

Figure 44: Cross-sectional areas of endoprosthesis

Functional loading (as captured by *Taylor et al (2001)* of the femur results in a peak net moment on the femur during jogging (11.5 BWcm), and a peak torsional moment during stair descent (1.3 BWcm); Section 4.4.2. Based on this loading (for a 70 kg individual, Appendix A-5), the stresses in each of the 12 different cross sections are calculated to ensure that failure by fatigue is avoided, Figure 45.

Stresses are calculated according to the formula (Shigley, Mischke & Budynas n.d.) below, detailed in Appendix E-5.

$$\sigma_1 = \frac{\sigma_x + \sigma_y}{2} + \sqrt{\left(\frac{\sigma_x + \sigma_y}{2}\right)^2 + \tau_{xy}^2}$$

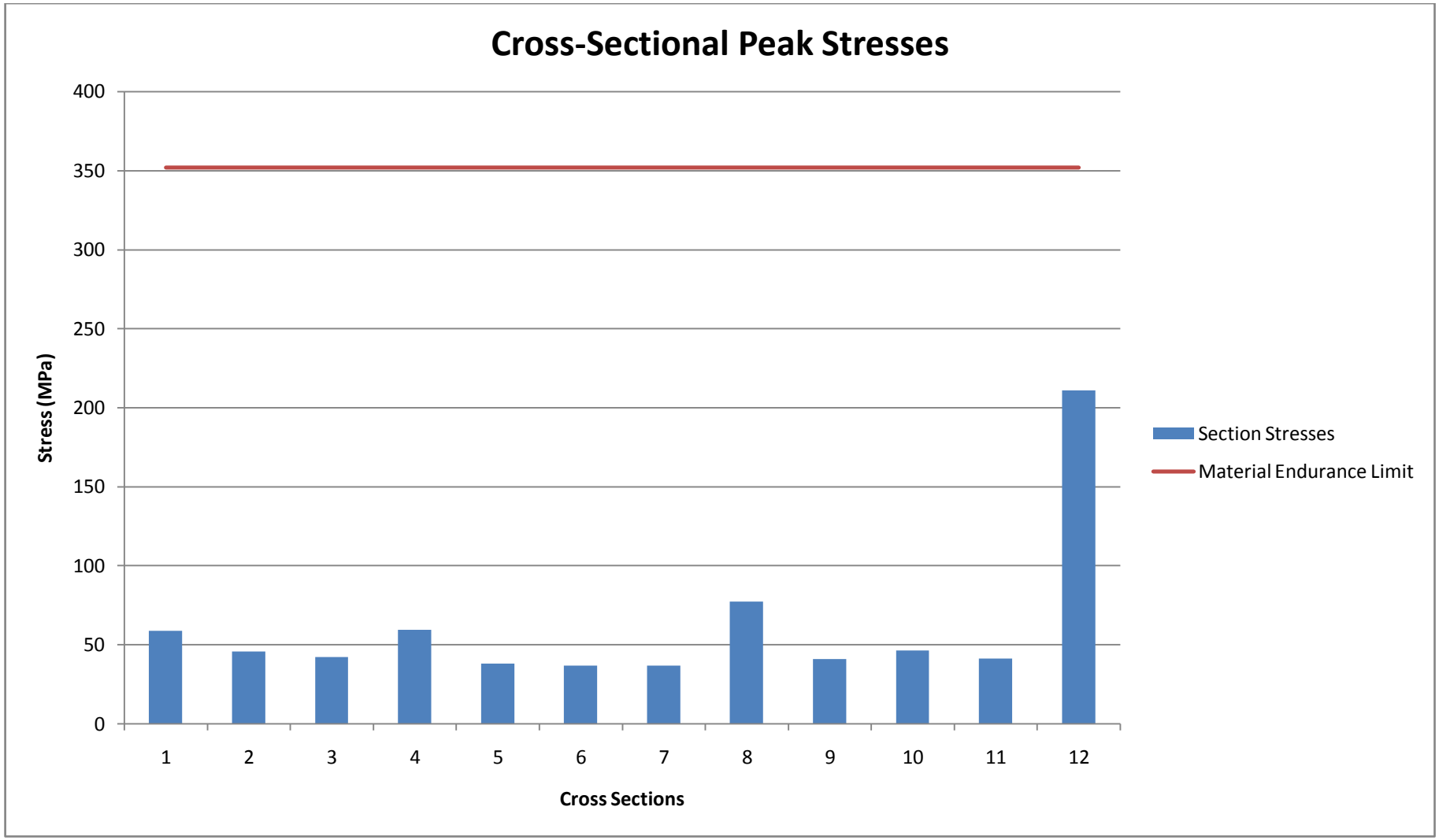

Figure 45: Endoprosthesis material stress due to functional loading for a 70 kg individual

It can be seen that all 12 sections experience stresses far below the fatigue strength of medical grade titanium (approx. 350 MPa, Appendix A-2 Table 21) and as such both static and fatigue failure are unlikely. The overall device exhibits a minimum safety factor of 1.6, section 12.

5.2. Power, Control and Feedback (Vicatos, Ginsberg & Parsons 2011)

The electronic system is required to:

- Couple motor drive energy through the patient's skin
- Generate signals suitable for motor operation (steps)
- Monitor motor rotation
- Permit programming by medical personnel
- Optionally allow for in-vivo data capture
- Withstand conditions associated with standard medical procedures including sterilisation and diagnostics.

This electronic system can be separated into three distinct categories: Internal, External, and Program (allowing configuration).

5.2.1. Internal

Contained within the extendible endoprosthesis and implanted in the patient are a motor, motor drive circuit, power-receiving coil and regulation circuit, the power for which is supplied through inductance from a coil outside the patients' body across the skin.

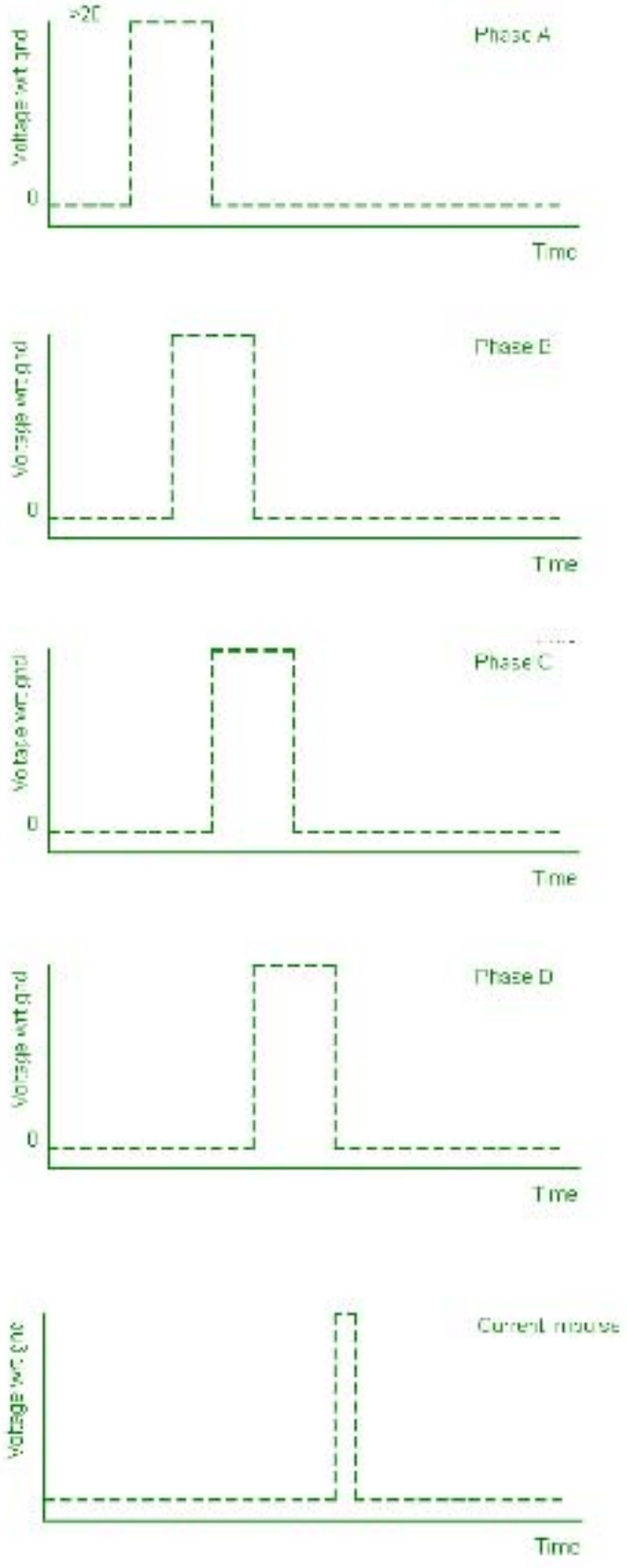

Figure 46: Phased drive signals (A-D) and impulse

Shown in Figure 46, are the phased electrical signals required to cause rotation of the motor. Repeatedly supplied to the motor, these signals (phase A-D) generate rotation of the motor output shaft.

In order to monitor the motor rotation, a current impulse is drawn from the motor drives' power supply within the body which similarly causes a current impulse to be drawn from the external power supply. Monitoring the power consumption, the current impulses indicate the completion of the four 'steps' taken by the motor (corresponding to the four phases). The current impulse occurs shortly after the completion of Phase D pulse, also shown in Figure 46.

Some of the materials contained within the motor and gearbox, together with the circuit components are likely to cause inflammatory responses due to bio-incompatibility. This resulted in the endoprosthesis being designed in such a way so as to isolate these parts, avoiding all contact with body fluids and in turn limiting the possible sterilisation methods to Gamma. The need to withstand ionizing radiation means that conventional microcontroller technology cannot be used as radiation damages the contents of many memory types including Flash and EEPROM. Additionally, the circuit components for internal placement must be as small as possible. In order to comply with these requirements, the circuit was approached differently, resulting in a hard-wired circuit for control rather than a program controlled one (shown in Appendix D-3).

An alternating current is generated in the receiving coil (charge coil), implanted immediately beneath the patients' skin, when coupled with the external power coil. This current is converted to direct current and the energy is briefly stored within capacitors. When a voltage sufficient to successfully turn the motor is reached, a voltage 'pulse' is generated. The four phases of the motor are then activated successively through time delay circuits. The final time delay circuit in the cascade results in the drawing of a current impulse from the charge coil, causing the capacitors to discharge. It is this current impulse which provides the feedback for monitoring of rotation. Following the current impulse, the capacitors begin charging again and the process repeats and the waveforms indicated in figure are generated as long as the charge coil is affected by a suitable alternating magnetic field.

Further enhancement of the extendible endoprosthesis is achievable through the attachment of strain gauges to the titanium body, measuring extension force as well as functional loads. With the resulting data being transmitted across the skin, either by conventional radio techniques or through coded patterns of current impulses (similar to that of rotation monitoring).

5.2.2. External

Using an Ergo case (B7015209 – See Appendix D-4), shown in Figure 47, to house the external electronics, the unit can be strapped to the patient, the case curvature providing a snug fit with the limb.

Figure 47: ERGO Case

This close contact with the skin ensures the supply of an alternating magnetic field to the internal charge coil below the skin. The circuitry within this unit allows for monitoring of the internally generated current impulse, measuring the number of steps taken by the motor. There is no limit on the circuit components, as in the case of the internal electronics, because sterilisation of the unit is not required due to it being housed external to the patient. The circuitry operates according to the flow chart shown in Figure 31, Section 4.7. A block diagram of the external system is shown in Figure 48 below.

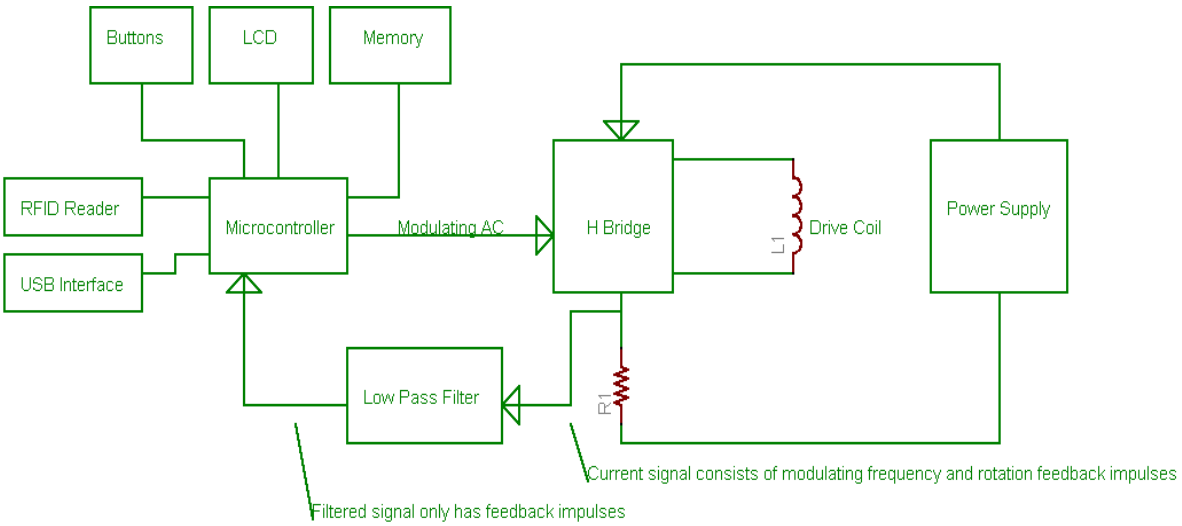

Figure 48: Block diagram of external electronic system

The use of a microcontroller within the external unit allows for computer interface, typically USB. Various parameters can then be transferred to the unit and stored in memory, such as the total extension required over a given period, as well as limits on daily extensions. Each extension operation results in a count down on the total extension programmed, indicated to the user on an LCD mounted on the case (Figure 49).

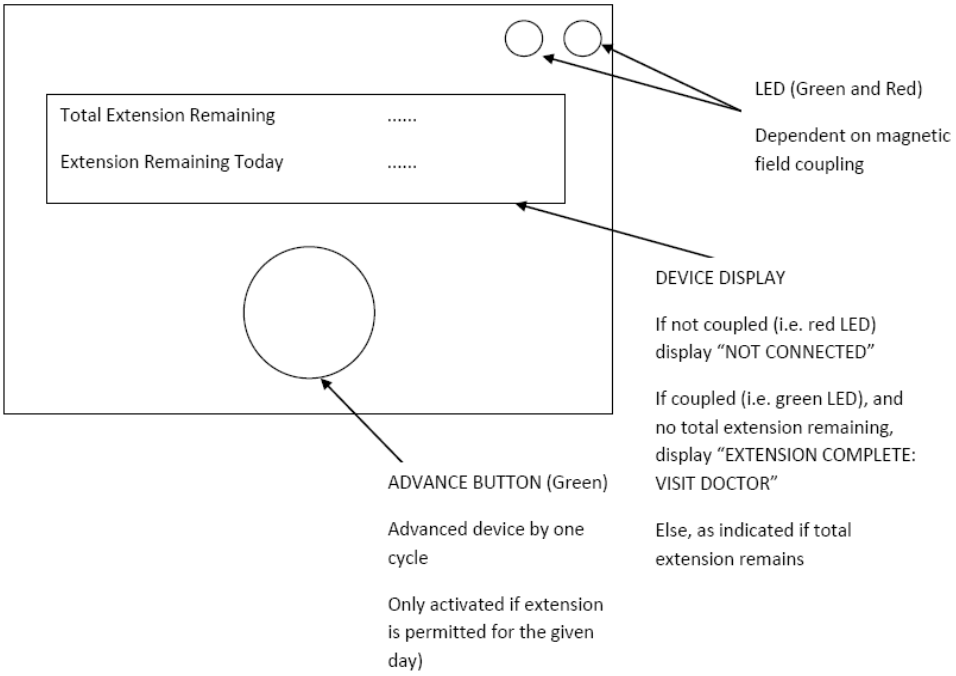

Figure 49: ERGO case extension interface

LEDs present on the face of the ERGO case indicate coupling between the external drive coil and internal charge coil, failing which extension is not permitted. A single button on the unit allows the patient to begin an extension operation within the limits of the pre-programmed parameters. In the event that coupling is lost, the unit stores the amount of extension carried out and updates the remaining for the programmed period. An optional RFID reader allows for the unit to paired with and identify a specific endoprosthesis, ensuring the correct device is being extended.

The drive frequency is selected to be in the 100 kHz to 1 MHz range, avoiding the ionizing and thermal range of frequencies that would be harmful to the patient.

5.2.3. Program

Medical personnel will be required to program the device (external control unit) by entering the amount of extension required and time frame into a computer based application, an example of which is shown in Figure 50 below. Having set extension parameters, the settings could be transferred to the control unit via USB or similar.

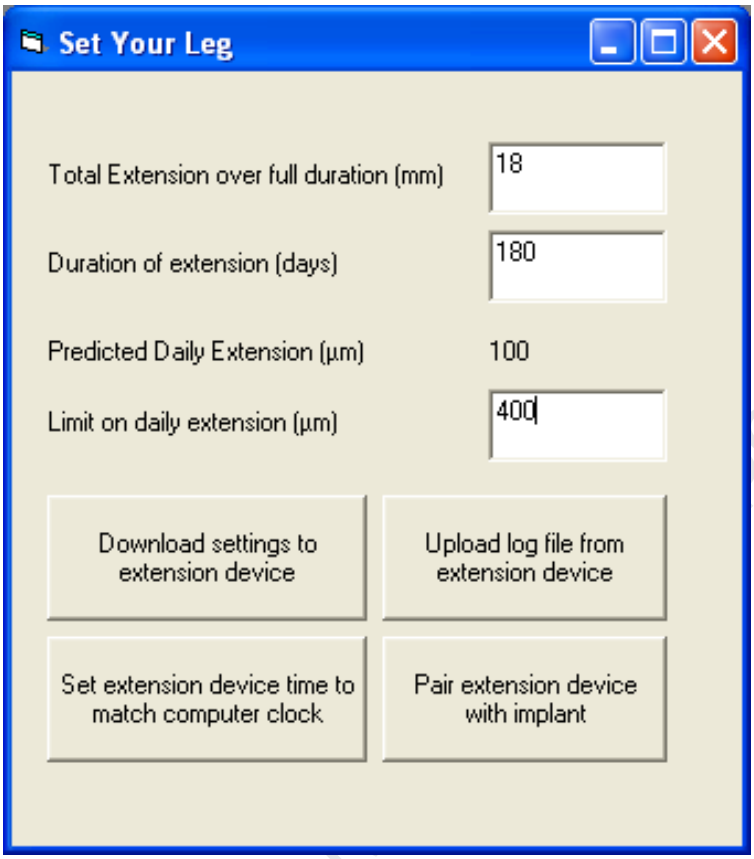

Figure 50: Screenshot of program interface

5.3. Sealing

In order to prevent contact of body tissue and fluids with the gearbox, motor and drive electronics, sealing is required at three points, namely drive shaft, power cable and prosthetic joint connection.

The seal between the extension module and the attaching prosthetic joint is outside the scope of this dissertation however, for the purposes of testing, this seal was modelled with an M24x1 threaded plug, as shown in Appendix D-1-2. This could be reduced to a standard Morse taper without the thread for attachment to a prosthetic joint.

The wall of the drive unit casing is too thin to accommodate an effective means of sealing the electrical cable connecting the receiving coil under the skin and drive circuitry within the device.

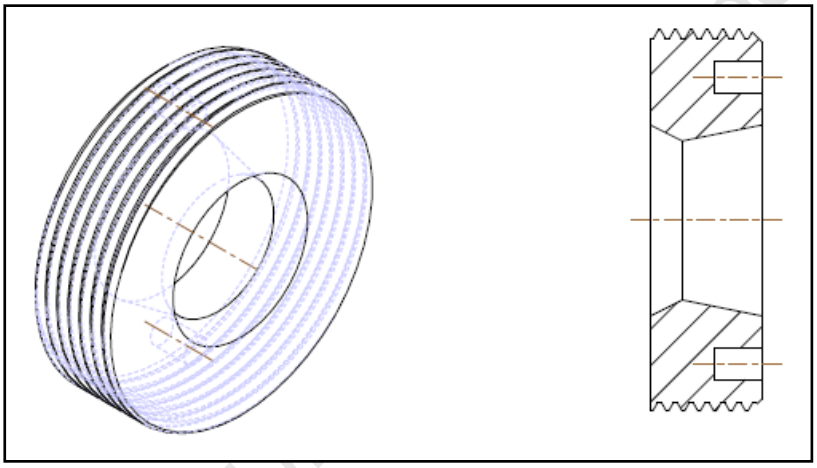

Figure 51: UHMWPE seal

The UHMWPE drive shaft seal is above in Figure 51. The circumference of the seal is threaded, M24x1 (tight thread) and seals against the corresponding internal thread of the drive unit casing. A central hole through the seal is required for the drive shaft. Sealing at this point is achieved by a tolerance on both the drive shaft seal surface and seal central hole to generate an interference fit and still allow for rotation of the drive shaft. A more detailed drawing of the location of the seal can be seen in Appendix D-1-2.

5.4. Sterilisation

The standard motor and gearbox provided by Piezo Motor and Wittenstein respectively, together with the custom drive electronics, contain biomedically incompatible materials and as such cannot come into contact with body tissue and or fluid. This requirement resulted in the development of seals to prevent this contact (Section 5.3). Effective sealing of the internal components presents difficulties to the sterilisation process, preventing the permeation of sterilising gases involved with autoclaving and ethylene oxide. As a result the only effective means of sterilisation is through gamma exposure.

The materials chosen for the design of the endoprosthesis were based on their compatibility with gamma radiation however, the components required for drive and operation of the endoprosthesis were supplied as standard from manufacturers. The materials that make up the gearbox were disclosed by Wittenstein and are deemed gamma compatible with the exception of a polymer gear stage used, which could diminish the life span of the gearbox. The required operating lifespan of the gearbox is minimal compared to that predicted for a gearbox not exposed to gamma and, as such, the effect of gamma radiation can be considered negligible. Piezo Motor Gmbh is unwilling to disclose the nature of the components within the motor and hence the resistance to gamma ray exposure is unknown and must be investigated.

5.5. Test Rig

In addition to the design of the device itself, it was also necessary to design and fabricate a test rig (Figure 52 and Appendix D-2) for the device in order to test the linear force output of the device.

The linear force of the endoprosthesis is measured by means of pressure change in a hydraulic cylinder. Attachment of the endoprosthesis to the hydraulic cylinder is facilitated by the internal thread at the end of the extension shaft which corresponds to that on the hydraulic cylinder. In order to ensure that the linear force of the device was transferred to the cylinder, backing plates were placed behind both the device and the cylinder. Additionally, to ensure axial alignment of the device and cylinder, a support/ guide plate is required for the device.

6. Results

6.1. Linear Force

The test rig shown in Appendix D-2 was set up and the experiment carried out according to Appendix B-1. This experiment was necessary to confirm the predicted capacity for linear extension, developing the necessary forces required to extend a typical femur, overcoming the tension of muscles and tendons. It was envisaged that the device would be capable of generating sufficient force to develop an extension of up to 6 mm, accommodating both regular daily extension as well as periodic extension similar to that of the Stanmore Mark V (Section 3.5).

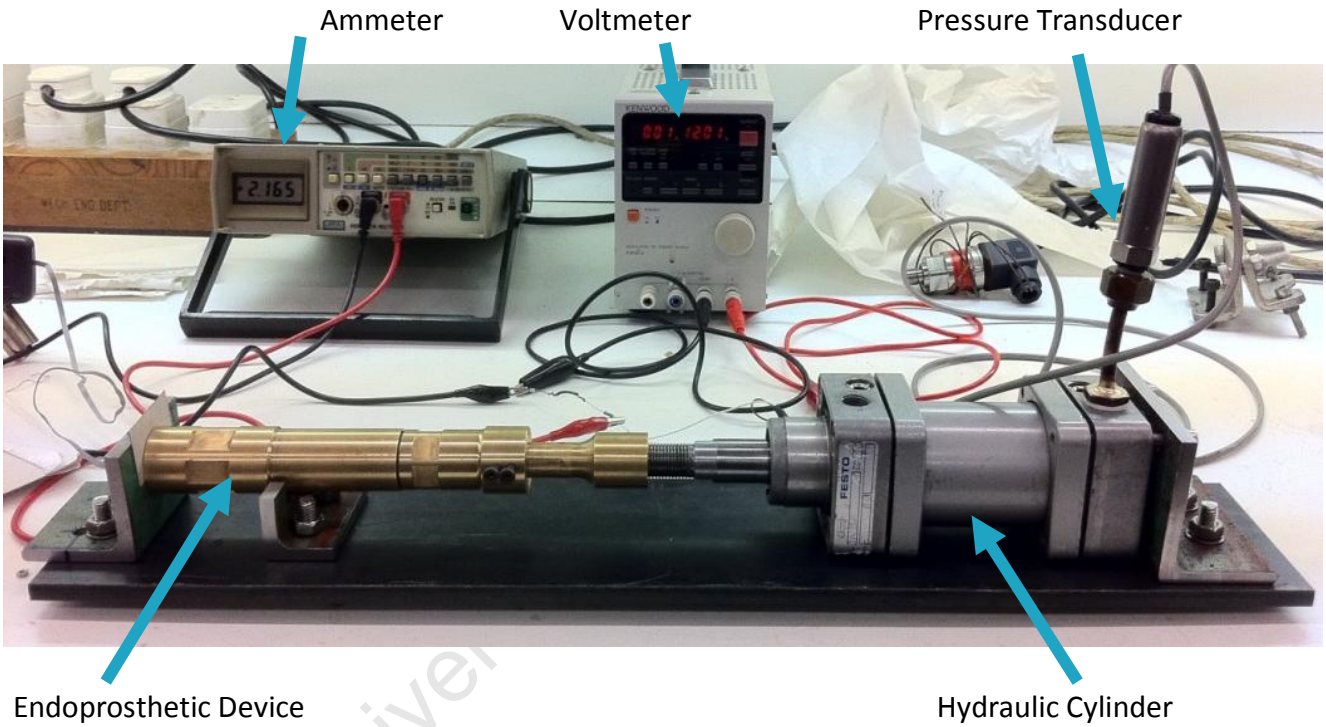

Figure 52: Linear force experiment apparatus

The linear force test was carried out on the brass prototype excluding the UHMWPE seal, shown together with the testing apparatus in Figure 52. The results of this initial test are shown in the graph below (Figure 53). The force was calculated based on the pressure change in a hydraulic cylinder (sampled at 5 minute intervals) and, as can be expected, the linear force versus operating time increases exponentially due to the incompressibility (bulk modulus) of the hydraulic fluid. The maximum distraction force for this experiment was limited to 40 kg (390 N) due to the material limits of brass. It can be seen that the linear force reached the maximum 40 kg for this experiment. This result is congruent with the predicted capabilities of the device.

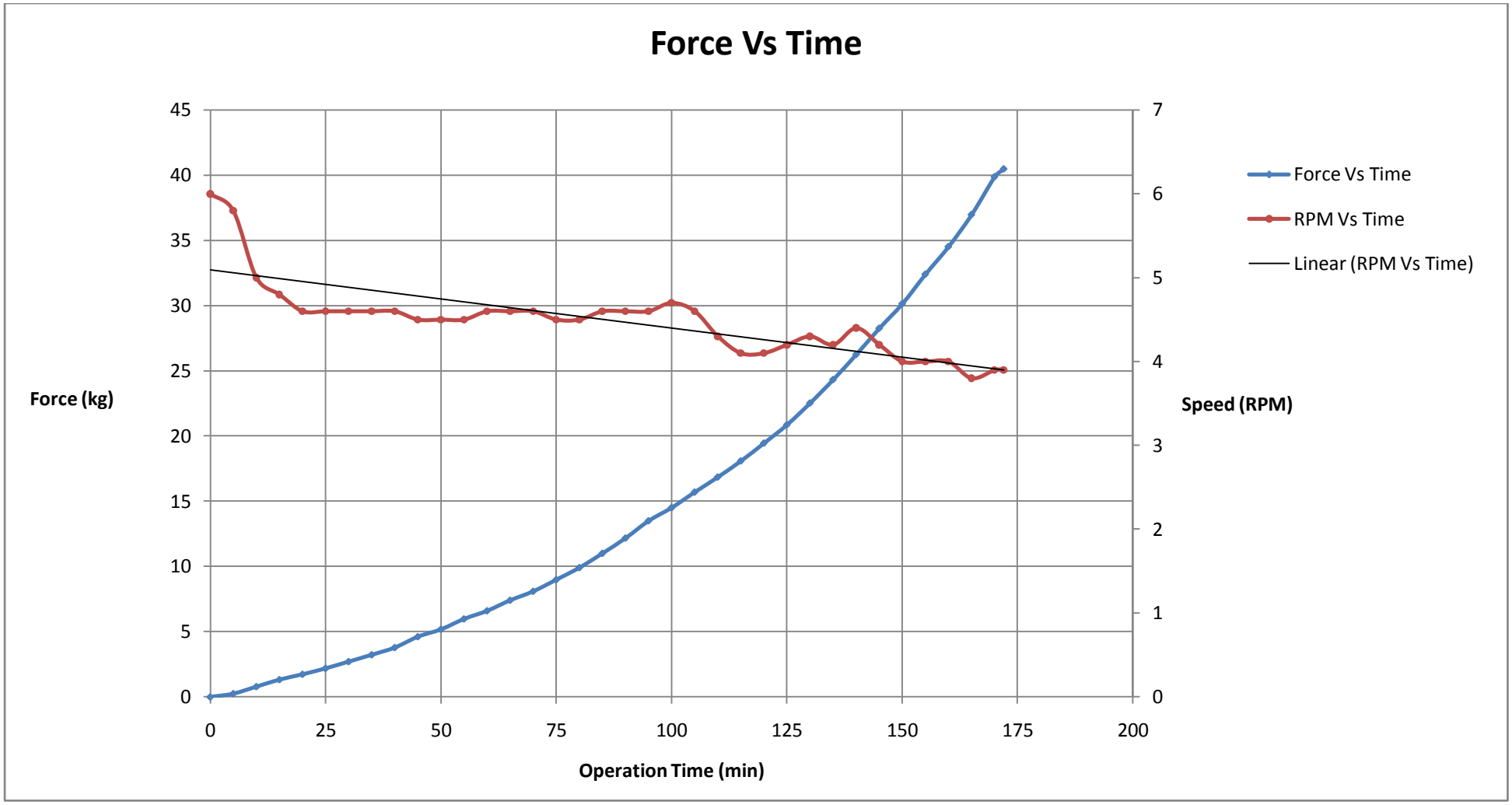

Figure 53: Results of linear force test

The rotational velocity of the piezo motor was recorded throughout the experiment and also sampled at five minute intervals together with the pressure readings. The RPM of the motor was measured visually, marking a point on the motor and timing a revolution. The variation of the motor RPM versus experiment time is shown the graph. It is noted that the RPM of the motor decreases linearly with time and/or device linear force. A further experiment (Appendix B-2) was developed to investigate this observation, and establish whether it was a result of strain on the motor, or merely a characteristic of the motor.

The linear force test on the device was repeated on the brass prototype, including the drive shaft seal. The results of which are shown in the graph below (Figure 54). A preload was applied to the device and the force tracked over a shorter period compared to the initial test. It can be seen from the graph that the results compare closely with those of the test without a seal (Figure 55). However, it can be seen that the motor rotational velocity does not compare similarly across both tests. This is attributed to the fact that the period for the test without a seal is significantly shorter than that with the seal, indicating that the motor speed varies over time and not due to strain, although this observation was investigated further, Section 6.2.

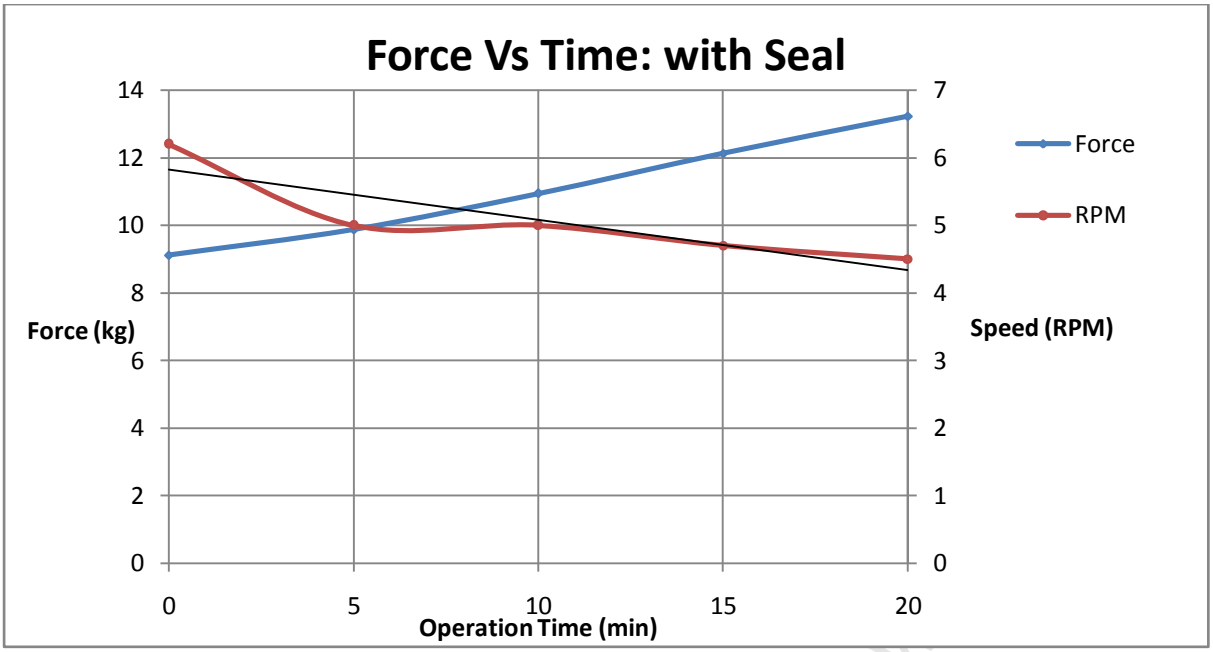

Figure 54: Linear force testing with UHMWPE seal

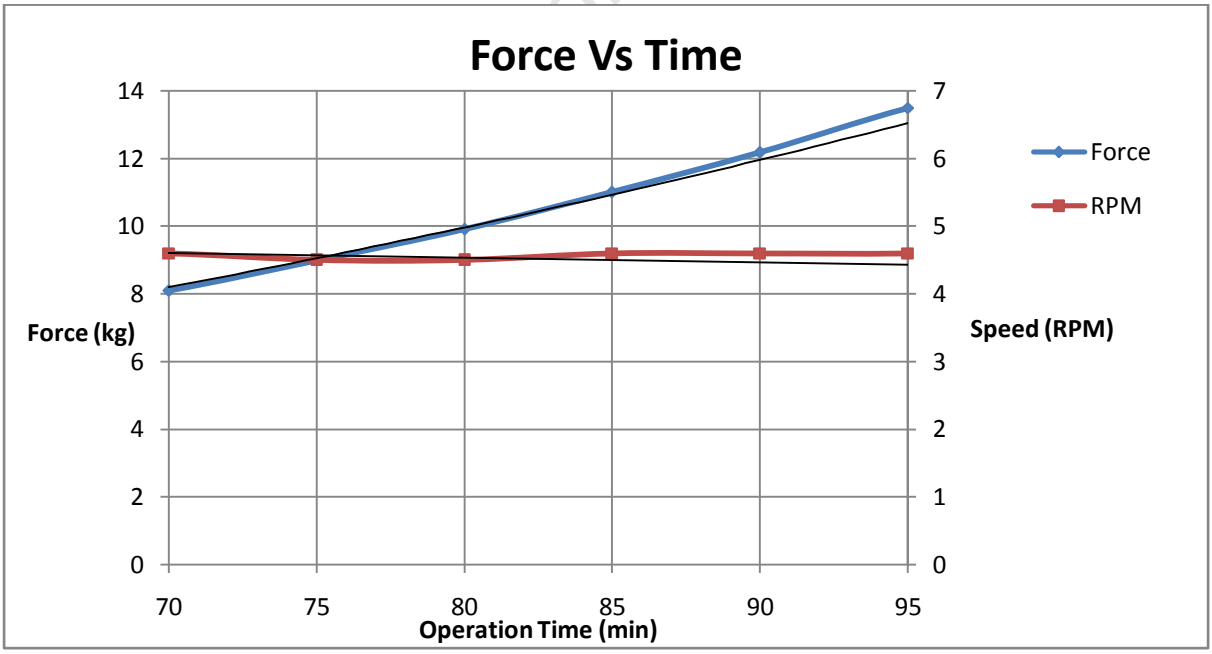

Figure 55: Linear force test without UHMWPE seal

Following the successful results of linear force testing, the growth module mechanism was fabricated in medical grade titanium (Ti6Al4V), shown in Figure 56.

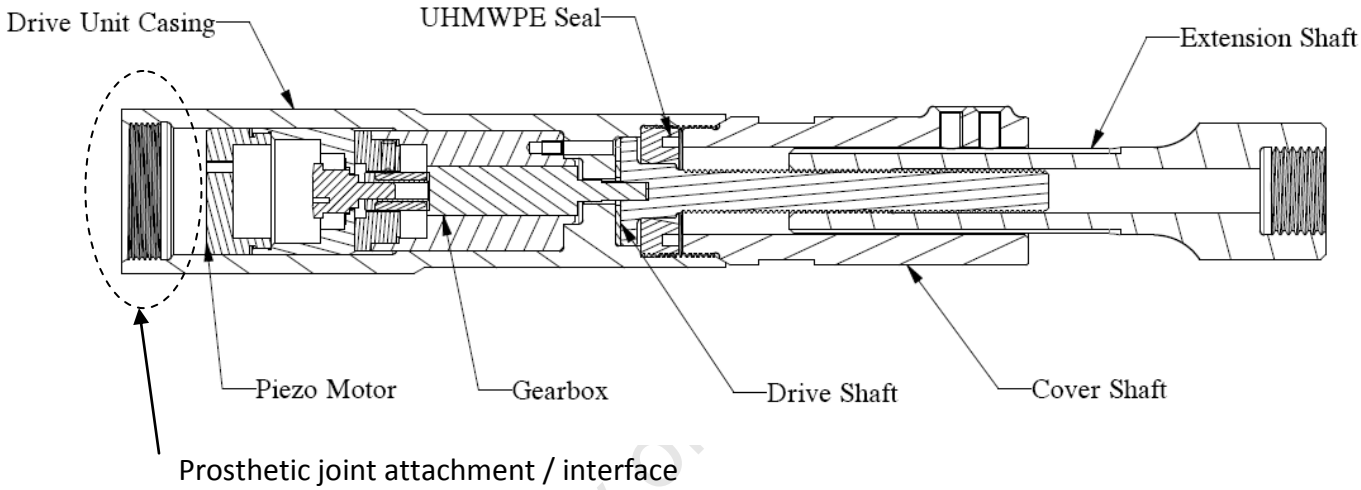

Figure 56: The trial titanium endoprosthetic growth module mechanism

6.2. Piezo Motor Rotational Velocity

Observation from the linear force experiments indicated that the motor RPM and the device linear force expressed an inverse relationship. Monitoring of extension is achieved through the electronic control circuitry of the motor, sending a pulse back on completion of one revolution irrespective of time. Although a decrease in rotational velocity has not effect on the operation, it was necessary to assess whether this was a characteristic of the motor or a result of strain due to the increasing loads which could mean that the motor would eventually seize. In order to examine this more closely, the piezo motor was operated alone, without any external loads on the output. The results of this experiment are shown below (Figure 57).

The graph shows that the motor RPM decreases over time, tending toward a constant. This observation is similar to that observed in the linear force experiment (Section 6.1.) It is noted that in the absence of a motor load, the settled RPM of the motor is greater than that of the initial experiment. It is therefore apparent that the loading has an influence on the RPM of the motor, although this influence is not large and is unlikely to cause seizure of the motor.

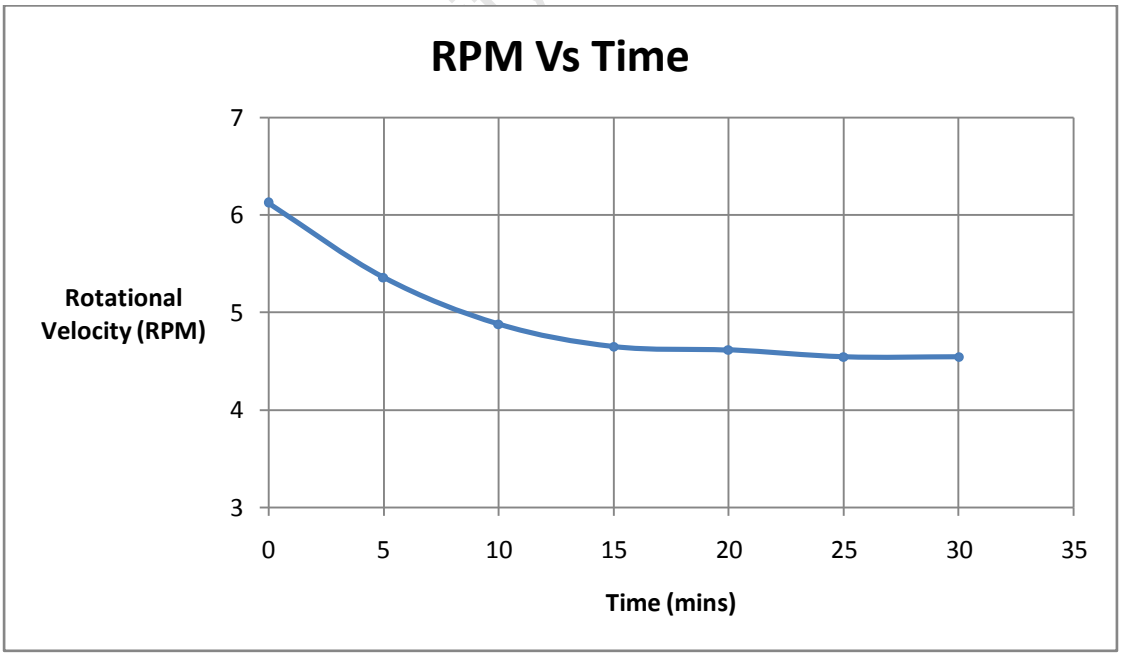

Figure 57: Piezo motor speed characteristics at no-load conditions

6.3. Seal Testing

6.3.1. Sealing

The UHMWPE seal on the drive shaft is required to prevent the passage of bodily fluid, as contact with the biologically incompatible materials of the drive unit could result in a negative physiological response.

Seal testing was carried out according to the experiment outlined in Appendix B-4. No fluid was seen to pass through the seal after a period of 48 hours under periodic rotation and flexing of the drive shaft.

6.3.2. Frictional Torque

In addition to frictional losses in the thread of the drive shaft, the drive unit must also generate torque to overcome the friction due to the UHMWPE seal. The investigation into the magnitude of this torque was carried out according to Appendix B-5.

The device was assembled as shown in Figure 58, without the extension shaft and drive unit, allowing the drive shaft to rotate relative to the drive unit casing and cover shaft. The end of the drive shaft was clamped in a fixed position, and a mass attached to a screw extending from the cover shaft. The mass moment arm was varied until the drive unit casing and extension shaft rotated relative to the drive shaft, indicating that the frictional torque of the seal was overcome.

The frictional torque of the seal was found to be between 28 and 36 Nmm (Appendix A-1-3), and as such has negligible influence on the linear output force of the extension mechanism.

Figure 58: Seal friction testing

6.4. Inductive Power Transfer

The driving circuit provided by Piezo Motor SE, designed to operate the piezo motor, generates a sinusoidal output for driving the motor's piezo crystals. Changing the drive signal to a square wave resulted in a significant space saving on the circuit board which was required due to the limited space available. As such it was necessary to establish whether a square wave could in fact drive the motor. Following correspondence with the manufacturer in confirming the operation of the motor under a square wave input, it was necessary to investigate the potential for inductive power transfer across biological tissue.

Cow muscle tissue was used (cow shank) for testing of inductive coupling. The receiving and transmitting coils were placed on either side of a section of muscle tissue (Figure 59). The thickness of the tissue was gradually reduced until power transfer was achieved, approximately 10 mm. The drive frequency was maintained at 130 kHz, and as such there were no thermal effects on the muscle tissue.

Figure 59: Wireless power transfer across tissue

6.5. Gamma Testing

Gamma radiation is the expected method of sterilisation for the device and as such, the effects of this radiation on electronic components needed to be tested (Irradiation Certificate shown in Appendix H-1).

6.5.1. Electronics

Of all the electronics used in the drive circuitry, the only components sensitive to gamma radiation were the op-amps. The original op-amps (series LM358) used in the prototype circuitry failed after 25 kGy radiation. Following this result, two alternative op-amp series were tested (MC33078 and LM833). After irradiation (25 kGy) the op-amps were operational, but required more power than previously. The results of the LM833 were deemed to be inconclusive as this series had failed in the first test with the LM358 series.

Based on the results of gamma irradiation, the op-amp chosen for the drive circuitry was the MC33078. The increased power demand of the op-amp is easily accommodated for in the power circuitry.

6.5.2. Piezo Motor

Following exposure to 25 kGy radiation, the piezo motor functioned normally.

6.6. MRI Testing

A piezo motor was chosen for the drive unit in an effort to develop an endoprosthetic extension module compatible with MRI imaging. In order to test this compatibility, the extension module was subjected to a 3 Tesla MRI. To model the implant conditions and achieve contrast with biological tissues, the device replaced a section of bone within a cow shank (tibia), shown in Figure 60.

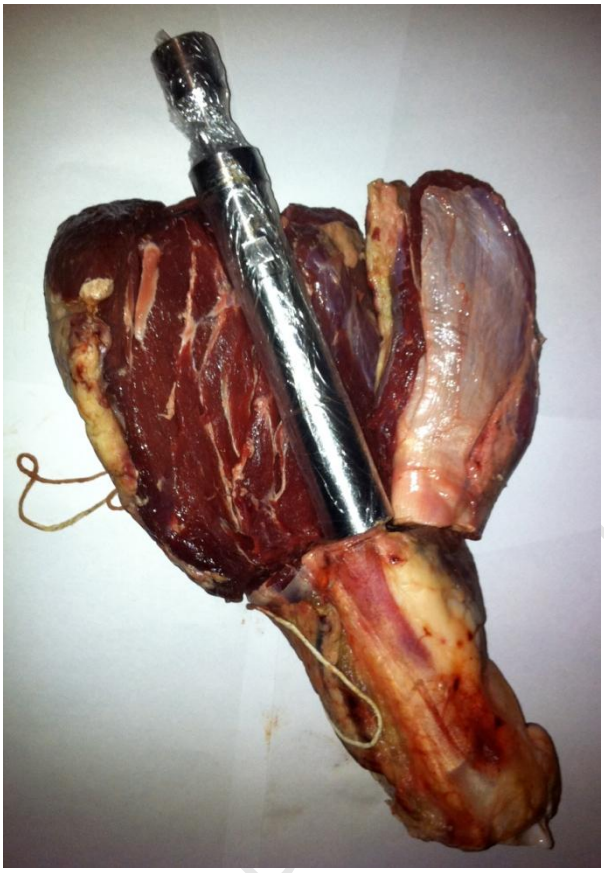

Figure 60: Endoprosthetic device implanted in cow shank

Figure 61 shows the image produced under MRI, a void exists along the length of the shank, corresponding to the location of the extension device. The ankle joint of the shank can be seen in the bottom of the image. The 3 Tesla MRI produced a dark shadow but no scatter artefacts as one would have expected from stainless steel parts. This result indicates that the current device is incompatible with MRI at 3 Tesla.

Figure 61: MRI image of extension module implanted in cow shank

7. Conclusion

A literature review of the progressive development of extendible endoprostheses was carried out, with specific focus on those designed by Stanmore Implants Worldwide. Stanmore designs were focused upon as the company has contributed to all categories of extendible endoprostheses including modular, minimally-invasive and non-invasive, the latest being the Mark V JTS, categorised as non-invasive. The JTS overcomes considerable disadvantages of earlier designs, specifically the need for surgically facilitated extension. Extension is achieved non-invasively by a rotating magnetic field external to the body, inducing the rotation of an internal magnet, driving a power screw. The ferromagnetic materials contained within the JTS drive mechanism make it incompatible with MRI, limiting the diagnostic techniques available for follow-up. While surgery is not necessary to extend the JTS, it requires a cumbersome coil apparatus to be operated by a physician. As a result, the extensions are only carried out periodically, requiring large extensions (approximately 6 mm at six months).

Based on the review of both past and currently available devices, areas for improvement were noted, specifically relating to frequency of extensions and MRI compatibility. This required the development of a new extendible endoprosthesis. Before the development of the new design, the requirements of such a device needed to be addressed. Crucial design requirements include device dimensions, biocompatibility, sterilisation, loading, drive (including powering and control), extension rate and sealing.

The overall length of the device limited to the typical tumour resection length of 115 mm (80-200 mm). Additionally, the maximum remaining femoral growth for an 8-year-old male patient is approximately 140 mm contributed by both the proximal and distal epiphyses, requiring that the device be capable of facilitating a maximum of approximately 100 mm (10-year old male distal femur, Section 4.2) of growth over the remaining period of growth. To provide this extension, the device must be capable of generating the linear force required to overcome muscle tension (avg. approximately 500 N at 6 mm). Additionally, the patient is expected to continue with typical activities such as walking, stair ascent and descent, as well as jogging. The extendible endoprosthesis must be capable of withstanding

the stresses resulting from these activities. The materials used for the device are limited to those that are biocompatible, as well as compatible with sterilisation techniques. Furthermore, the absence of ferromagnetic materials within the device allows for the use of MRI for follow-up assessment. Finally, the control, power and feedback of the drive mechanism were considered.

The designed extension mechanism includes a piezo motor containing no ferromagnetic material and generating a stall torque of 80 Nmm. The torque of the motor is stepped through a gearbox (RR 196:1) resulting in the gearbox maximum output torque of 3 Nm (Rated Gearbox Torque). An M8x1 threaded drive shaft connected to the gearbox output shaft was chosen for the drive shaft capable of developing the linear force of 500 N required for an extension of 6 mm with 2 Nm of torque. The functional length of the device is 95 mm, and the cover and extension shaft lengths may be varied to suit the patient, allowing for different overall extension lengths.

The drive unit for the device is powered and controlled wirelessly using inductive coupling across the patient's skin. A pulse is sent back from the motor after completing four phase pulses, activating the piezo crystals and turning the motor 4 µrad. In this way, the amount of extension achieved can be monitored. The external unit is designed to be pre-programmed, permitting the patient to carry out extension procedures at home with follow up visits with the physician scheduled periodically to assess progress. The ability to carry out extensions at home allows extensions to be carried out frequently (daily), achieving an extension rate similar to natural growth.

Several aspects of the design required testing, specifically linear force, sterilisation compatibility, MRI compatibility, seal testing, wireless power transfer and device control. The capacity for extension was investigated through force testing, using a test rig and hydraulic cylinder measuring the force pressure. Sterilisation of the device is limited to gamma radiation and, as such, the radiation effects on certain components of the drive and control circuitry was tested to ensure compatibility. Similarly, MRI testing was carried out to assess the effects of device components on imaging quality. Finally, seal testing was carried

out to ensure that no fluids entered the drive mechanism, coming into contact with biologically incompatible materials.

Linear force testing was carried out on the brass prototype, generating a 40kg extension force (limited due to material properties of brass), capable of effecting a 4 mm extension of the femur. The device has a predicted maximum extension force of approximately 800 N, and is capable of achieving extension > 6 mm under tissue resistance.

The designed UHMWPE seal proved effective, preventing the penetration of fluids into the drive unit casing while permitting rotation of the drive shaft. The sealing contact between the seal and the drive shaft results in friction. A torque of between 28 and 36 Nmm is required to overcome this friction, having a negligible effect on the linear output force of the device.

All electronic components used in the extendible endoprosthesis were operational following gamma irradiation (25kGy), confirming that the device is compatible with gamma sterilisation.

Imaging of the extendible endoprosthesis was not possible using a 3 Tesla MRI, as it gave inconclusive results.

The capacity for wireless power transfer was tested across muscle tissue. With a drive frequency of 130 kHz, transmission across approximately 10 mm of tissue was achieved without any thermal affects on the tissue. This result confirmed that the drive unit of the device can be powered wirelessly across the patient's skin.

Overall the designed device is an acceptable alternative to currently available extendible endoprosthesis. Added advantages to this device include the potential for MRI compatibility with little to no distortion effects, and the capacity for minor daily extension to be carried out in a home setting (reducing strain on surrounding muscle tissue).

Recommendations

- MRI testing was carried out using a very powerful 3 Tesla MRI, which may be the reason the device could not be resolved in the images. It is recommended that further MRI testing be carried out, as images of previously designed medical grade titanium endoprosthesis have been achieved, even with the presence of ferromagnetic materials.

- In the current design both the motor and gearbox were supplied as standard products from the manufacturer. It is recommended that these components be custom designed to exclude any ferromagnetic materials as well as to improve mechanical output and input connections to facilitate interface between the two.

- The electrical cable linking the subcutaneous power receiving coil and the drive electronics housed within the drive unit casing must be sealed to prevent tissue fluid entering the drive unit casing. The minimal wall thickness of the designed endoprosthesis cannot accommodate an effective mechanical seal. As such, it is recommended that the cable pass through the attaching prosthetic joint (Figure 56). The attaching joint would have sufficient material and space for cable sealing, alternatively, special biocompatible 'glue' material is needed to provide sealing between the cable and implant.

References

Anderson, M & Green, WT 1948, 'Lengths of the Femur and Tibia', *American Journal of Disease of Children*, vol 75, pp. 279 - 290.

Anderson, M, Green, WT & Messner, MB 1963, 'Growth and Prediction of Growth in the Lower Extremities', *Journal of Bone and Joint Surgery*, vol 45 , pp. 1 - 14.

Bigata, X, Ribera, M, Bielsa, I & Ferrandiz, C 2001, 'Adverse Granulomatous Reaction After Cosmetic Dermal Silicone Injection', *American Society for Dermatologic Surgery*, no. 27, pp. 198-200.

Board, CNE 2008, *Osteosarcoma - Childhood*, viewed 22 July 2009, <http://www.cancer.net/patient/Cancer+Types/Osteosarcoma+-+Childhood>.

Board, CNE 2009, *Tests and Procedures*, viewed 22 July 2009, <http://www.cancer.net/patient/All+About+Cancer/Newly+Diagnosed/Tests+and+Procedures>.

Bone: Histology of the growth plate, viewed 23 April 2009, <http://www.gla.ac.uk/ibls/US/fab/tutorial/generic/bone5.html>.

Cancer Imaging, viewed 21 July 2009, <http://imaging.cancer.gov/imaginginformation/cancerimaging>.

Cool, WP, Carter, SR, Grimer, RJ, Tillman, RM & Walker, PS 1997, 'Growth after Extendible Endoprosthetic Replacement of the Distal Femur', *The Journal of Bone and Joint Surgery*, vol 79 - B, no. 6, pp. 938 - 942.

Davis, JR 2003, 'Sterilization of Implants', in JR Davis (ed.), *Handbook of Materials for Medical Devices*, ASM International.

Delepine, G, Delepine, N, Desbois, JC & Goutallier, D 1998, 'Expanding Prostheses in Conservative Surgery for Lower Limb Sarcoma', *International Orthopaedics*, vol 22, no. 1, pp. 27 - 31.

Dominkus, M, Krepler, P, Schwamies, E, Windhager, R & Kotz, R 2001, 'Growth Prediction in Extendable Tumor Prostheses in Children', *Clinical Orthopaedics and Related Research*, no. 390, pp. 212 - 220.

Duda, GN, Schneider, E & Chao, EYS 1997, 'Internal Forces and Moments in the Femur During Walking', *Journal of Biomechanics*, vol 30, no. 9, pp. 993-941.

Eckardt, JJ, Safran, MR, Eilber, FR, Rosen, G & Kabo, JM 1993, 'Expandable Endoprosthetic Reconstruction of the Skeletally Immature After Malignant Bone Tumor Resection', *Clinical Orthopaedics and Related Research*, no. 297, pp. 188 - 202.

Grimer, RJ 2005, 'Surgical Options for Children with Osteosarcoma', *Lancet Oncology*, no. 6, pp. 85-92.

Grimer, RJ, Taminiau, AM & Cannon, SR 2002, 'Surgical Outcomes in Osteosarcoma', *Journal of Bone and Joint Surgery*, vol 84-B, no. 3, pp. 395-400.

Gupta, A, Meswania, J, Blunn, G, Cannon, SR & Briggs, TWR 2006, 'Stanmore Non-Invasive Growing Arthrodesis Endoprosthesis in the Reconstruction of Complicated Total Knee Arthroplasty: A Case Report', *The Knee*, vol 13, no. 3, pp. 247 - 251.

Gupta, A, Meswania, J, Pollock, R, Cannon, SR, Briggs, TWR, Taylor, S & Blunn, G 2006, 'Non-Invasive Distal Femoral Expandable Endoprosthesis for Limb-Salvage Surgery in Paediatric Tumours', *The Journal of Bone and Joint Surgery*, vol 88, no. 5, pp. 649 - 654.

How is Ostesarcoma Treated? 2009, viewed 23 July 2009, <http://www.cancer.org/docroot/CRI/content/CRI_2_4_4X_How_is_osteosarcoma_treated_52.asp?rnav=cri>.

Kapukaya, A, Subasi, M, Kandiya, E, Ozates, M & Yilmaz, F 2000, 'Limb Reconstruction with the Callus Distraction Method after Bone Tumour Resection', *Archive of Orthopaedic and Trauma Surgery*, no. 120, pp. 215-218.

Kotz, R, Dominkus, M, Zettl, T, Ritschl, P, Windhager, R, Gadner, H, Zielinski, C & Salzer-Kuntschik, M 2002, 'Advances in bone tumour treatment in 30 years with respect to survival and limb salvage. A single institution experience', *International Orthopaedics*, no. 26, pp. 197-202.

Kurtz, SM 2004, *The UHMWPE Handbook: Ultra High Molecular Weight Polyethylene in Total Joint Replacement*.

Kutz, M 2009, *Biomedical Engineering and Design Handbook*, 2nd edn, McGraw-Hill.

Letson, GD, D'Amato, G, Windham, TC & Muro-Cacho, CA 2003, 'Extendable Prostheses for the Treatment of Malignant Bone Tumors in Gowing Children', *Current Opinion in Orthopaedics*, vol 14, no. 6, pp. 413 - 418.

Lewis, MM 1986, 'The Use of an Expandable and Adjustable Prosthesis in the Treatment of Childhood Malignant Bone Tumors of the Extremity', *Cancer*, vol 57, pp. 499 - 502.

Lewis, VO 2005, 'Limb Salvage in the Skeletally Immature Patient', *Current Oncology Reports*, no. 7, pp. 285-292.

Maresh, MM 1955, 'Linear Growth of Long Bones of Extremities from Infancy through Adolescence', *American Journal of Disease of Children*, vol 89, pp. 725 - 742.

Mehlman, CT & Cripe, TP 2008, *Osteosarcoma*, viewed 20 April 2009, <http://emedicine.medscape.com/article/1256857-overview>.

Meswania, JM, Walker, PS, Sneath, RS & Grimer, RJ 1998, 'In vivo distraction forces in extendible endoprostheticc replacements - a study of 34 patients', *Proceedings of the Institution of Mechanical Engineers*, vol 212, no. H, pp. 151 - 155.

MRI of the Body (Chest, Abdomen, Pelvis), viewed 22 July 2009, <http://www.radiologyinfo.org/en/info.cfm?pg=bodymr>.

Myers, GJC, Abudu, AT, Carter, SR, Tillman, RM & Grimer, RJ 2007, 'Endoprosthetic Replacement of the Distal Femur for Bone Tumors: Long Term Results', *The Journal of Bone & Joint Surgery*, vol 89 - B, no. 4, pp. 521 - 526.

Neel, MD & Letson, GD 2001, 'Modular Endoprostheses for Children With Malignant Bone Tumors', *Cancer Control*, vol 8, no. 4, pp. 344 - 348.

Neel, MD, Wilkins, RM, Rao, BN & Kelly, CM 2003, 'Early Multicenter Experience With a Noninvasive Expandable Prosthesis', *Clinical Orthopaedics and Related Research*, no. 415, pp. 72-81.

Nordian, *Gamma Compatible Materials: Reference Guide*, viewed 15 January 2011, <http://www.nordion.com/documents/Gamma_Compatible_Materials_List.pdf>.

Oprea, M, Schnoring, H, Sachweh, J, Ott, H, Biertz, J & Vazquez-Jimenez, J 2009, 'Allergy to Pacemaker Silicone Compounds: Recognition and Surgical Management', *The Society of Thoracic Surgeons*, no. 87, pp. 1275-1277.

Rosner, B, Prineas, R, Loggie, J & Daniels, SR 1998, 'Percentiles for body mass index in U.S. children 5 to 17 years of age', *The Journal of Pediatrics*, pp. 211-222.

Schiller, C, Windhager, R, Fellinger, EJ, Salzer-Kuntschik, M, Kaider, A & Kotz, R 1995, 'Extendable Tumour Endoprostheses for the Leg in Children', vol 77 - B, no. 4, pp. 608 - 614.

Schindler, OS, Cannon, SR, Briggs, TWR & Blunn, GW 1997, 'Stanmore Custom-Made Extendible Distal Femoral Replacements: Clinical Experience in Children with Primary Malignant Bone Tumours', *Journal of Bone and Joint Surgery*, vol 79, pp. 927 - 937.

Schindler, OS, Cannon, SR, Briggs, TWR, Blunn, GW, Grimer, RJ & Walker, PS 1998, 'Use of Extendable Total Femoral Replacements in Children with Malignant Bone Tumours', *Clincical Orthopaedics and Related Research*, vol 1, no. 357, pp. 157 - 170.

Serhan, HA, Varnavas, G, Dooris, AP, Patwardhan, A & Termiadianos, M 2007, 'Biomechanics of the posterior lumbar articulating elements', vol 22.

Shigley, JE, Mischke, CR & Budynas, RG 2004, 'Fatigue Failure Resulting from Variable Loading', in *Mechanical Engineering Design*, 7th edn.

Shigley, JE, Mischke, CR & Budynas, RG, 'Load and Stress Analysis', in *Mechanical Engineering and Design*, 7th edn.

Shigley, JE, Mischke, CR & Budynas, RG, 'The Mechanics of Power Screws', in *Mechanical Engineering Design*, 7th edn.

Snyder, RW & Helmus, MN, 'Cardiovascular Biomaterials', in *Biomedical Engineering and Design Handbook*.

Stamore Implants, W, 'JTS Drive Unit: Operations Manual'.

Szpalski, M, Gunzberg, R & Mayer, M 2002, 'Spine Arthroplasty: a historical review', vol 11 (Suppl.2).

Taylor, ME, Tanner, KE, Freeman, MAR & Yettram, AL 1996, 'Stress and strain distribution within the intact femur: compression or bending?', *Med. Eng. Phys.*, vol 18, pp. 122 - 131.

Taylor, SJG & Walker, PS 2001, 'Forces and moments telemetered from two distal femoral replacements during various activities', *Journal of Biomechanics*, vol 34, pp. 839 - 848.

Teoh, SH 2007, *Engineering Materials for Biomedical Applications*, World Scientific Publishing Co.

Thermometrics, Precision Temperature Sensors, *Wire Selection*, viewed 22 February 2011, <http://www.thermometricscorp.com/wircabmat1.html>.

Titanium Ti-6Al-4V (Grade 5), STA, viewed 20 July 2011, <http://www.matweb.com/search/DataSheet.aspx?MatGUID=b350a789eda946c6b86a3e4d3c577b39&ckck=1>.

Tortora, GJ & Grabowski, SR 2003, 'Medical Imaging', in *Principles of Anatomy and Physiology*, John Wiley & Sons, Inc.

Tortora, GJ & Grabowski, SR 2003, *Principles of Anatomy & Physiology*, John Wiley & Sons, Inc.

Tortora, GJ & Grabowski, SR 2003, 'Structure of Bone', in *Principles of Anatomy and Physiology*.

Tortora, GJ & Grabowski, SR 2003, 'The Cellular Level of Organization', in *Principles of Anatomy and Physiology*.

Tung-Wu, L, Taylor, SJG, O'Conner, JJ & Walker, PS 1997, 'Influence of muscle activity on the forces in the femur: an in vivo study', *Journal of Biomechanics*, vol 30, pp. 1101 - 1106.

Tupman, G S 1962, 'A Study of Bone Growth in Normal Children and its relationship to Skeletal Maturity', *The Journal of Bone and Joint Surgery*, vol 44B, no. 1.

Unwin, PS & Walker, PS 1996, 'Extendible Endoprostheses for the Skeletally Immature', *Clincal Orthopaedics and Related Research*, vol 322, pp. 179 - 193.

Vicatos, G, Ginsberg, S & Parsons, A 2011, 'Patent Application: Endoprosthesis'.

What is Cancer - Childhood Cancers, viewed 23 July 2009, <http://www.cancer.org/docroot/CRI/content/CRI_2_4_1x_Whats_Is_Cancer_-_Childhood_Cancers.asp?rnav=cri>.

What Is Cancer? 2009, viewed 1 October 2009, <http://www.cancer.org/docroot/CRI/content/CRI_2_4_1x_What_Is_Cancer.asp?sitearea=>.

What is Osteosarcoma? 2009, viewed 21 April 2009, <http://www.cancer.org/docroot/CRI/content/CRI_2_4_1X_What_is_osteosarcoma_cancer_52.asp?sitearea=>.

Wicart, P, Mascard, E, Missenard, G & Dubousset, J 2002, 'Rotationplasty after failure of a knee prosthesis for malignant tumour of the distal femur', *The Journal of Bone & Joint Surgery*, vol 84-B, no. 6, pp. 865-869.

Yoshida, Y, Iwata, S, Ueda, T, Kawai, A, Isu, K & Ryu, J 2008, 'Current State of Extendable Prostheses for the Lower Limb in Japan', *Surgical Oncology*, vol 17, pp. 65 - 71.

Zamanian, A & Hardiman, C 2005, 'Electromagnetic Radiation and Human Health: A Review of Sources and Effects', *High Frequency Electronics*, pp. 16-26.

Appendix A

A. Tables

A-1. Dimensions: Femur and Tibia

Values for stature, length of femur and tibia at consecutive chronological ages, lengths measured from orthoroentgenograms and includes both proximal and distal epiphyses (Anderson, Green & Messner 1963).

Table 8: Female dimensions; stature, femur and tibia

Female Dimensions (50 Girls) (Anderson, Green & Messner 1963)												
Age	**Stature**				**Femur**				**Tibia**			
yrs	**mm**				**mm**				**mm**			
	Mean	*Std Dev*			*Mean*	*Std Dev*			*Mean*	*Std Dev*		
			Max	Min			Max	Min			Max	Min
8	1281	47.8	1424.4	1137.6	331	16.3	379.9	282.1	263	13.9	304.7	221.3
9	1338	47.8	1481.4	1194.6	350	17.1	401.3	298.7	280	15	325	235
10	1399	52.4	1556.2	1241.8	370	18.2	424.6	315.4	298	16.7	348.1	247.9
11	1466	59.3	1643.9	1288.1	392	20	452	332	316	18.4	371.2	260.8
12	1532	63.6	1722.8	1341.2	411	21.2	474.6	347.4	332	19.5	390.5	273.5
13	1583	61.4	1767.2	1398.8	424	21.2	487.6	360.4	342	19.4	400.2	283.8
14	1608	61.6	1792.8	1423.2	431	21.5	495.5	366.5	345	19.7	404.1	285.9
15	1623	60.2	1803.6	1442.4	432	21.8	497.4	366.6	346	19.8	405.4	286.6
16	1629	61	1812	1446	433	22	499	367	346	20	406	286
17	1638*	63.7*	1829.1	1446.9	433*	22.1*	499.3	366.7	347*	20*	407	287
18	1649*	61*	1832	1466	433*	22.1*	499.3	366.7	347*	20*	407	287

* Figures are based on 21-42 girls, since data were not available on all subjects at these ages (Anderson, Green & Messner 1963)

Table 9: Male dimensions; stature, femur and tibia

Male Dimensions (50 Boys) (Anderson, Green & Messner 1963)												
Age	**Stature**				**Femur**				**Tibia**			
yrs	**mm**				**mm**				**mm**			
	Mean	*Std Dev*			*Mean*	*Std Dev*			*Mean*	*Std Dev*		
			Max	Min			Max	Min			Max	Min
8	1276	59.4	1454.2	1097.8	328*	15.3*	373.9	282.1	259*	15.5*	305.5	212.5
9	1333	61.5	1517.5	1148.5	346*	17.8*	399.4	292.6	271*	18.6*	326.8	215.2
10	1385	65.8	1582.4	1187.6	364	18.7	420.1	307.9	286	18.9	342.7	229.3
11	1435	69.4	1643.2	1226.8	382	20.7	444.1	319.9	301	20.7	363.1	238.9
12	1494	77.2	1725.6	1262.4	402	22.3	468.9	335.1	318	22.7	386.1	249.9
13	1563	91.3	1836.9	1289.1	423	25.2	498.6	347.4	336	24.9	410.7	261.3
14	1637	95.4	1923.2	1350.8	443	25.8	520.4	365.6	353	25.4	429.2	276.8
15	1698	86.8	1958.4	1437.6	458	23.8	529.4	386.6	364	23.4	434.2	293.8
16	1732	77.4	1964.2	1499.8	466	22.7	534.1	397.9	369	22.1	435.3	302.7
17	1750	74.1	1972.3	1527.7	469	23	538	400	371	22.1	437.3	304.7
18	1759	73.7	1980.1	1537.9	470	23.5	540.5	399.5	371	22.2	437.6	304.4

* Figures are based on 31-49 boys, since data were not available on all subjects at these ages (Anderson, Green & Messner 1963)

Table 10: Remaining growth in distal femur

Remaining Distal Femoral Growth (mm)						
Age	Female			Male		
	Average	Max	Min	Average	Max	Min
8	65	98	41	-	-	-
9	52	86	31	-	-	-
10	41	72	22	72	97	48
11	28	47	16	61	84	38
12	17	28	7	48	72	28
13	7	15	1	29	57	16
14	3	7	0	14	30	40
15	0	4	0	4	10	10
16	-	-	-	1	6	0
17	-	-	-	0	2	0

Table 11: Remaining growth in proximal tibia

Remaining Proximal Tibial Growth (mm)						
Age	Female			Male		
	Average	Max	Min	Average	Max	Min
8	41	60	25	-	-	-
9	33	51	19	-	-	-
10	26	43	11	46	67	30
11	16	28	9	38	56	23
12	8	15	3	30	47	16
13	3	8	0	18	34	10
14	0	3	0	7	22	1
15	0	1	0	2	7	0
16	-	-	-	0	3	0
17	-	-	-	0	1	0

A-2. Growth Rates: Femur and Tibia

Table 12: Female growth rates; stature, femur and tibia

Female Growth Rate																
Age Interval	**Stature**				**Femur**						**Tibia**					
yrs	**mm**				**mm**						**mm**					
	Mean	*Std Dev*			*Mean (pa)*	*Std Dev*	*Mean Limits (pa)*		*Mean (pm)*	*Mean (pd)*	*Mean (pa)*	*Std Dev*	*Mean Limits (pa)*		*Mean (pm)*	*Mean (pd)*
			Max	Min			Max	Min					Max	Min		
8.5	57	7.7	80.1	33.9	20	2.8	28.4	11.6	1.667	0.056	17	2.9	25.7	8.3	1.417	0.047
9.5	60	13.9	101.7	18.3	20	3.2	29.6	10.4	1.667	0.056	18	3.6	28.8	7.2	1.500	0.050
10.5	67	17	118	16	21	3.5	31.5	10.5	1.750	0.058	18	3.8	29.4	6.6	1.500	0.050
11.5	65	19.1	122.3	7.7	19	5.2	34.6	3.4	1.583	0.053	16	5.6	32.8	0	1.333	0.044
12.5	52	22	118	0	14	6.7	34.1	0	1.167	0.039	10	6.3	28.9	0	0.833	0.028
13.5	25	15	70	0	6	5	21	0	0.500	0.017	4	4.1	16.3	0	0.333	0.011
14.5	14	11.5	48.5	0	2	3	11	0	0.167	0.006	1	2.4	8.2	0	0.083	0.003
15.5	7	7.9	30.7	0	1	2	7	0	0.083	0.003	0	1.4	4.2	0	0	0
16.5	4*	5.8*	21.4	0	0*	0.6*	1.8	0	0	0	0*	0.4*	1.2*	0	0	0
17.5	2*	4.6*	15.8	0	0*	0*	0	0	0	0	0*	0*	0*	0	0	0

*Figures are based on 35-44 children only, since data were not available on every subject at these ages

Table 13: Male growth rates; stature, femur and tibia

Male Growth Rate																
Age Interval	**Stature**				**Femur**						**Tibia**					
yrs	**mm**				**mm**						**mm**					
	Mean	*Std Dev*			*Mean (pa)*	*Std Dev*	*Mean Limits (pa)*		*Mean (pm)*	*Mean (pd)*	*Mean (pa)*	*Std Dev*	*Mean Limits (pa)*		*Mean (pm)*	*Mean (pd)*
			Max	Min			Max	Min					Max	Min		
8.5	57	8.8	83.4	30.6	20*	2.7*	28.1	11.9	1.667	0.056	16*	2.2*	22.6	9.4	1.333	0.044
9.5	52	9.1	79.3	24.7	18*	3.2*	27.6	8.4	1.500	0.050	15*	2.7*	23.1	6.9	1.250	0.042
10.5	50	8	74	26	18	3.4	28.2	7.8	1.500	0.050	15	2.8	23.4	6.6	1.250	0.042
11.5	59	16	107	11	19	4.2	31.6	6.4	1.583	0.053	17	4.2	29.6	4.4	1.417	0.047
12.5	69	21.6	133.8	4.2	21	5	36	6	1.750	0.058	18	4.9	32.7	3.3	1.500	0.050
13.5	74	20.2	134.6	13.4	20	5.2	35.6	4.4	1.667	0.056	17	5.8	34.4	0	1.417	0.047
14.5	60	25.6	136.8	0	15	7.9	38.7	0	1.250	0.042	11	6.8	31.4	0	0.917	0.031
15.5	35	23.7	106.1	0	8	7.3	29.9	0	0.667	0.022	5	7.7	28.1	0	0.417	0.014
16.5	18	17.4	70.2	0	3	3.8	14.4	0	0.250	0.008	2	2.5	9.5	0	0.167	0.006
17.5	9	10.4	40.2	0	1	1.7	6.1	0	0.083	0.003	0	0.8	2.4	0	0	0

*Figures are based on 35-44 children only, since data were not available on every subject at these ages

A-3. Femur and Tibia Distraction Forces

Table 14: Loads due to distraction for femur and tibia (Meswania et al. 1998)

Loads due to Extension								
	Femur				Tibia			
Extension	Load Range		Average Load	Regression Load	Load Range		Average Load	Regression Load
	Upper	Lower			Upper	Lower		
mm	N	N	N	N	N	N	N	N
0	578	1	135	122	422	16	142	130
1	734	10	196	188	534	47	196	189
2	890	19	257	253	645	77	250	248
3	1046	28	319	319	757	108	304	308
4	1201	37	380	385	869	139	358	367
5	1357	46	441	450	980	169	412	426
6	1513	55	502	516	1092	200	466	485

A-4. Femoral Loading for Various Activities

Table 15: Peaks and troughs of axial force and moments (mean of n cycles) for gait activities (Taylor & Walker 2001)

Activity	n Gait Cycles	Weeks post op	Axial Compression (BW)		Antero-Posterior (AP) Moment (BWcm)		Medio-Lateral (ML) Moment (BWcm)		Torque (BWcm)		Speed
			Peak	Trough	Peak	Trough	Peak	Trough	Peak	Trough	m/s
Walking	8-9	52	2.17	0.25	6.6	-1.2	4.3	-0.6	0.8	-0.4	1.1
	8-9	108	2.62	0.33	7.7	-1.3	5	-0.4	0.4	-0.5	1.17
	8-10	132	2.8	0.24	8.5	-0.8	4.4	-0.4	0.4	-0.6	1.32
Ascending Stairs	6-7	52	2.14	0.34	6.3	-0.4	5.4	-2	1.1	-0.2	0.45
	5-6	108	2.4	0.48	6.9	-0.4	4.9	-2.3	0.4	-0.4	0.47
	4-5	132	2.44	0.43	9	-1.3	3.7	-1.8	0.8	-0.7	0.51
Descending Stairs	4-6	52	2.68	0.34	7.1	-1.1	3.5	-1.6	1.3	-0.4	0.51
	4-5	108	2.9	0.52	6.6	-1.2	4	-2.4	0.9	-0.4	0.51
	4-6	132	3.09	0.45	9.5	-0.8	2.8	-1.9	1	-0.4	0.56
Jogging	6-8	52	3.08	0.46	8.3	-0.7	5.5	-1.9	0.9	-0.7	1.7
	8-9	108	3.11	0.65	7	-1.1	6.7	-2.3	0.3	-0.5	1.88
	7-8	132	3.6	0.39	9.4	-0.5	6.4	-3.3	0.5	-0.4	1.92

A-5. BMI: Male and Female

Table 16: Mean BMI for males and females by age (Rosner et al. 1998)

	Male				Female			
Age	BMI	Std Dev	Stature	Body Mass *	BMI	Std Dev	Stature	Body Mass *
yrs	kg/m2		mm	kg	kg/m2		mm	kg
5	15.8	1.6	-	-	15.6	1.8	-	-
6	16.0	1.7	-	-	15.9	2.0	-	-
7	16.4	1.9	-	-	16.2	2.2	-	-
8	16.8	2.3	1276	27.4	16.8	2.6	1281	27.6
9	17.5	2.7	1333	31.1	17.5	3.1	1338	31.3
10	18.2	3.2	1385	34.9	18.3	3.4	1399	35.8
11	18.9	3.5	1435	38.9	19.2	3.7	1466	41.3
12	19.5	3.6	1494	43.5	20.3	4.1	1532	47.6
13	20.2	3.6	1563	49.3	21.0	4.1	1583	52.6
14	20.7	3.6	1637	55.5	21.5	4.2	1608	55.6
15	21.6	3.8	1698	62.3	21.9	4.2	1623	57.7
16	22.1	3.7	1732	66.3	22.2	4.3	1629	58.9
17	22.8	3.9	1750	69.8	22.5	4.5	1638	60.4

*body mass calculated according to Appendix E-8

A-1. Experiment Results

A-1-1. Linear Force

Table 17: Results of linear force testing

	Time	Resistance	Voltage	Current	Pressure		Load			Speed
							Force	Load	True Load	
		R	V	I	P	P	F	L		
	min	Ω	V	A	Bar	kPa	N	kg	Cum. kg	~ RPM
Zero		249.4	1.1984	0.0048	0.4026	40.26	79.04	8.06	-	-
Start	0	249.3	1.1980	0.0048	0.4027	40.27	79.08	8.06	0.00	6
	10	249.2	1.2172	0.0049	0.4422	44.22	86.83	8.85	0.79	5
	20	249.2	1.2405	0.0050	0.4895	48.95	96.11	9.80	1.74	4.6
	30	249.1	1.2645	0.0051	0.5381	53.81	105.66	10.77	2.71	4.6
	40	249.0	1.2908	0.0052	0.5920	59.20	116.23	11.85	3.79	4.6
	50	249.0	1.3255	0.0053	0.6616	66.16	129.91	13.24	5.18	4.5
	60	248.9	1.3603	0.0055	0.7326	73.26	143.85	14.66	6.60	4.6
	70	248.9	1.3975	0.0056	0.8074	80.74	158.52	16.16	8.10	4.6
	80	248.8	1.4420	0.0058	0.8979	89.79	176.30	17.97	9.91	4.5
	90	248.8	1.4983	0.0060	1.0111	101.11	198.52	20.24	12.18	4.6
	100	248.8	1.5560	0.0063	1.1276	112.76	221.41	22.57	14.51	4.7
	110	248.7	1.6139	0.0065	1.2447	124.47	244.39	24.91	16.85	4.3
	120	248.7	1.6785	0.0067	1.3745	137.45	269.89	27.51	19.45	4.1
	130	248.7	1.7549	0.0071	1.5281	152.81	300.05	30.59	22.53	4.3
	140	248.7	1.8470	0.0074	1.7141	171.41	336.55	34.31	26.25	4.4
	150	248.6	1.9434	0.0078	1.9087	190.87	374.77	38.20	30.14	4
	160	248.6	2.0520	0.0083	2.1271	212.71	417.66	42.57	34.51	4
	170	248.6	2.1850	0.0088	2.3946	239.46	470.18	47.93	39.87	3.9
End	180	248.6	1.3500	0.0054	0.7152	71.52	140.43	14.32	6.25	

A-1-2. Motor Rotational Velocity

Table 18: Results of motor rotational velocity testing

Time	1 Rev (s)	RPM
0	9.8	6.1
5	11.2	5.4
10	12.3	4.9
15	12.9	4.7
20	13	4.6
25	13.2	4.5
30	13.2	4.5

A-1-3. Seal Friction

Table 19: Results of seal friction testing

Seal	Mass (kg)	Moment Arm (m)	Frictional Torque(Nm)
Sample 1	0.0908	0.0398<l<0.0406	0.03581
Sample 2	0.0908	0.0317<l<0.032	0.02837

A-2. Properties of Medical Grade Titanium (Ti6Al4V)

Table 20: Properties of Ti6Al4V (Titanium Ti-6Al-4V (Grade 5), STA n.d.)

Physical Properties	Value	Units	Comments
Density	4.43	g/cc	
Mechanical Properties			
Hardness, Brinell	379	-	
Hardness, Knoop	414	-	
Hardness, Rockwell C	41	-	
Hardness, Vickers	396	-	
Tensile Strength, Ultimate	1170	MPa	
Tensile Strength, Yield	1100	MPa	
Elongation at Break	10	%	
Modulus of Elasticity	114	GPa	Average Tension and Compression
Compressive Yield Strength	1070	MPa	
Notched Tensile Strength	1550	MPa	
Ultimate Bearing Strength	2140	MPa	
Bearing Yield Strength	1790	MPa	
Poissons Ratio	0.33	-	
Charpy Impact	23	J	V Notch
Fatigue Strength	160	MPa	Kt (Stress Concentration Factor)= 3.3, Cycles 1e7
	700	MPa	Un-notched, Cycles 1e7
Fracture Toughness	43	MPa√m	
Shear Modulus	44	GPa	
Shear Strength	760	MPa	Ultimate Shear Strength

Table 21: Calculated endurance limit (Based on Dimensions and Loading) See Appendix E-7

Endurance Limit	Value	Units	Comments
Max	406	MPa	Φ 8 mm
Min	352	MPa	Φ 30 mm

Appendix B

B. Experiments

B-1. Linear Force

Aim	To investigate the validity of predicted linear force of the designed device versus the actual linear force achieved in a practical application.
Apparatus	• The device, assembled • Hydraulic cylinder • Test Rig (see Appendix) • Pressure Transducer (8 Bar) • DC power supply • 250 Ohm Resistance (240 Ohm and 10 Ohm resistors) • Conductive Wire • Digital Meter • Stop Watch • Hydraulic fluid (23?)
Method	- Prime cylinder with hydraulic fluid and mount pressure transducer, ensuring no air bubbles in the cylinder. - Assemble the test rig according to Diagram, including mounting of the hydraulic cylinder - Assemble test circuit according to diagram - Calibrate hydraulic cylinder and pressure transducer, checking zero error - Place extension device in test rig as indicated in diagram - Adjust to ensure zero load on the extension device - Attached piezo motor control device to the motor - Set DC power supply to 12 V - Measure resistance of resistors in series using digital meter - Measure zero load voltage, using digital meter - Turn motor on, beginning test - Sample resistance and voltage every 5 mins using the digital meter, further measure the rotational velocity of the piezo motor every 5 mins using the stop watch until the desired and predicted output force for brass is achieved - Record result in a spreadsheet, calculating pressure, at sample times, based on the voltage output of the pressure transducer - Based on the pressure reading of the transducer calculated the applied linear force
Results	The recorded data from the experiment are shown in Table 17, and presented graphically in Section 6.1

B-2. Motor Rotational Velocity Characteristics

Aim	To investigate the variation in rotational velocity of the piezo motor with respect to time
Apparatus	• Piezo motor • Piezo motor driver • Stop watch
Method	- Connect the driver to the piezo motor - Initiate rotation of the piezo motor with the driver - At 5 min intervals record the rotational velocity of the motor
Results	The results are shown in Table 18, Appendix A-1-2 and represented graphically in Section 6.2.

B-3. Wireless Power Transfer

Aim	To investigate the capability of the external circuit in providing sufficient power to the internal circuitry to drive the motor.
Apparatus	• Drive assembly • Custom drive circuitry and receiving coil • External power circuitry including driving inductive coil • Power supply • Oscilloscope • Beef shank
Method	- Connect the external power circuitry to the power supply - Place the drive circuitry and receiving coil in the beef shank, under muscle and fat tissue - Starting with a large separation, align the axes of the driving and receiving coils - Observe motor output, if no rotation observed, resect some tissue reducing separation distance and repeat test
Results	Motor rotation was achieved with a separation of approximately 10mm, yielding a positive result for wireless powering of the device across skin and tissue

B-4. Seal Efficacy

Aim	To investigate the efficacy of the seal in preventing the passage of fluid.
Apparatus	• The device, assembled with UHMWPE seal and without the drive unit • Water • Red dye
Method	- Mix water and dye, pouring into the cavity for the drive unit - Leave for a period of two days under gravity, periodically rotating and flexing the drive shaft
Results	During the course of the experiment, no fluid was observed to have leaked past the UHMWPE seal.

B-5. Seal Friction

Aim	To investigate the torque required to overcome the static friction between the seal and the drive shaft.
Apparatus	• Two sample seals of type 2 • The device, assembled without extension shaft and drive unit • Vice • Weights (90.8g) • M4 Screws of various lengths
Method	- Rotation of the drive shaft is prevented using vice grips, leaving the drive unit casing and cover shaft free to rotate relative to the drive shaft - An M4 screw is inserted into the corresponding hole in the cover shaft, and the device is rotated until the screw is horizontal - The fixed mass is suspended from the screw and the moment arm length adjusted until the applied torque is sufficient to overcome the static friction, at which point the length of the moment arm is recorded - Procedure repeated using second seal
Results	The torque required to overcome the friction was calculated according to Appendix E-6, and the results shown in Appendix A-1-3

Appendix C

C. Equipment Specifications

C-1. Gearbox

Table 22: GCP022 gearbox specifications

Manufacturer/Supplier	Wittenstein Inc 1249 Humbracht Tel: (630) 540 5300 Fax: (630) 736 6100 Web: http://wittenstein-us.com/Motors.html
Contact	Thompson, Geoff Geoff.Thompson@wittenstein-us.com
Product	Motor Gearbox Unit GCP 022 (3 Stage)
Ratio	196
Nominal Output Torque (Nm)	1.5
Peak Output Torque (Nm)	3
Mass (g)	100
Efficiency	0.85
Mass Moment of Inertia (kgm2)	0.004
Torsional Backlash (arcmin)	50
Torsional Stiffness (Nm/arcmin)	0.20
Temperature Range (0C)	Max +90
Protection Class	44
Average Lifetime (hr)	approximately 10 000

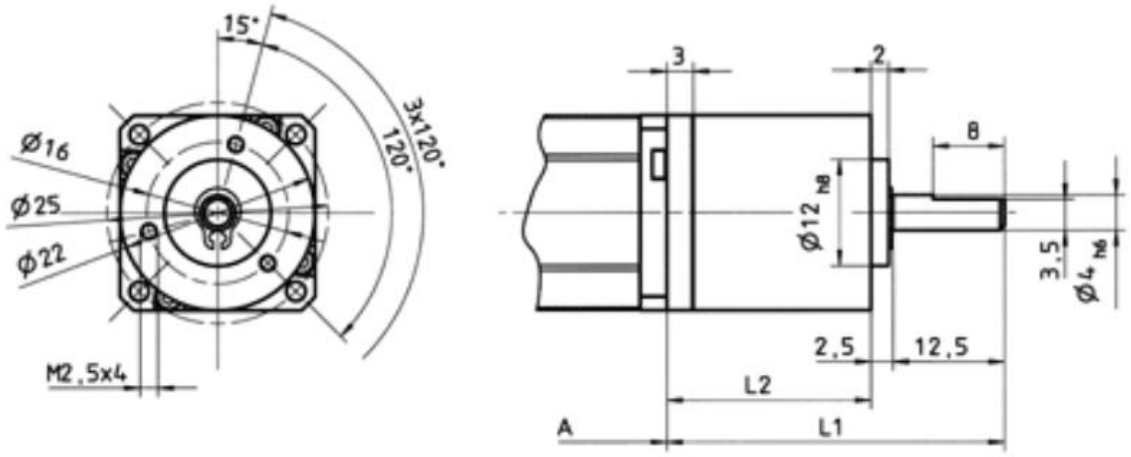

Figure 62: Wittenstein GCP022 gearbox

C-2. Motor

Table 23: Piezo motor specifications

Manufacturer/Supplier	Piezo Motor Stålgatan 14 SE-754 50 Uppsala Sweden Tel: +46 (0) 18-489 51 71 Fax: : +46 (0)18-489 50 01 Web: http://www.piezomotor.se/
Contact	Lindkvist, Olle olle.lindkvist@piezomotor.se
Product	Piezo Legs Rotary Motor
Angular Range	360 deg
Maximum Speed	14 RPM
Resolution	<1 µrad
Max Voltage	48 V
Stall Torque (max)	80 Nmm
Holding Torque (max)	90 Nmm
Surface	Bare metal
Material	Stainless steel
Connector	JST BM05B-SRSS-TB
Mechanical Size	32 x 23 mm
Weight	60 g
Operating Temp	-20 to +70 ^{o}C

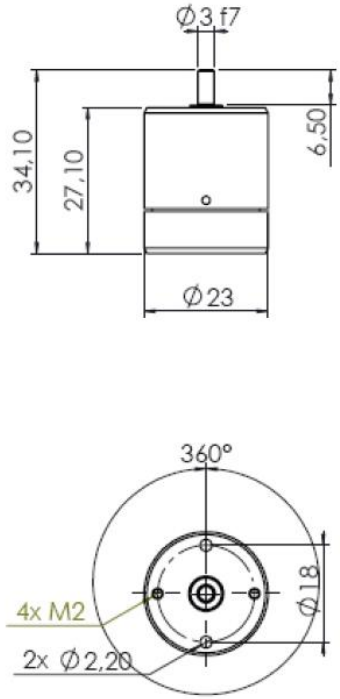

Figure 63: Rotary piezo motor

C-3. Stanmore JTS

Table 24: Stanmore JTS specifications (Gupta et al. 2006)

Component	Specification	Value	Unit
Gearbox (Epicyclic)	Diameter	21.5	mm
	Length	18.5	mm
	Reduction Ratio	13061:1	-
	Output Torque	4	Nm
Magnetic Disc (NdFeB toroidal)	Synchronous Speed	3000	RPM
Power Screw	Axial Thrust	1350	N
	Pitch	1	mm
	Extension Rate	0.23	mm/min

Appendix D

D. Technical Drawings

D-1. Endoprosthetic Growth Module Mechanism

D-1-1. Device Assembly: Exploded

001	Piezo Motor (As Supplied)
002	Adaptor Plate (Ti6Al4V)
003	Transition Shaft (Ti6Al4V)
004	Gearbox (As Supplied)
005	Drive Unit Casing (Ti6Al4V)
006	Spacing Plate (Ti6Al4V)
007	Seal (UHMWPE)
008	Cover Shaft (Ti6Al4V)
009	Drive Shaft (Ti6Al4V)
010	Extension Shaft (Ti6Al4V)

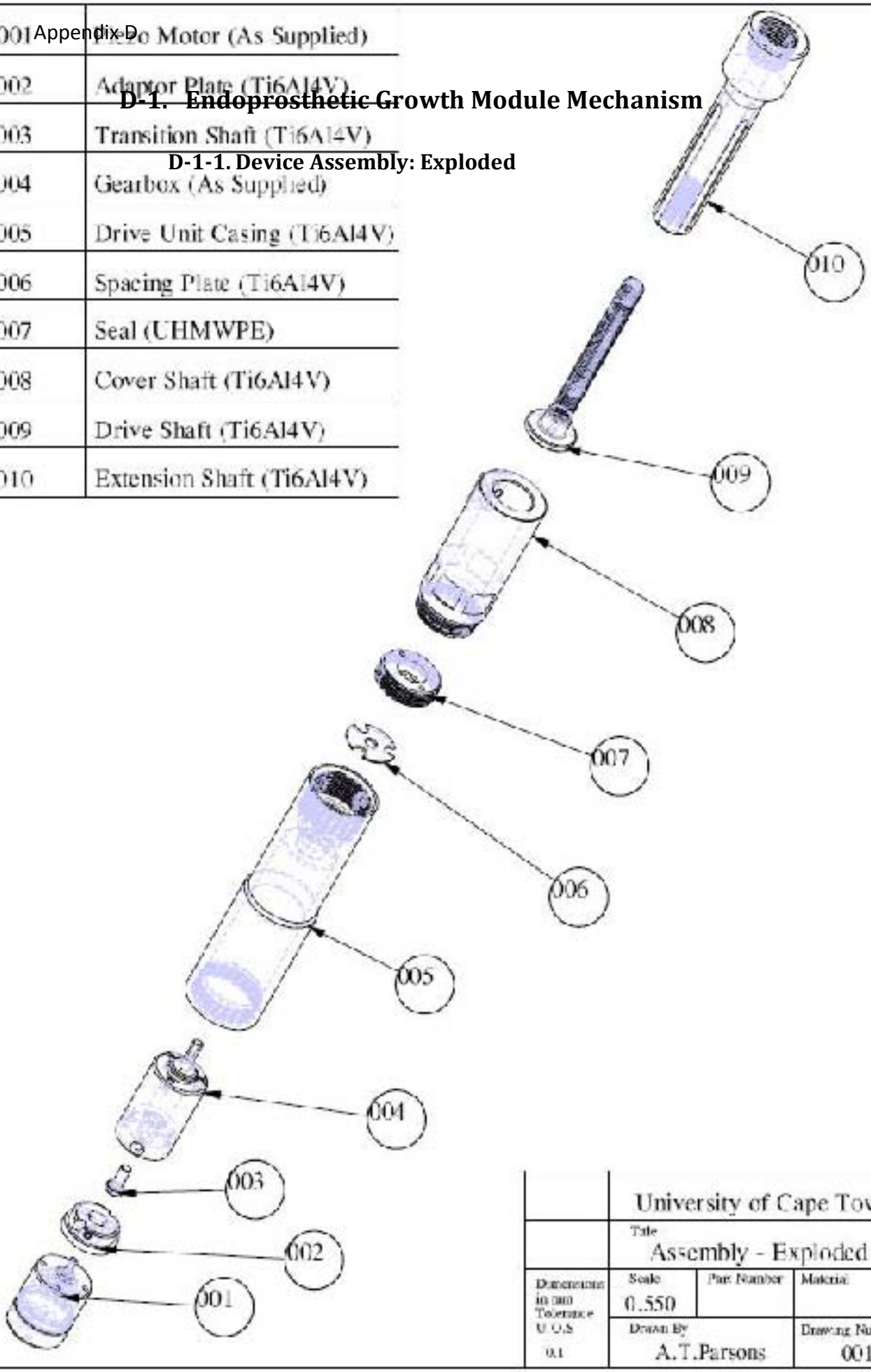

	University of Cape Town		
	Title: Assembly - Exploded		
Dimensions in mm Tolerance U.O.S 0.1	Scale: 0.550	Part Number:	Material:
	Drawn By: A.T.Parsons		Drawing Number: 001

D-1-2. Device Assembly: Cross Section

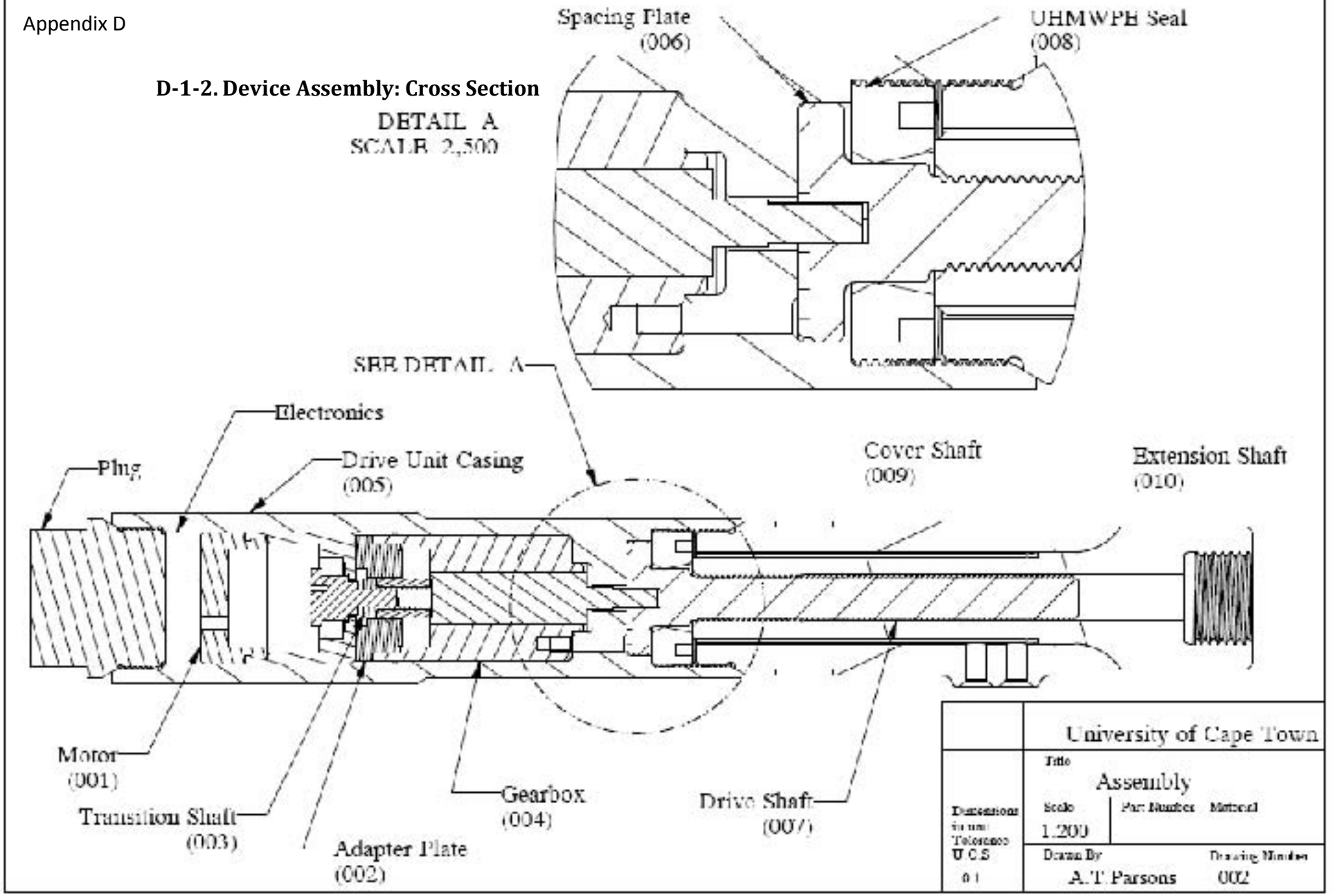

D-1-3. Piezo Motor

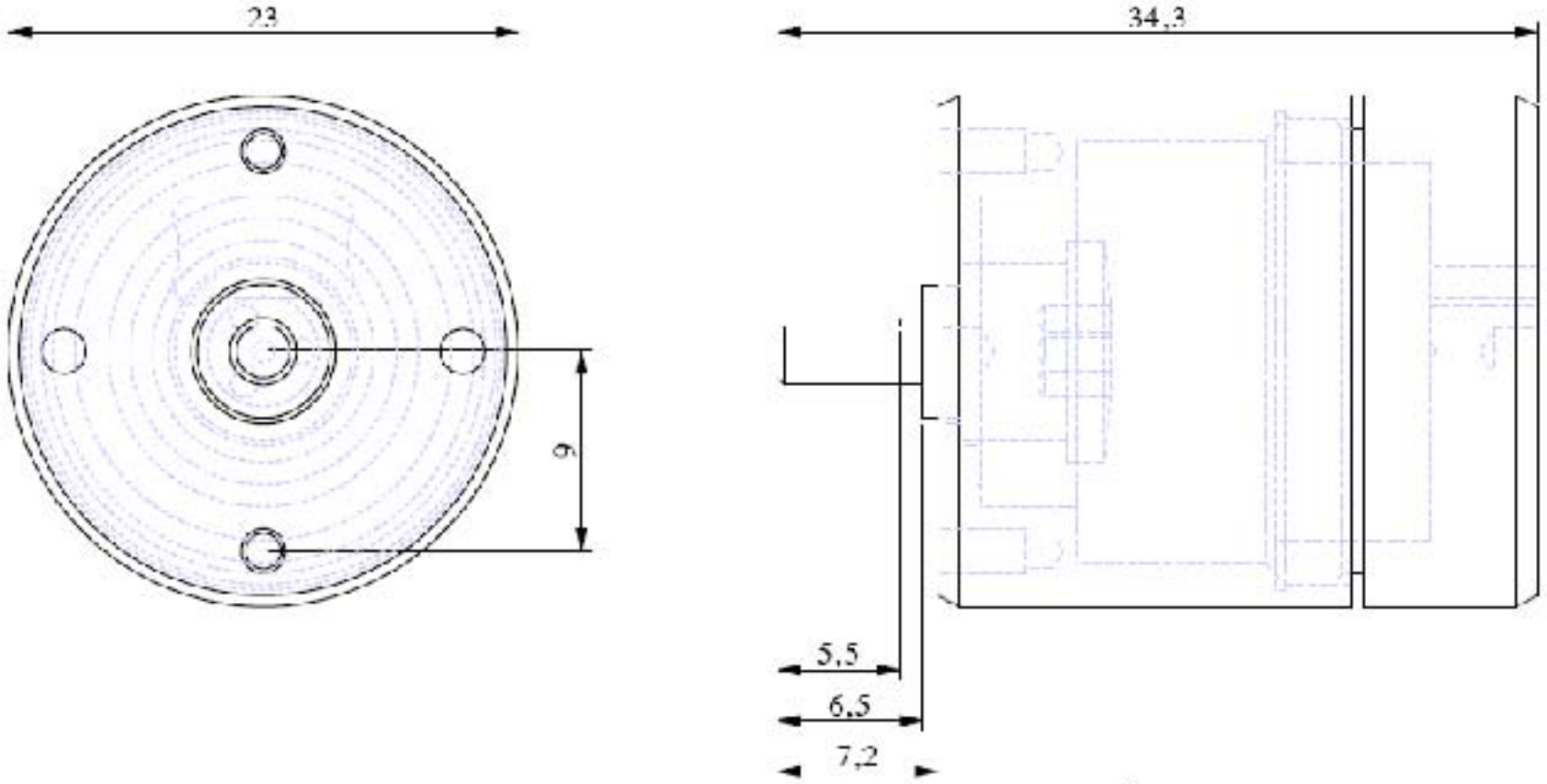

University of Cape Town				
Title: Piezo Motor				
Dimensions in mm Tolerance +/- 0.5	Scale: 5.500	Part Number: 001	Sheet: 01	Of: 01
0.1	Drawn By: A.T.Parsons		Drawing Number: 001	

D-1-4. Adaptor Plate

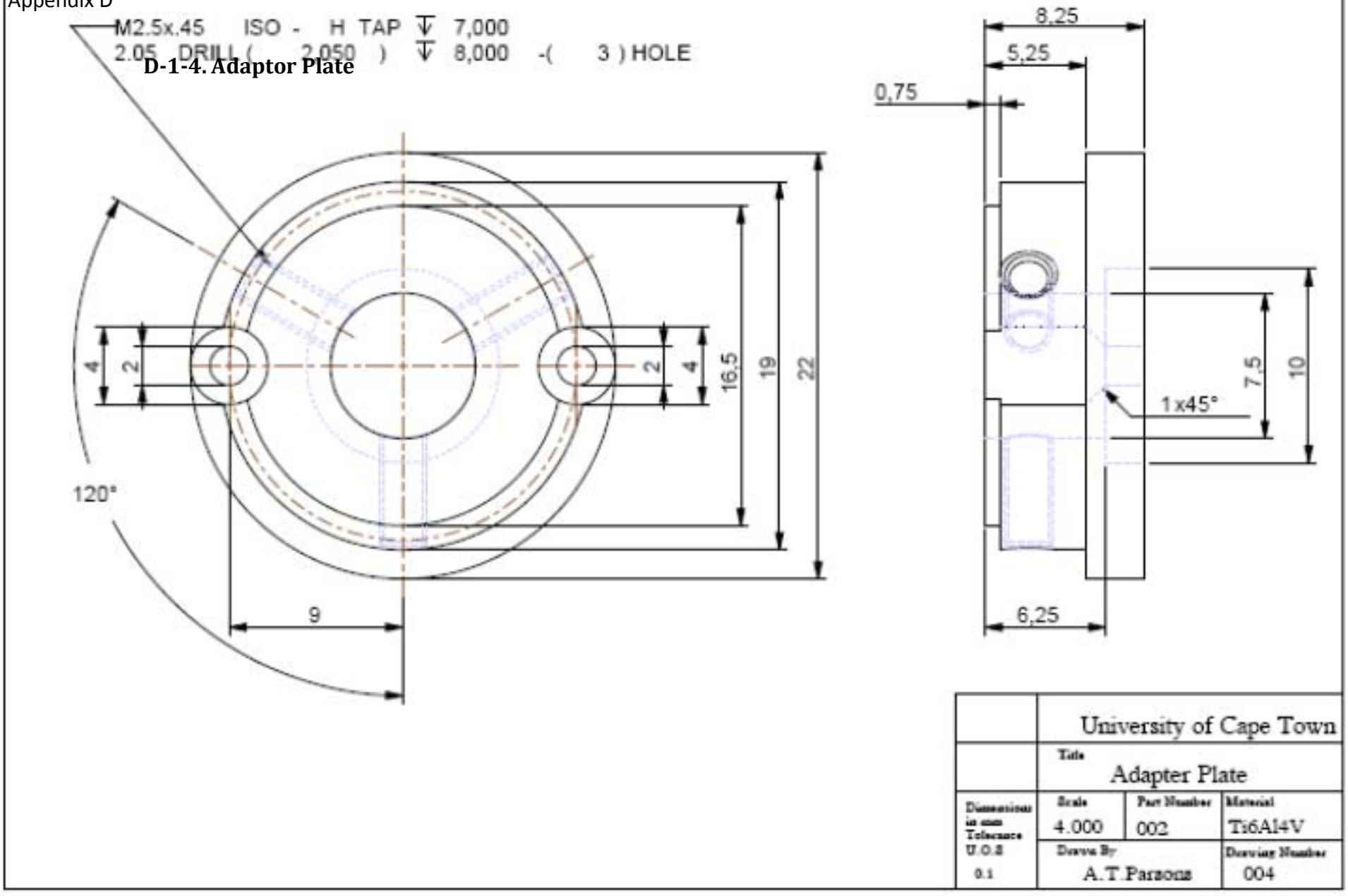

D-1-5. Transition Shaft

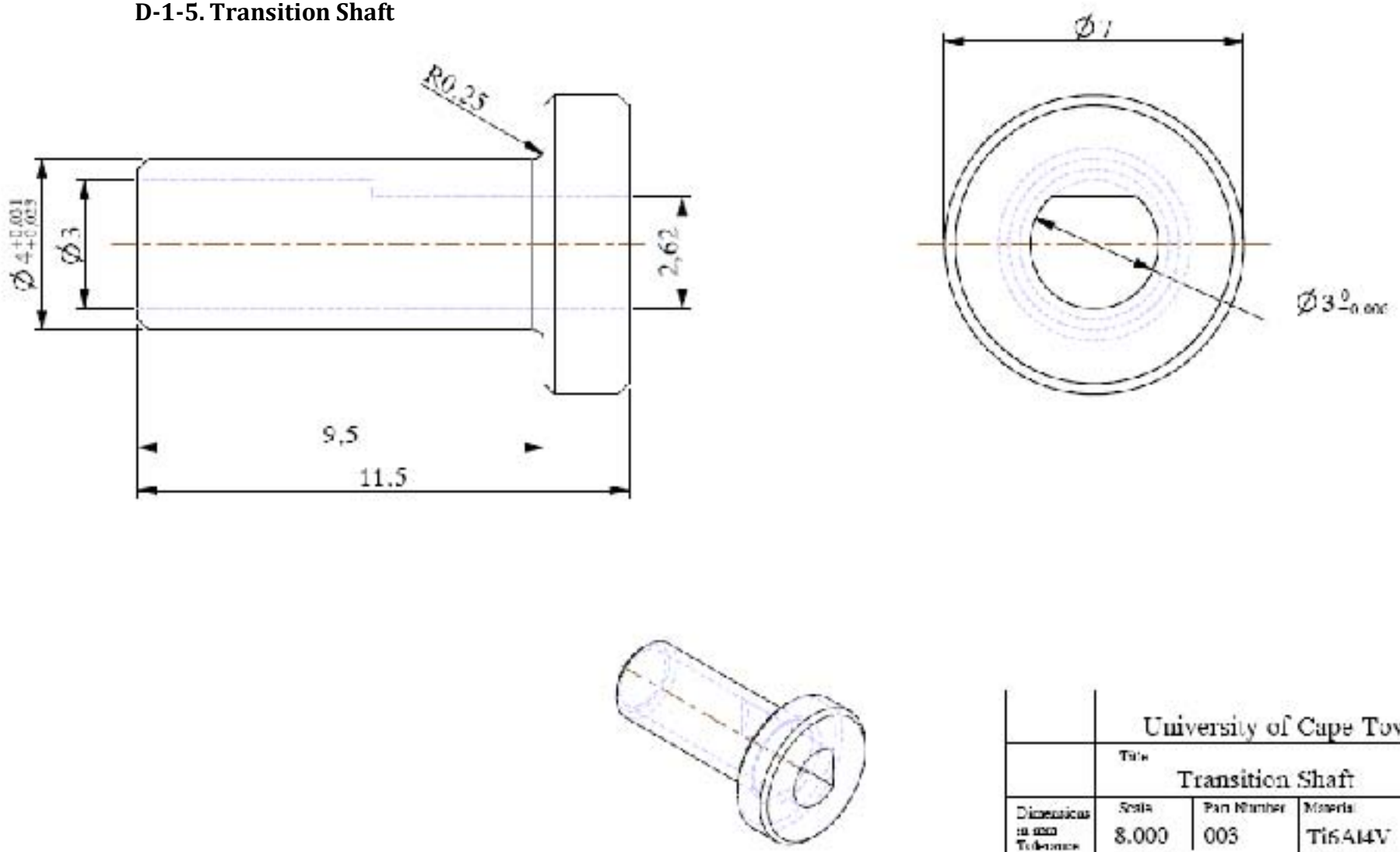

	University of Cape Town		
	Title: Transition Shaft		
Dimensions in mm Tolerance: U.O.S 0.1	Scale: 8.000	Part Number: 003	Material: Ti6Al4V
	Drawn By: A.T Parsons		Drawing Number: 005

D-1-6. Gearbox

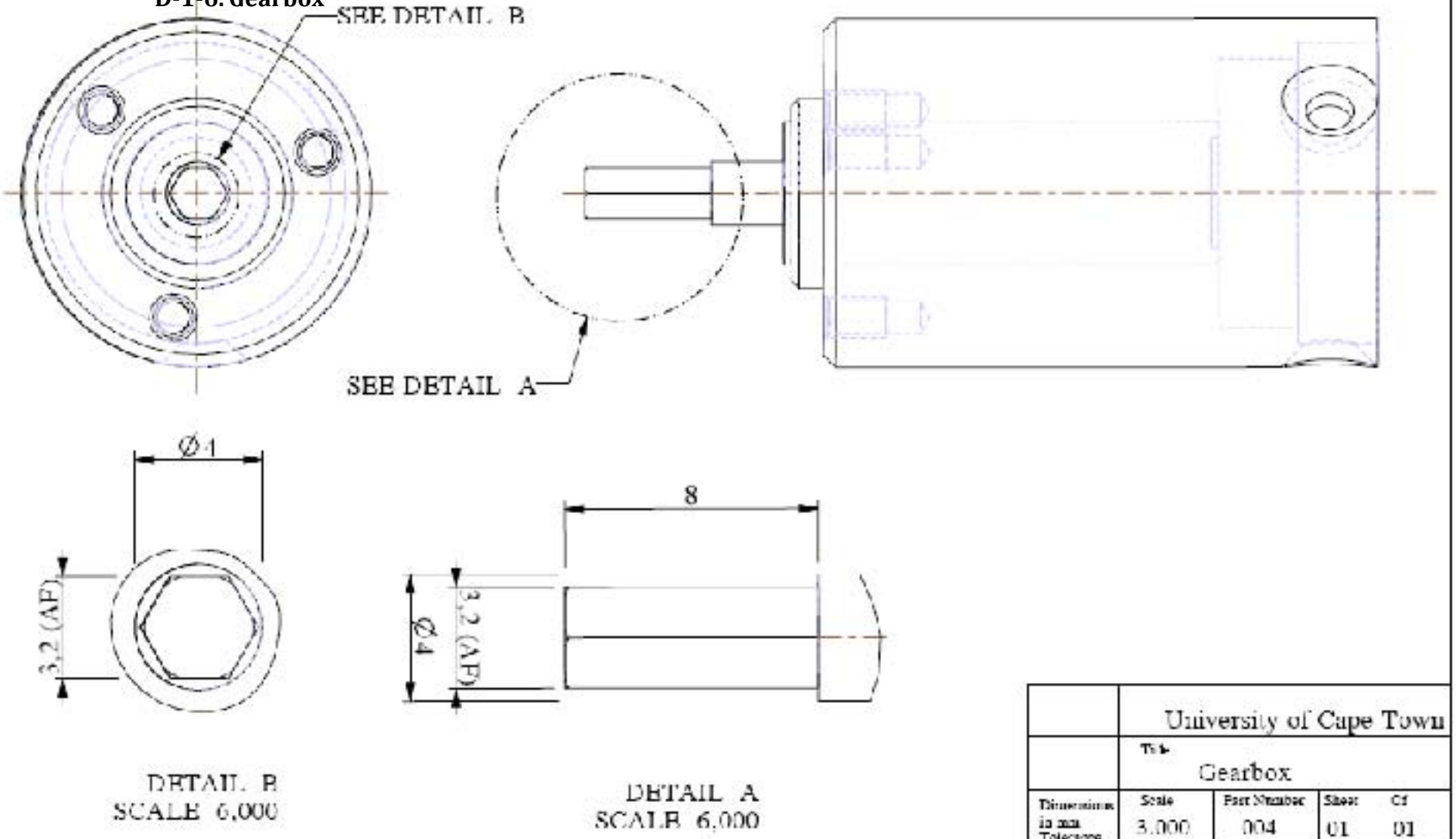
SEE DETAIL B
SEE DETAIL A
Ø4
3.2 (AF)
8
Ø4
3.2 (AF)
DETAIL B
SCALE 6.000
DETAIL A
SCALE 6.000
University of Cape Town
Title
Gearbox
Dimensions in mm
Tolerance
U.O.S
Scale
3.000
Part Number
004
Sheet
01
Of
01
Drawn By
A.T.Parsons
Drawing Number

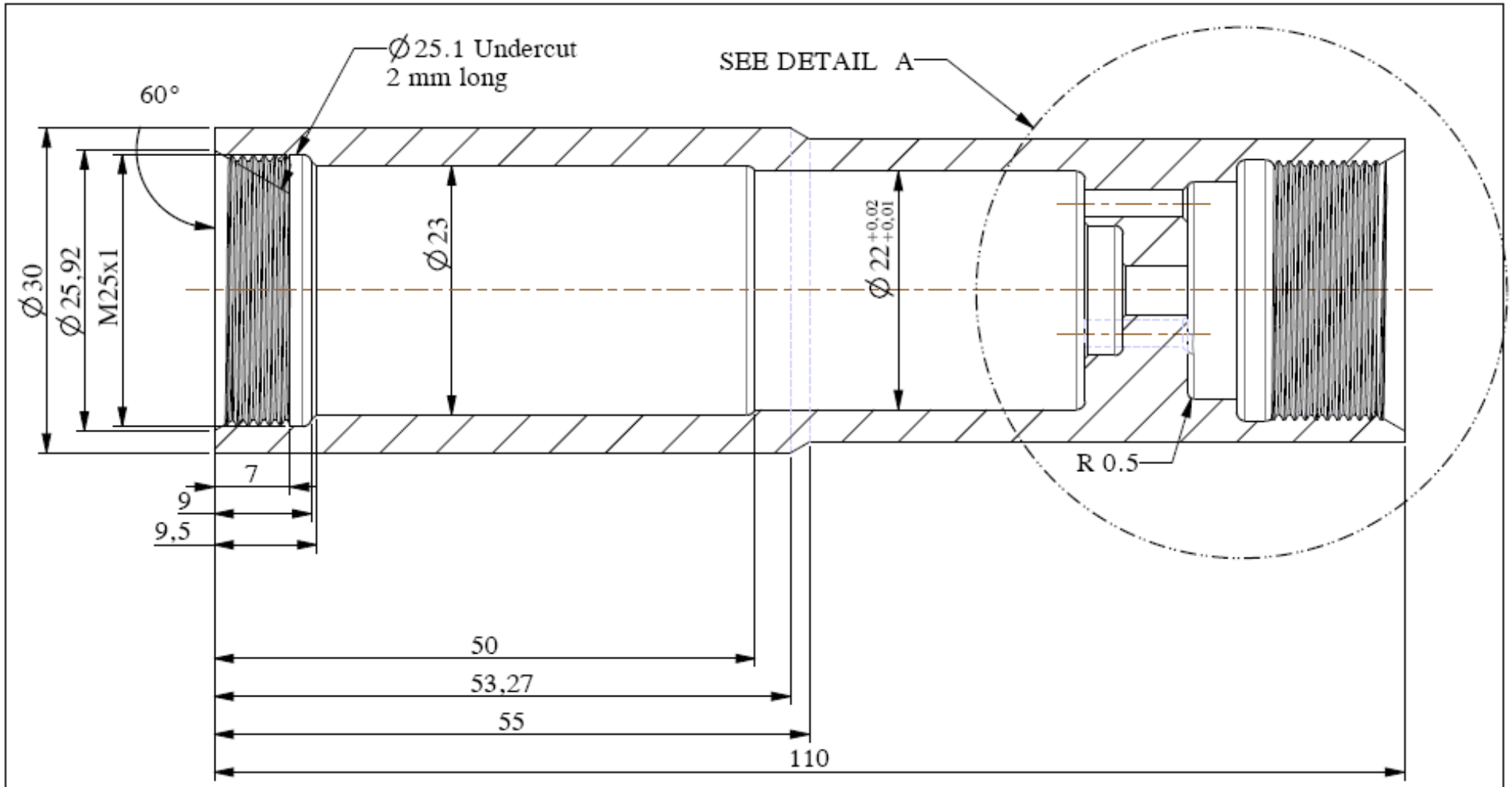

All Rounds 0.8
Unless Stated

Break All Corners

	University of Cape Town		
	Title: Drive Unit Casing		
Dimensions in mm Tolerance U.O.S 0.1	Scale: 2.000	Part Number: 005	Material: Ti6Al4V
	Drawn By: A.T.Parsons		Drawing Number: 008

D-1-8. Drive Unit Casing: Detail A

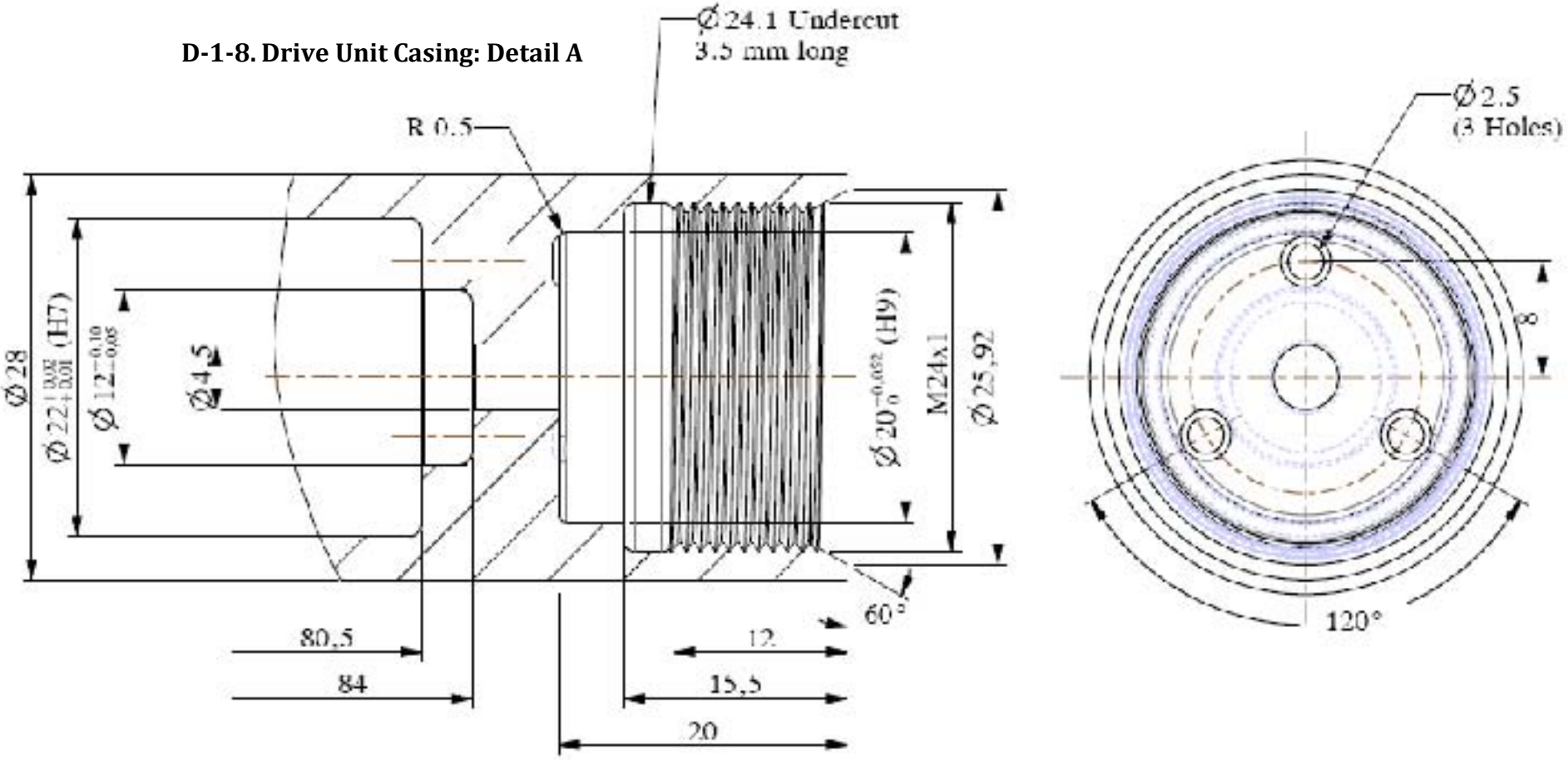

All Rounds 0.8
Unless Stated

Break All Corners

	University of Cape Town		
	Title: Drive Unit Casing Detail A		
Dimensions in mm Tolerance 0.05	Scale: 2.000	Part Number: 005	Material: Ti6Al4V
3.1	Drawn By: A.T.Parsons		Drawing Number: 008

D-1-9. Spacing Plate

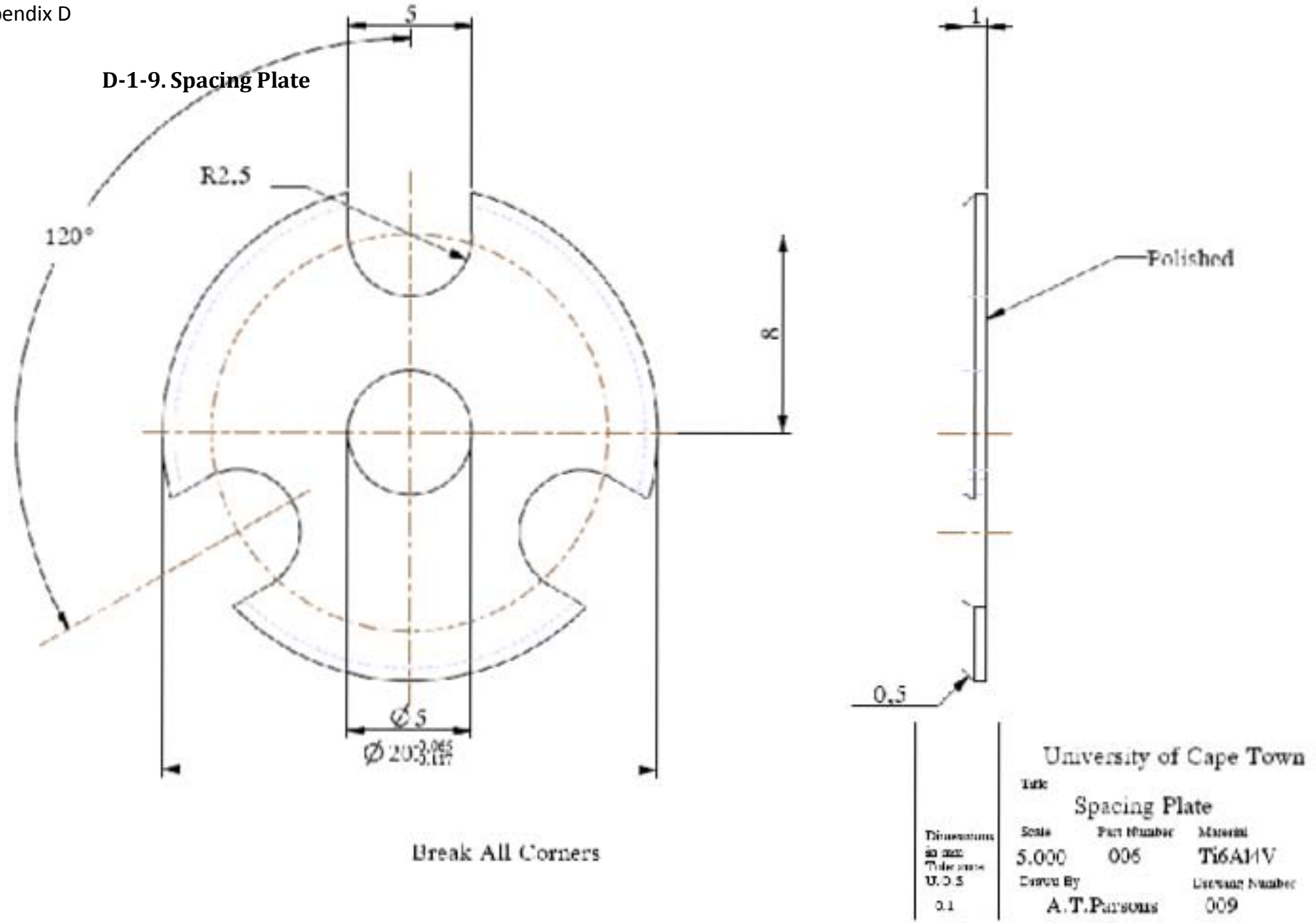

D-1-10. Drive Shaft

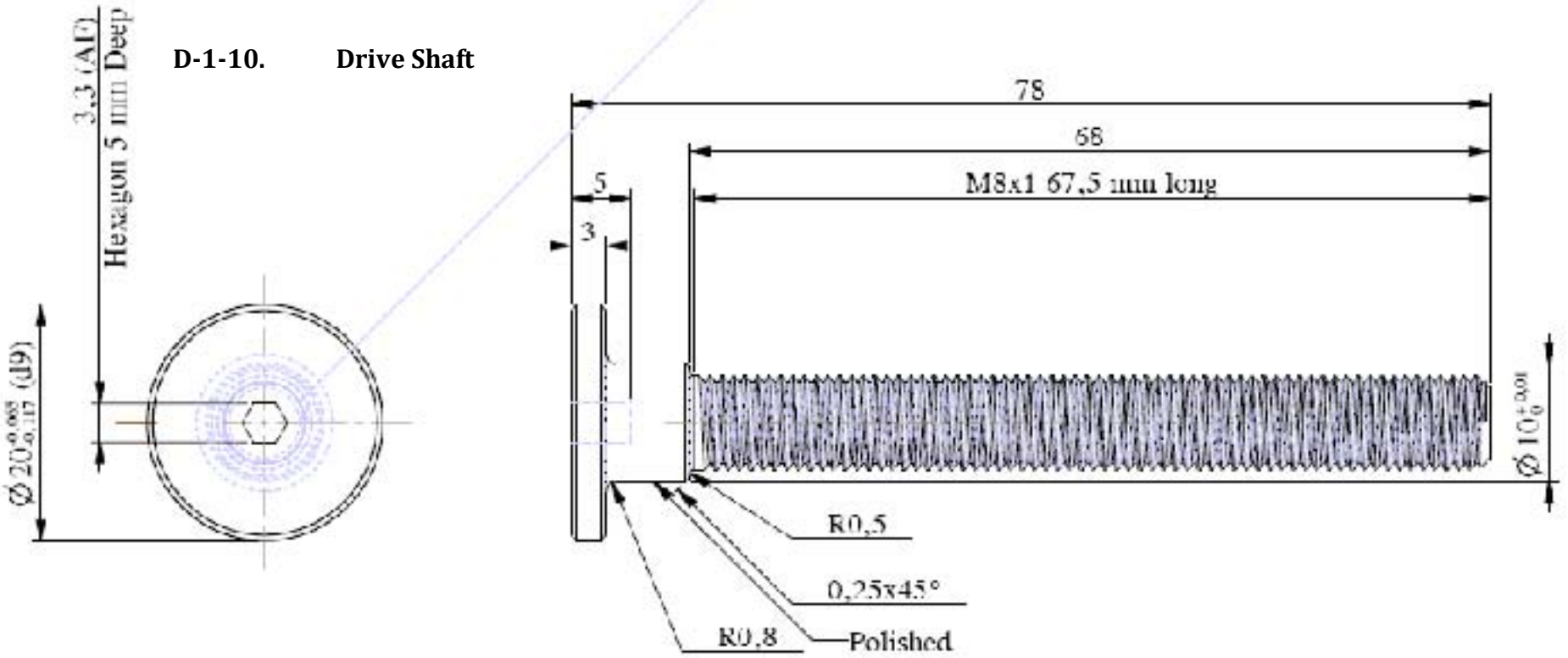

All Chamfers 1x45°
Unless stated

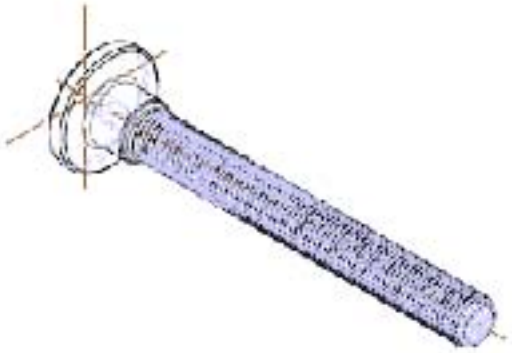

Dimensions in mm Tolerance U.O.S 0.1	University of Cape Town		
	Title: Drive Shaft		
	Scale: 2.000	Part Number: 007	Material: Ti6Al4V
	Drawn By: A.T.Parsons		Drawing Number: 010

D-1-11. UHMWPE Seal

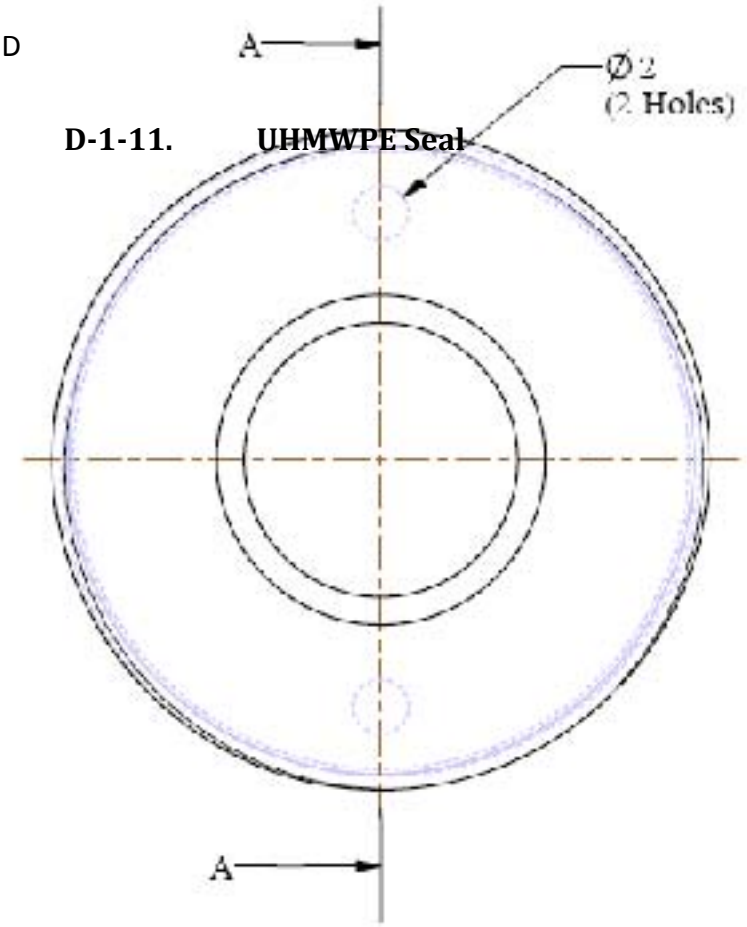

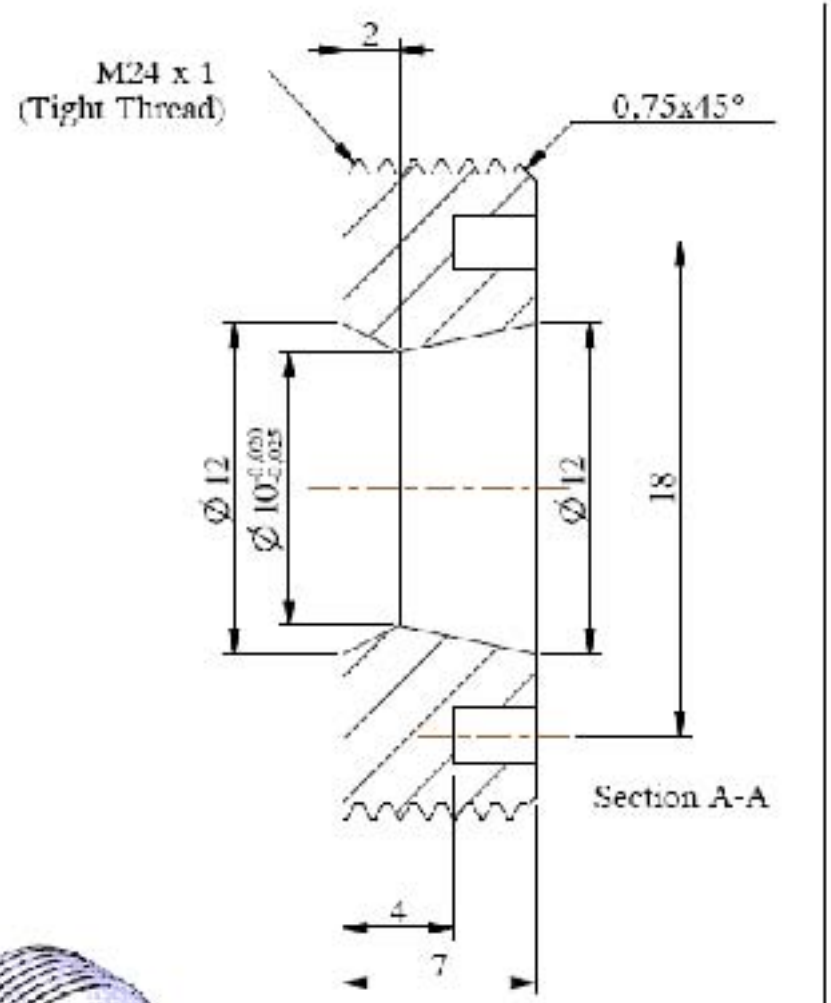

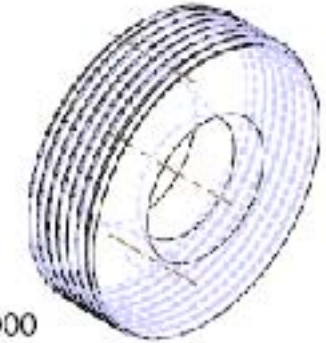

SCALE 2.000

University of Cape Town				
Title: UHMWPE Seal				
Dimensions in mm Tolerance U.O.S 0.1	Scale 4.000	Part Number 007	Sheet 01	Of 01
	Drawn By A.T. Parsons		Drawing Number	

D-1-12. Cover Shaft

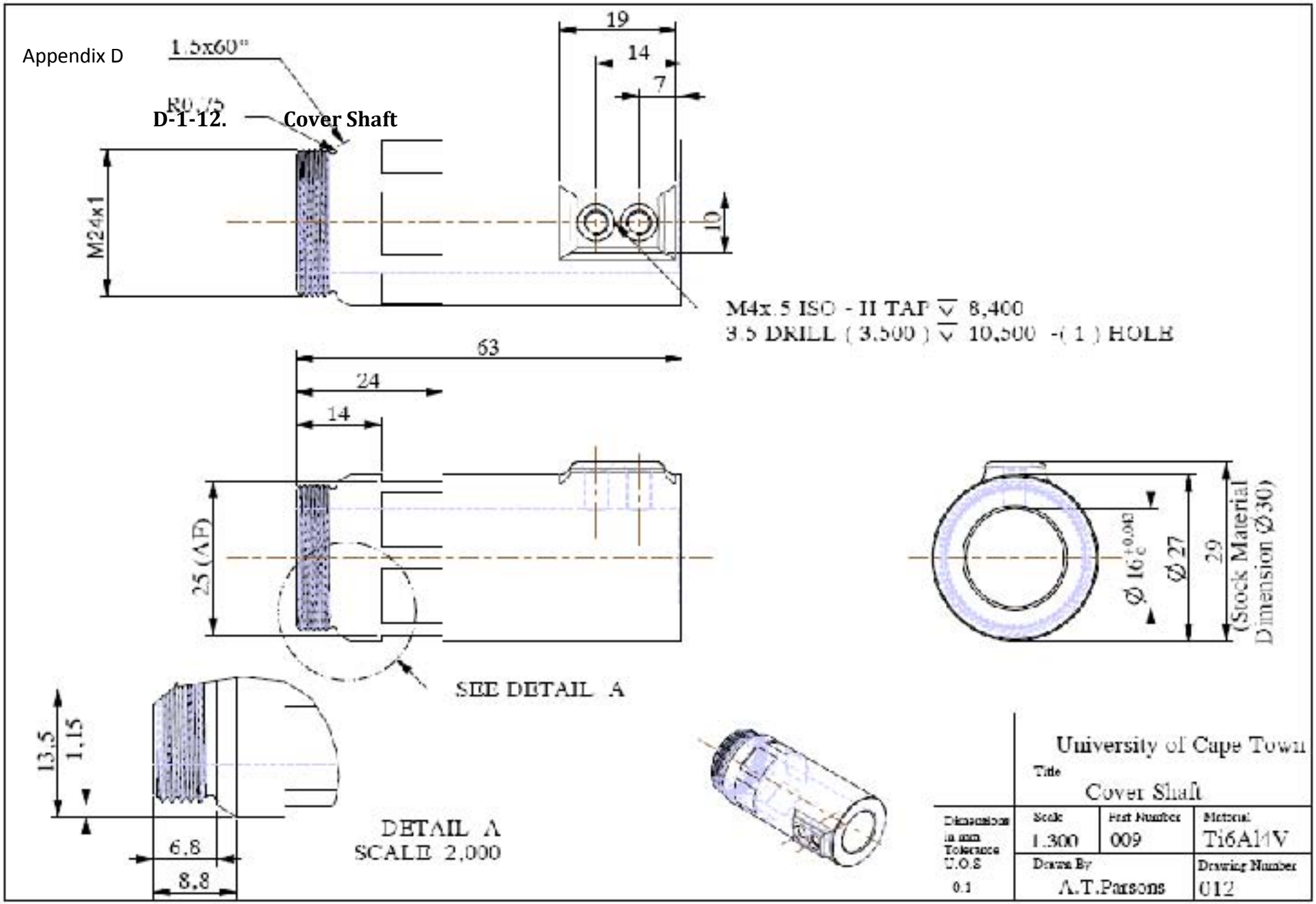

D-1-13. Extension Shaft

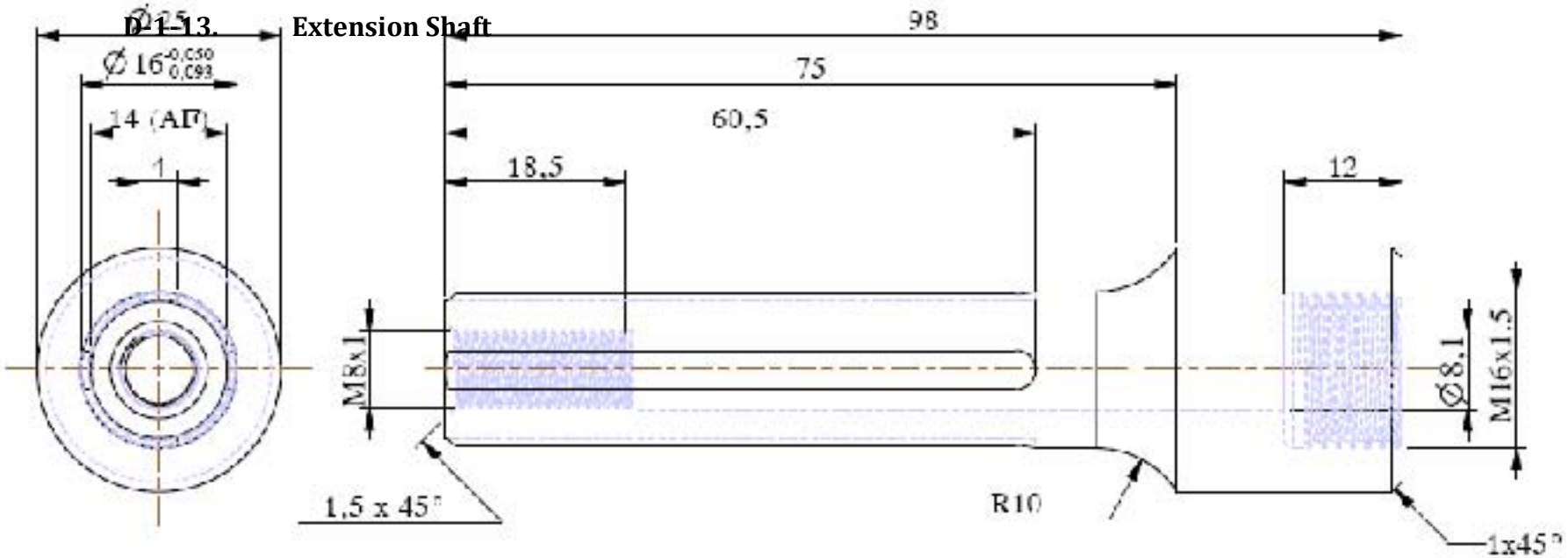

All Rounds 0.8
Unless Stated

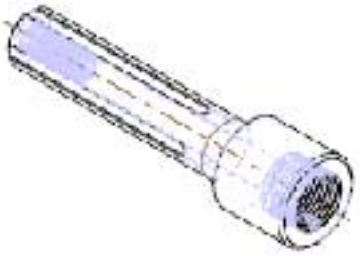

Dimensions in mm Tolerance U.O.S 0.1	University of Cape Town		
	Title: Extension Shaft		
	Scale: 1.600	Part Number: 010	Material: Ti6Al4V
	Drawn By: A.T. Parsons		Drawing Number: 013

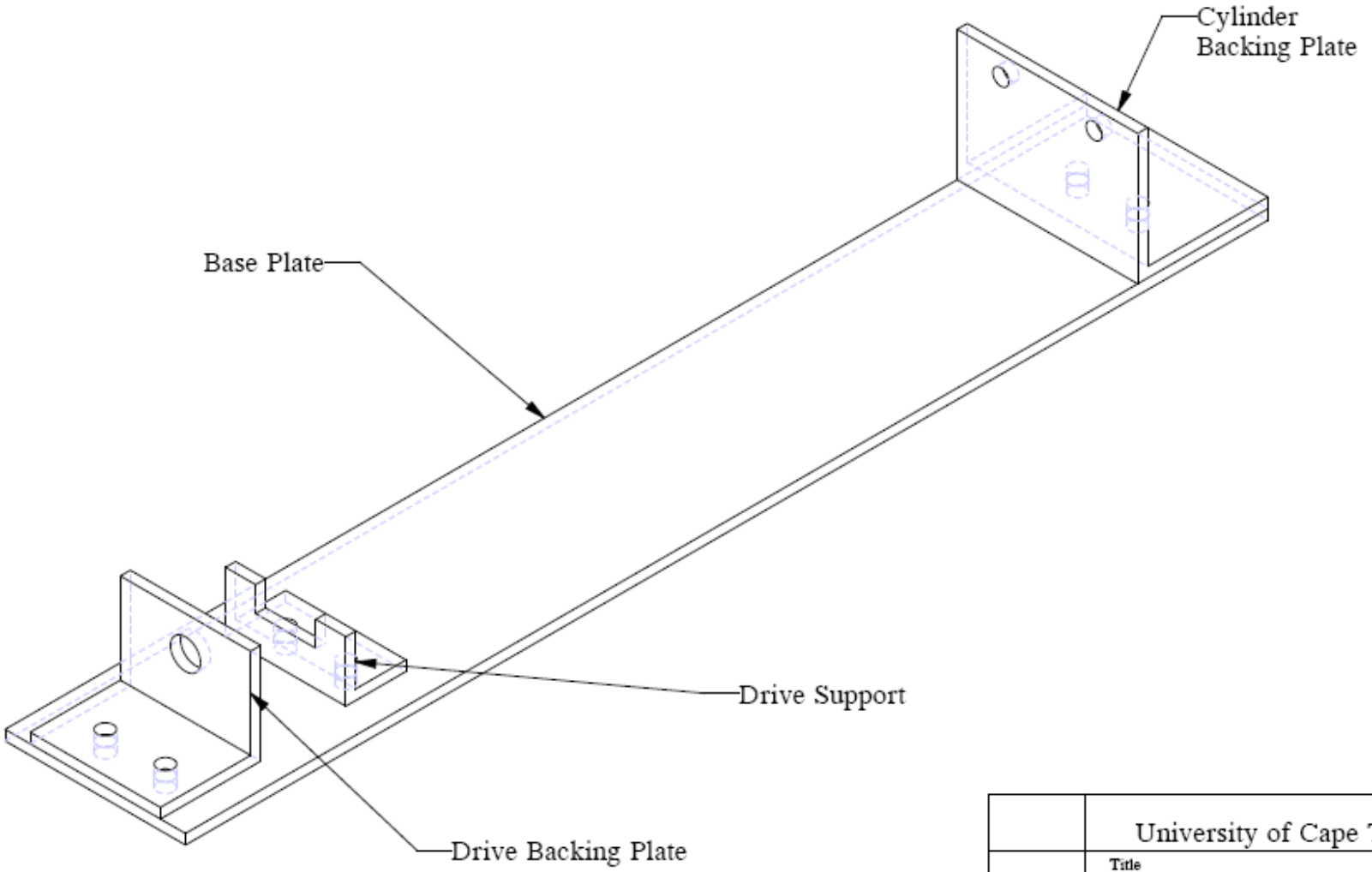

	University of Cape Town			
	Title: Test Rig Assembly			
Dimensions in mm Tolerance U.O.S 0.1	Scale: 0.500	Date:	Sheet:	Of:
	Drawn By: A.T.Parsons		Drawing Number:	

D-2-2. Base Plate

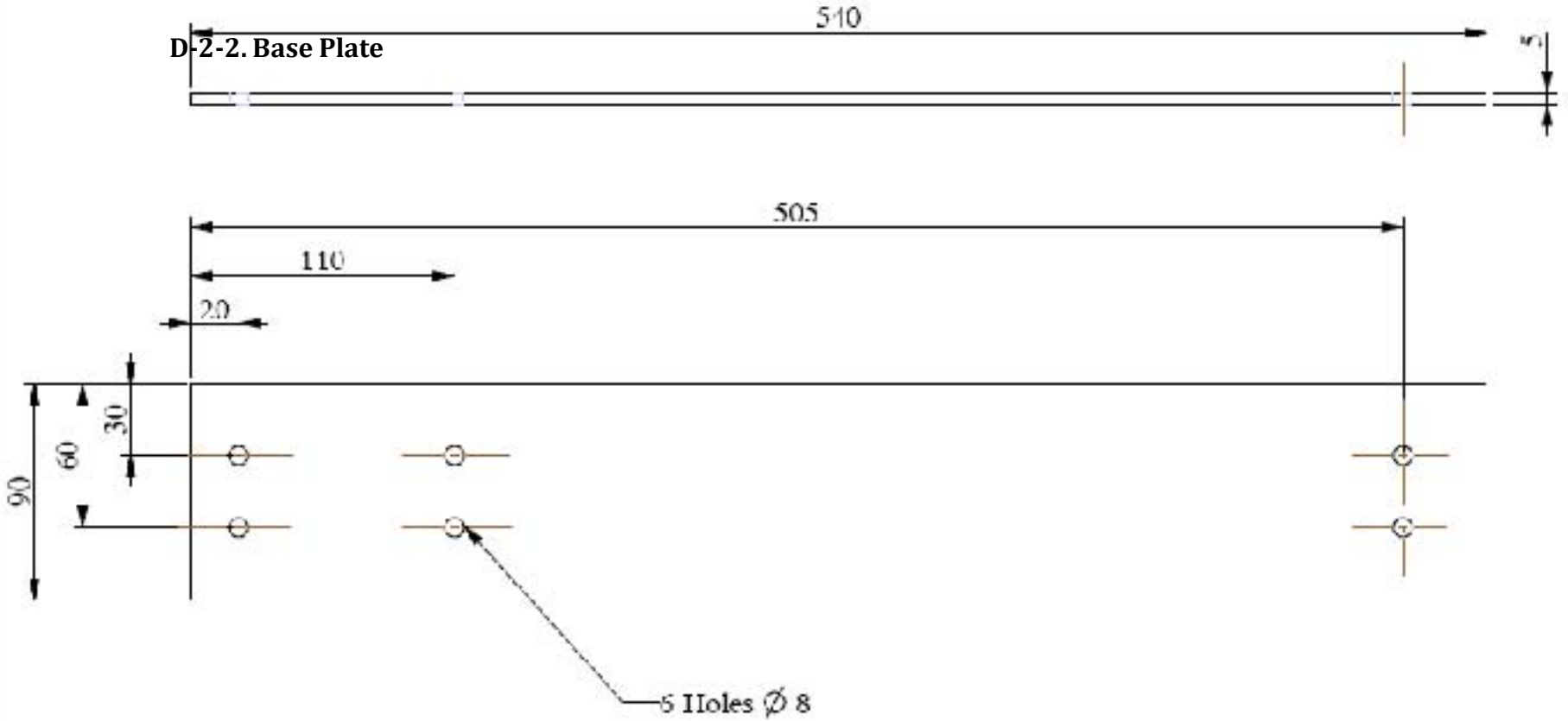

	University of Cape Town
Dimensions in mm Tolerance U.O.S 0.1	Title: Base Plate Scale: 0.400 Date: Sheet: Of Drawn By: A.T.Parsons Drawing Number:

D-2-3. Cylinder Backing

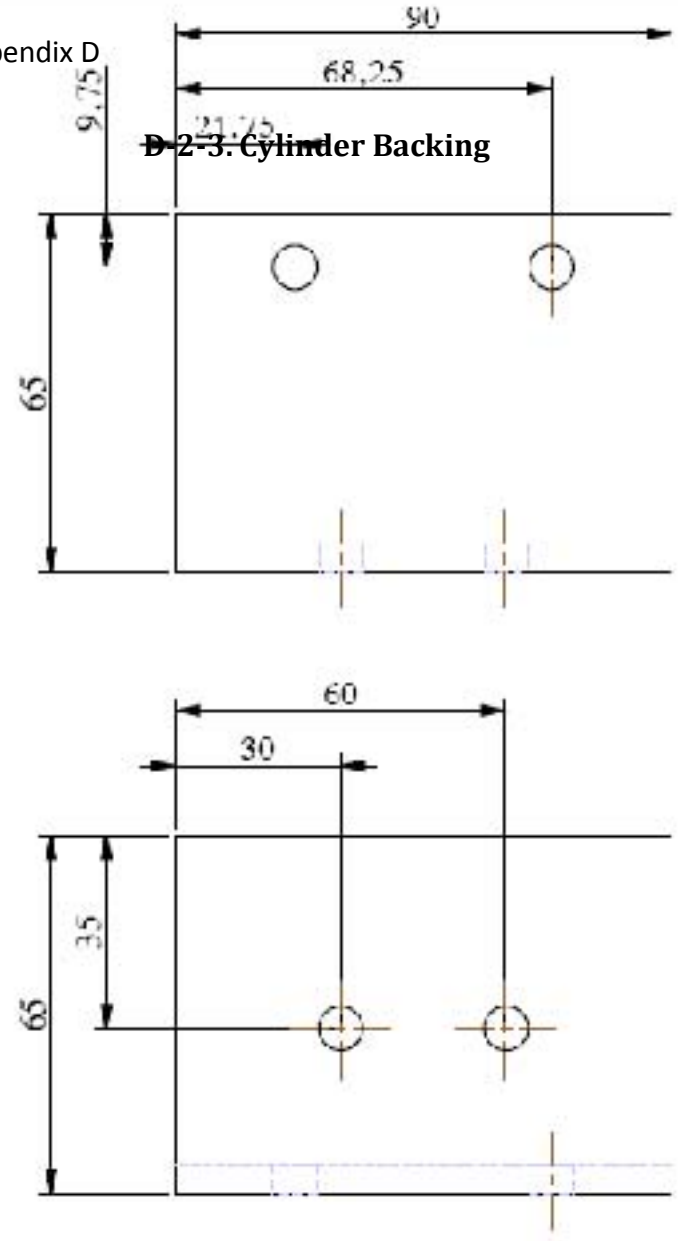

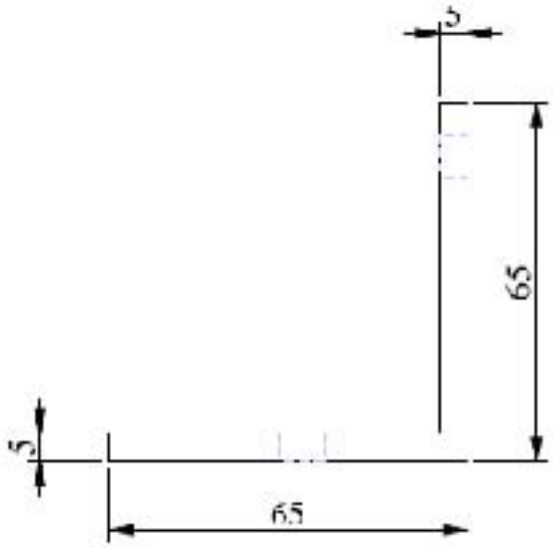

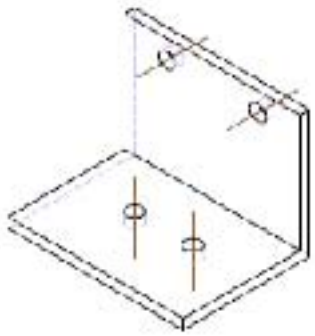

SCALE 0.400

	University of Cape Town		
	Title: Cylinder Backing Plate		
Dimensions in mm Tolerance ±0.5	Scale 0.800	Date	Sheet Of
0.1	Drawn By A.T.Parsons		Drawing Number

D-2-4. Device Backing

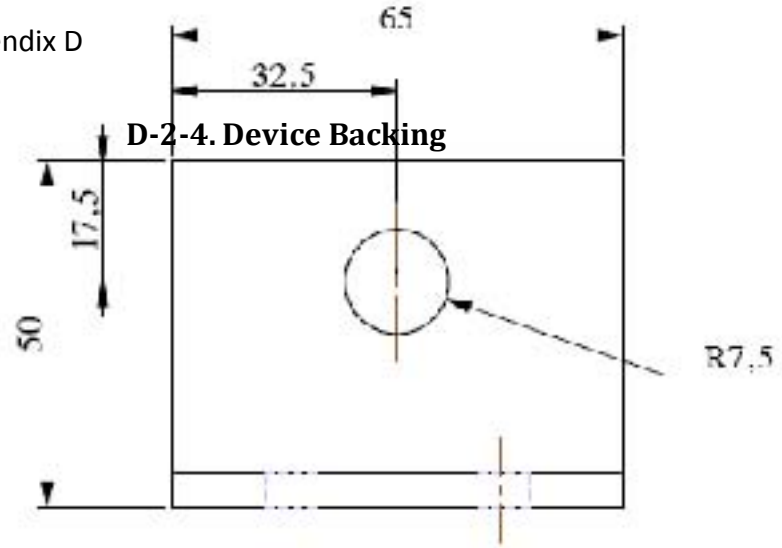

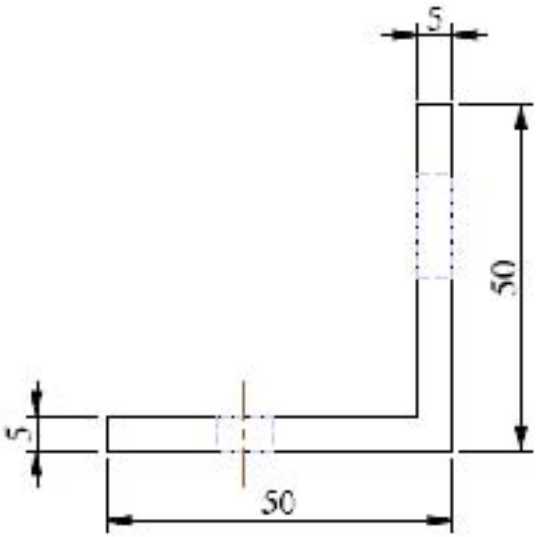

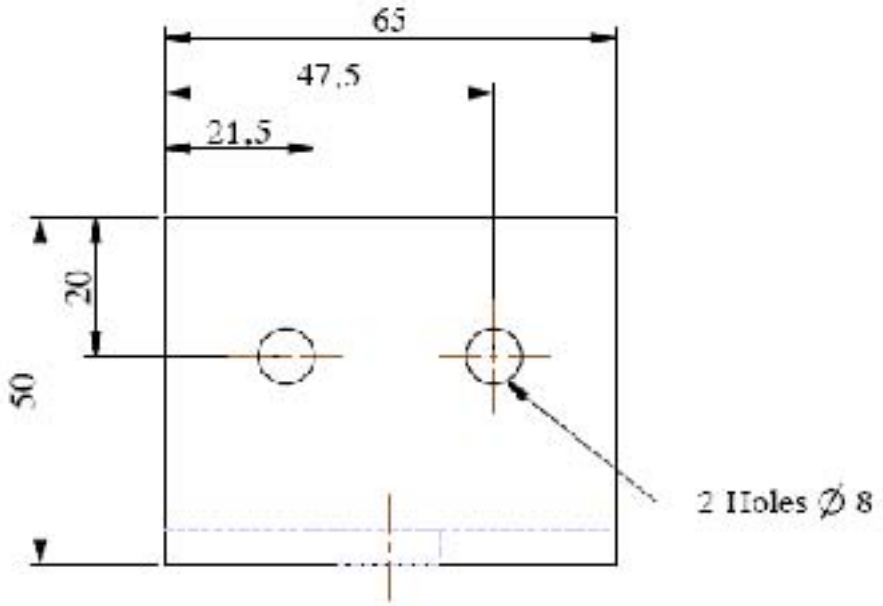

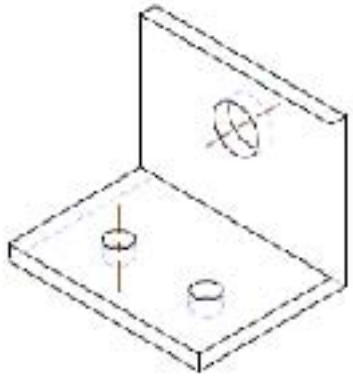

SCALE 0.600

	University of Cape Town
	Title: Drive Backing Plate
Dimensions in mm. Tolerance: U.O.S 0.1	Scale: 1.000 Date: Sheet: Of Drawn By: A.T.Parsons Drawing Number:

D-2-5. Device Support

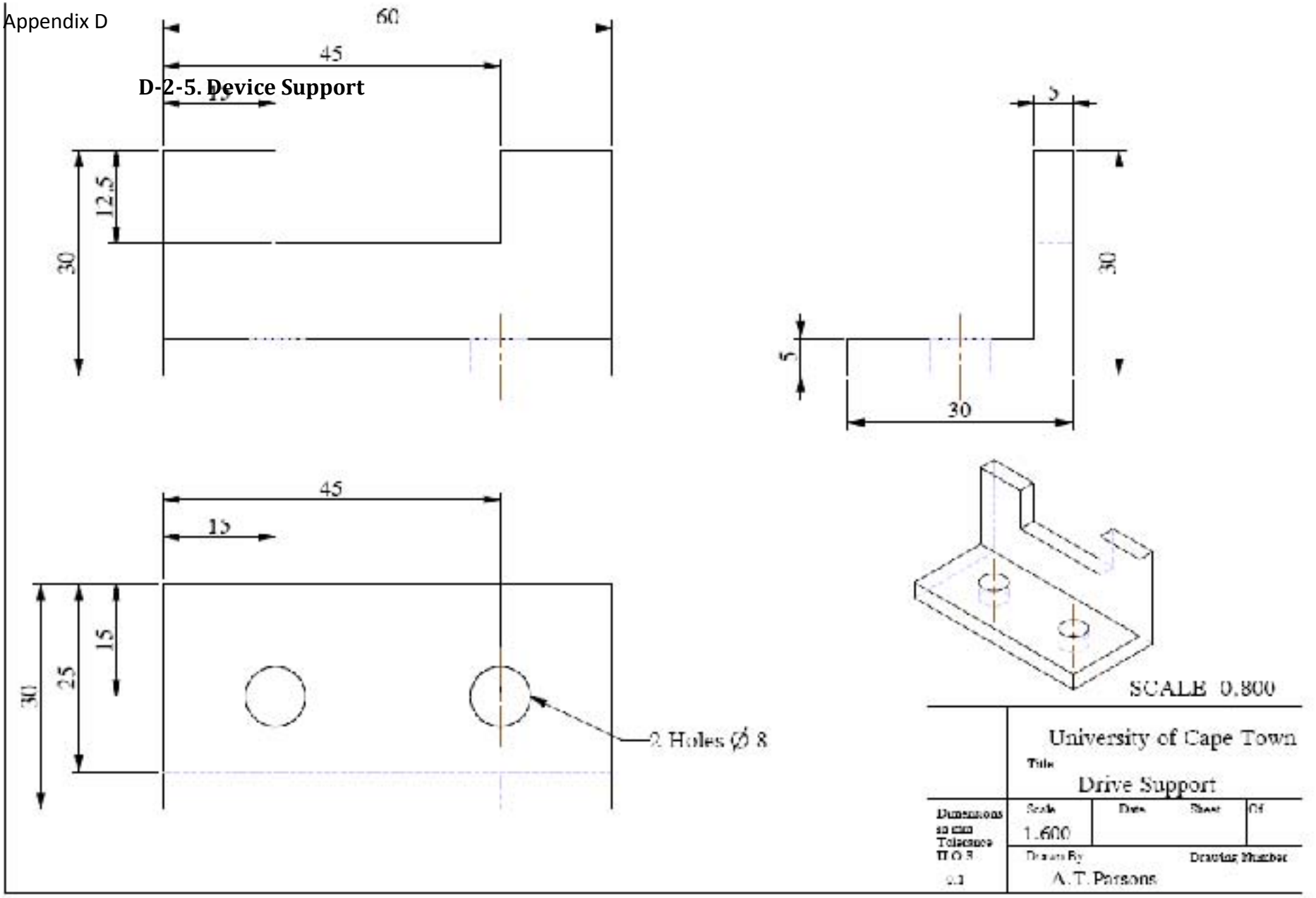

D-3. Circuit Diagram

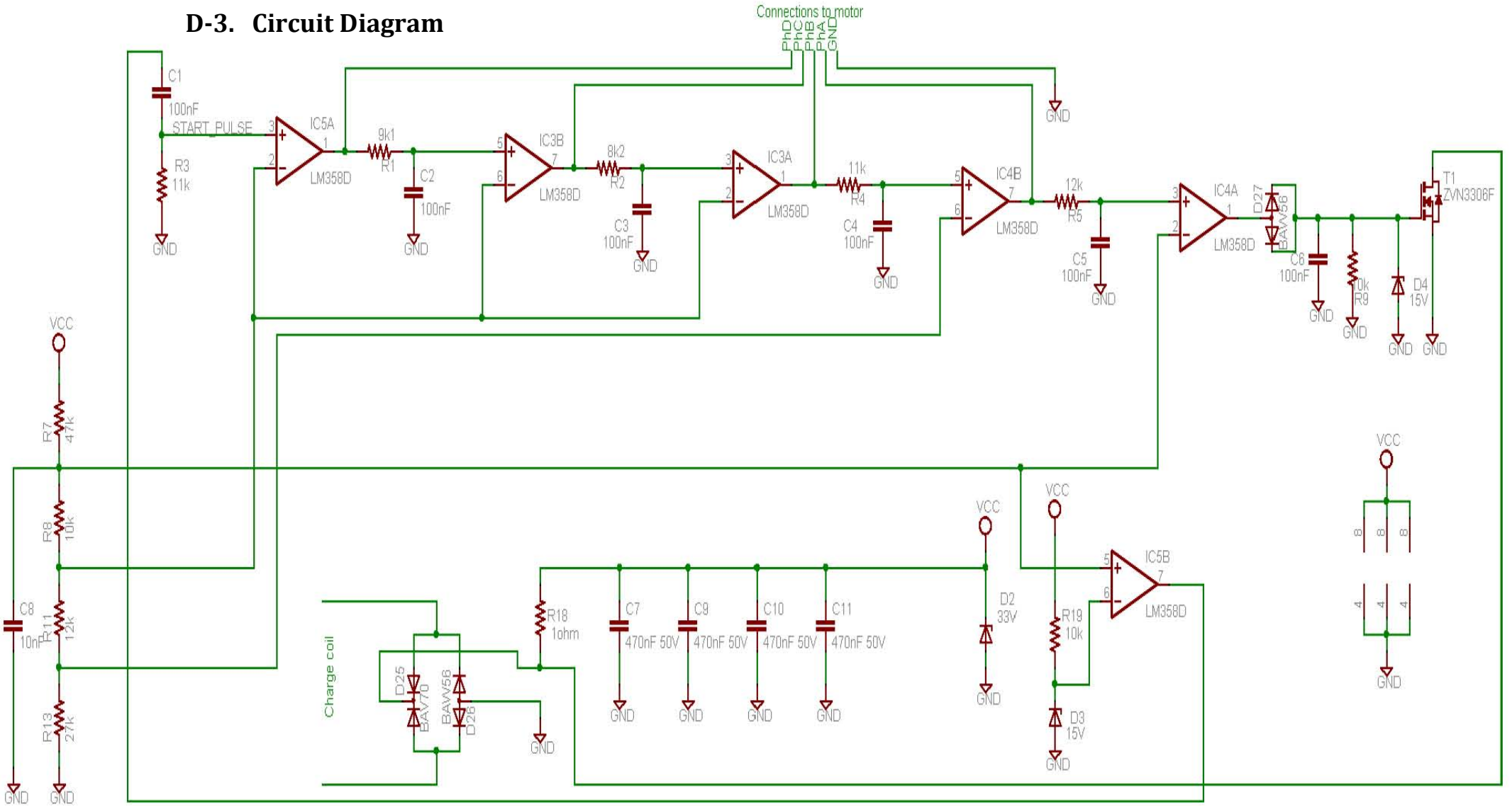

D-4. ERGO Case

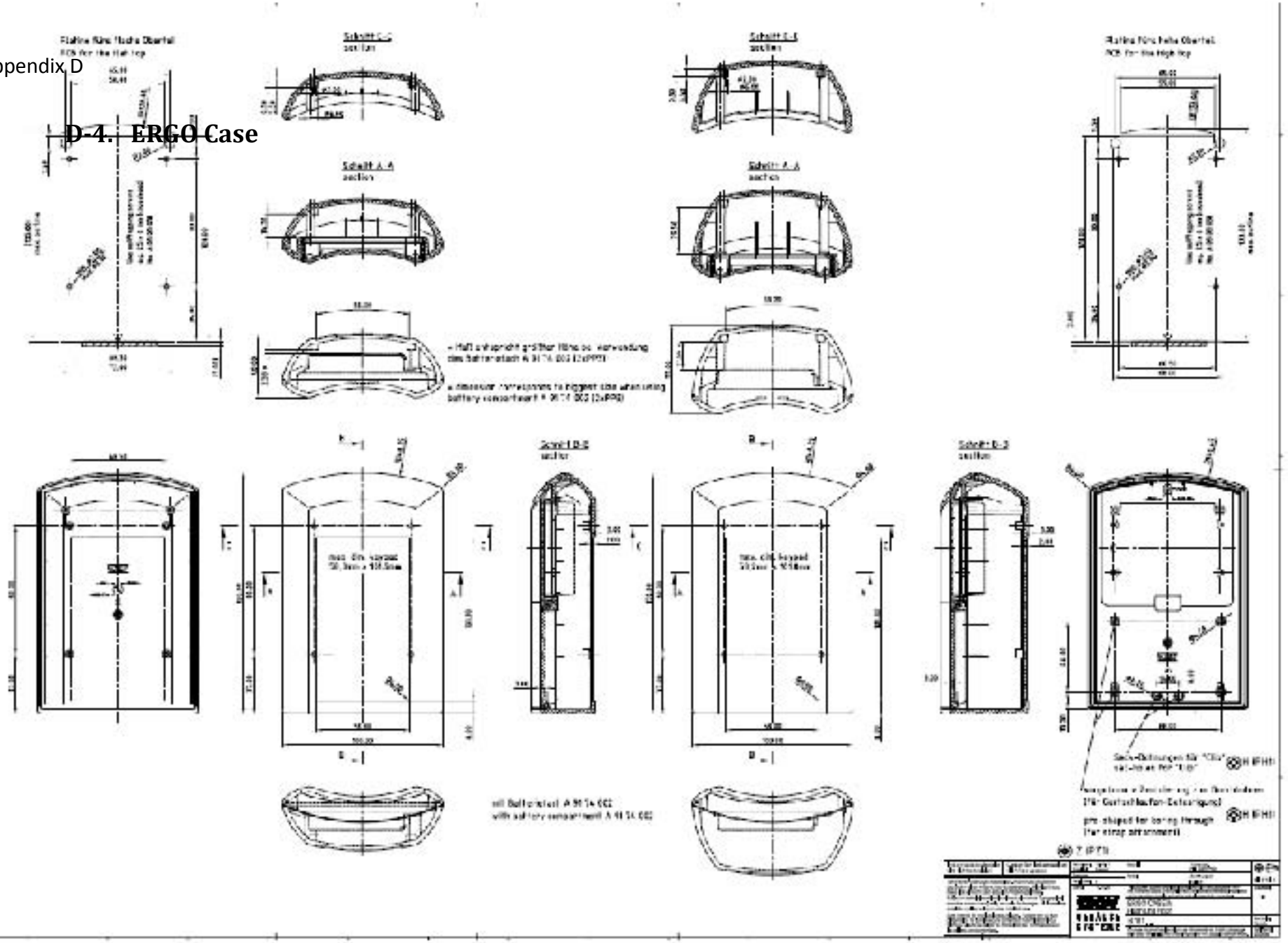

Appendix E

E. Calculations

E-1. Thread Dimensions

$$d_m = d - {}^{p}/_{2}$$

$$d_r = d - p$$

Where

$d = thread\ nominal\ diameter\ (m)$

$d_m = thread\ mean\ diameter\ (m)$

$d_r = thread\ minor\ diameter\ (m)$

$p = thread\ pitch\ (m)$

E-2. Thread Torque

$$\pi f d_m > l\ is\ the\ condition\ for\ self\ locking\ threads$$

$$T_R = \left(\frac{F d_m}{2}\right)\left(\frac{l + \pi f d_m}{\pi d_m - f l}\right)$$

$$T_L = \left(\frac{F d_m}{2}\right)\left(\frac{\pi f d_m - l}{\pi d_m + f l}\right)$$

Where

$T_R = raising\ torque\ (Nm)$

$T_L = raising\ torque\ (Nm)$

$F = linear\ force\ (N)$

$d_m = thread\ mean\ diameter\ (m)$

$l = thead\ lead\ (m)$

$f = material\ coefficient\ of\ friction$

E-3. Collar Friction

$$T_c = \frac{F f_c d_c}{2}$$

Where

$T_c = Collar\ torque\ (Nm)$

$F = axial\ load\ (N)$

$f_c = coefficient\ of\ friction$

$d_c = mean\ collar\ diameter\ (m)$

E-4. Thread Stress

The thread-root bending stress is calculated according to the principle stress formula,

$$\sigma' = \frac{1}{\sqrt{2}}\left((\sigma_x - \sigma_y)^2 + (\sigma_y - \sigma_z)^2 + (\sigma_z - \sigma_x)^2 + 6(\tau_{xy}^2 + \tau_{yz}^2 + \tau_{zx}^2)\right)^{1/2}$$

$$\sigma_x = {}^{6(0.38F)}/_{\pi d_r p} \qquad \tau_{xy} = 0$$

$$\sigma_y = 0 \qquad \tau_{yz} = {}^{16T}/_{\pi d_r^3}$$

$$\sigma_z = 0 \qquad \tau_{zx} = 0$$

Where

$\sigma' = Von\ Mises\ Stress\ (Pa)$

$F = axial\ load\ (N)$

$d_r = thread\ minor\ diameter\ (m)$

$p = thread\ pitch\ (m)$

$T = screw\ torque\ (Nm)$

E-5. Material Stress

$$\sigma_1 = \frac{\sigma_x + \sigma_y}{2} + \sqrt{\left(\frac{\sigma_x + \sigma_y}{2}\right)^2 + \tau_{xy}^2}$$

$$\sigma_x = {}^{My}/_{I} \qquad I = {}^{\pi d^4}/_{64}$$

$$\sigma_y = 0$$

$$\tau_{xy} = {Tr}/{J} \qquad J = {\pi d^4}/{32}$$

Where

$\sigma_1 = principal\ stress\ (Pa)$

$M = moment\ (Nm)$

$y = distance\ from\ centroid\ (m)$

$d = material\ dimension\ (diameter\ (m))$

$I = second\ moment\ of\ area\ (m^4)$

$J = polar\ second\ moment\ of\ area\ (m^4)$

E-6. Seal Torque

Formula used to calculate the torque required to overcome static friction of UHMWPE Seal

$$T = W \times l$$

Where

$T = torque\ (Nm)$

$W = weight\ (N)$

$l = length\ of\ moment\ arm\ (m)$

E-7. Endurance Limit

Formulae used to calculate material endurance limit (Shigley, Mischke & Budynas 2004)

$$S_e = k_a k_b k_c S_e^{'}$$

$$k_a = 4.51 S_{ut}^{-0.265}$$

$$k_b = 1.24 d^{-0.107}$$

$$k_c = 1$$

$$S_e^{'} = 0.504 S_{ut}$$

Where

$S_e = material\ endurance\ limit$

$k_a = surface\ factor$

$k_b = size\ factor$

$k_c = loading\ factor$

$k_d = temperature\ modification\ factor$

$k_e = miscellaneous - effects\ modification\ Factor$

$S_e^{'} = rotary - beam\ test\ specimen\ endurance\ limit$

$S_{ut} = material\ ultimate\ tensile\ strength$

$d = material\ dimension\ (diameter\ (m))$

E-8. Body Mass

The data captured by *Taylor & Walker (2001)*, relating to femoral loading is quoted in body weight units (BW). In order to accurately predict the material stresses in the growth module, this unit needed to be quantified.

$$BMI = {}^{m}/_{h^2}$$

Where

$BMI = body\ mass\ index$

$m = mass\ (kg)$

$h = height\ (m)$

Appendix F

F. Correspondence

F-1. Piezo Motor

F-1-1. Drive Signal

SV: SV: Follow up.

From: "Olle Lindkvist" <Olle.Lindkvist@piezomotor.se>

To: "Adam PARSONS" <Adam.Parsons@uct.ac.za>

Date: Tuesday - October 5, 2010 8:41 AM

Subject: SV: SV: Follow up.

Attachments: Mime.822

Dear Adam,

Yes you can drive using a square wave.

Best regards

Olle Lindkvist

Global Sales Manager

PiezoMotor AB

-----Ursprungligt meddelande-----

Från: Adam PARSONS [mailto:Adam.Parsons@uct.ac.za]

Skickat: den 4 oktober 2010 11:30

Till: Olle Lindkvist

Ämne: Re: SV: Follow up.

Dear Olle,

The information provided in the spreadsheet is not particularly clear. I would just like to know whether it is possible to operate the rotary motor with a square wave? Was the design of the driver outsourced?

Regards

Adam

>>> "Olle Lindkvist" 09/30/10 1:48 PM >>>

Adam,

Here are some wave forms.

Best regards

Olle Lindkvist

Global Sales Manager

PiezoMotor AB

_____

Från: adam.parsons@uct.ac.za [mailto:adam.parsons@uct.ac.za]

Skickat: den 30 September 2010 13:47

Till: Olle Lindkvist

Ämne: Re: Follow up.

Dear Olle,

I was hoping to establish what possible inputs (voltage waveform) I can supply the rotary motor with.

The standard driver for the motor supplies a sinusoidal waveform to the motor. For my application, it is preferable to supply either a square or trapezoidal waveform; is the motor capable of operations with such waveforms, or will it be detrimental to the motor life span?

Much appreciated

Regards

Adam

-

Adam Parsons

Contact Info:

Cell: 084 011 2919

E-Mail (1): adam.parsons.84@gmail.com

E-Mail (2): adam.parsons@uct.ac.za

_____

From: "Olle Lindkvist"

Date: Thu, 30 Sep 2010 13:26:45 +0200

To: Adam PARSONS

Subject: Follow up.

Dear Adam,

I want to follow up our previous conversation as I received a messaged from our UK distributor.

Anything I can do for you?

Best regards

OLLE LINDKVIST

Global Sales Manager

PiezoMotor Uppsala AB

Stålgatan 14, SE-754 50 Uppsala, Sweden

Phone: +46 (0)18-489 50 00 Direct phone: +46(0) 18-489 51 71

Mobil: +46(0)70-514 30 20 Fax: +46 (0)18-489 50 01

www.piezomotor.com E-mail: olle.lindkvist@piezomotor.se

F-1-2. Gamma Sterilisation

Re: SV: Rotary Piezo Motor

From: Adam PARSONS

To: Olle.Lindkvist@piezomotor.se

BC:

Date: Friday - June 10, 2011 10:29 AM

Subject: Re: SV: Rotary Piezo Motor

Dear Olle,

Thank you.

We will be exposing the motor to 25 kGy, I will let you know what the results are.

Kind regards

Adam

>>> Olle Lindkvist 06/09/11 8:47 AM >>>

Dear Adam,

What may be affected are plastics and epoxy depending on the radiation and energy used. Still, we believe it will work although it is hard to estimate the affect on the lifetime.

The plastics used would only be the connector.

We think that you have to judge and test this.

Thanks

Best regards

Olle Lindkvist

Global Sales Manager

PiezoMotor AB

-----Ursprungligt meddelande-----

Från: Adam PARSONS [mailto:Adam.Parsons@uct.ac.za]

Skickat: den 8 juni 2011 18:03

Till: Olle Lindkvist

Ämne: Rotary Piezo Motor

Dear Olle,

I hope you are well.

What type of piezo ceramics are used in the rotary motor? Alternatively, would the motor be capable of withstanding a dose of gamma radiation (when off and not powered) for the purposes of sterilisation without detriment to the operation of the motor?

Thank you

Kind regards

Adam

UNIVERSITY OF CAPE TOWN

This e-mail is subject to the UCT ICT policies and e-mail disclaimer

published on our website at

F-2. Wittenstein

Appendix G

G. Patent

No. 2011/

UNIVERSITY OF CAPE TOWN
IYUNIVESITHI YASEKAPA • UNIVERSITEIT VAN KAAPSTAD

Department of Research & Innovation

Research Contracts & IP Services
University of Cape Town · Private Bag · Rondebosch · 7701 · South Africa
Research & Innovation Building · 2 Rhodes Avenue · UCT · Mowbray · 7701
Fax: +27 (0)21 650 5778 · Tel: +27 (0)21 650-3355
www.rcips.uct.ac.za

INTELLECTUAL PROPERTY DISCLOSURE FORM

IMPORTANT NOTE ON PUBLIC DISCLOSURE

Please contact RCIPS before making any public disclosure of an invention. Failure to do so may result in the loss of rights to patent protection. Certain forms of disclosure can be managed by maintaining confidentially under written agreement and RCIPS can assist with this.

Public disclosure occurs through oral presentation at meetings at which the audience is not solely comprised of UCT Staff and Students, all forms of publication no matter how informal (abstracts, posters, non-accredited journals) as well as by SUBMITTING A THESIS for examination. Special provisions exist, however, for maintaining theses confidential for a period.

For any questions please contact: Andrew.Bailey@uct.ac.za tel 021 650-2425

Cynthia.Best@uct.ac.za tel 021 650-3076

IP Services Reception tel 021 650-4015

Date Submitted: {Please submit electronically}

Invention Title: **NON INVASIVE ENDOPROSTHETIC GROWTH CONTROL DEVICE**

Contact Inventor: **GEORGE VICATOS**

Do any of the Inventors work in an MRC-funded Group, Unit or Centre? ~~**Yes**~~ **/ No**

Inventor/s

PLEASE ADD ADDITIONAL TABLES FOR INVENTORS AS NECESSARY – Include Inventors from other institutions – note their affiliation in Department & Group/Unit field.

NB. **Full names and you home address details are required by the Patent Office.**

If you leave UCT, please keep our office updated as to your contact details so that we can track you for the payment of any royalty income accruing to the inventors.
*

FULL names [as per ID document]	GEORGE VICATOS
Title [Mr/Ms/Prof/Dr]	Dr
Department & Unit/Group	MECHANICAL ENGINEERING

Faculty	EBE
Staff or Student Number	00264733
Tel no.	021 6502492
Cell no.	0834243404
Email address	George.vicatos@uct.ac.za
Residential Address	1 Huguenot Avenue, Oranjezicht, 8001
Postal address & code if external, or UCT internal mail delivery address.	MECHANICAL ENGINEERING DEPARTMENT
Nationality	GREEK (RSA RESIDENT)

FULL names [as per ID document] & title:	SAMUEL ISAAC GINSBERG
Title [Mr/Ms/Prof/Dr]	Mr
Department & Unit/Group	ELECTRICAL ENGINEERING
Faculty	EBE
Staff or Student	01362217
Tel no.	021 6505297
Cell no.	0722072137
Email	Samuel.ginsberg@uct.ac.za
Residential Address	45 Cottage Mews, Fitzpatric Road, Milneron, 7441
Postal address & code if external, or UCT internal mail delivery address.	ELECTRICAL ENGINEERING DEPARTMENT
Nationality	RSA

FULL names [as per ID document] & title:	ADAM THANE PARSONS
Title [Mr/Ms/Prof/Dr]	Mr
Department & Unit/Group	MECHANICAL ENGINEERING
Faculty	EBE
Staff or Student	1264906
Tel no.	021 6502492
Cell no.	0840112919
Email	adam.parsons @uct.ac.za
Residential Address	3 Ellerslie Rd, Wynberg, 7808
Postal address & code if external, or UCT internal mail delivery address.	MECHANICAL ENGINEERING DEPARTMENT

Nationality	UK (RSA RESIDENT)

Share in Intellectual Property Creatorship (add more rows if necessary)

Note UCT inventors should record "UCT" in the Institution column.

Name	**Inventor/Enabler**[1]	**Institution / Company / Private**	**% Share**[2]
GEORGE VICATOS	INVENTOR	**UCT**	33.333 (1/3)
SAMUEL GINSBERG	INVENTOR	**UCT**	33.333 (1/3)
ADAM PARSONS	INVENTOR	**UCT**	33.333 (1/3)
			100

Applicant Details

Name: University of Cape Town

Address: Lovers Walk
Rondebosch
7701
Cape Town
South Africa

Courier/Street/Postal Address (for general communication)

Research Contracts & IP Services
Research & Innovation Building
University of Cape Town
2 Rhodes Avenue (Cnr Main Road)
Mowbray
7701
South Africa

Advise RCIPS of any other party, e.g. a funder who may have certain rights to this intellectual property (even if they funded only part of the work).

[1] An "Inventor" must contribute intellectual property to the inventive step that resulted in the invention. An Enabler is not involved in the inventive step, but may have done significant work, as directed by the inventors to prove the concept. Inventors may wish identified Enablers to share in any royalty income accruing to the Inventors. Additional information can be obtained by contacting RCIPS.

[2] This share is the basis on which the Inventors' portion of possible royalty income will be shared. A default situation is where the inventors elect to share the proceeds equally.

NONE

Summary: What is your invention and what does it do? Mention its potential commercial or societal value and mention the products or services that a company may develop based on the technology. (One or two paragraphs)

It is an endoprosthetic device to replace bone tissue to skeletally immature patients. It provides length adjustment to limbs (humerus, femur, and tibia) without surgical intervention. It requires an electromagnetic signal which is transmitted through the skin. It provides a feedback signal from which the extension and the tension of the soft tissues are monitored.

There are very few devices that perform limb lengthening. These devices need minimal surgical procedures to lengthen. Only recently, motorised devices were introduced in the market, but these utilise permanent magnets internal to the device and cumbersome and heavy external induction coils.
To the contrary, the under development device, utilises the combination of a piezo-motor, gearbox and screw-thread to provide a lengthening force of 2000N, while the signal is transmitted from a patient-friendly control device.

Public Disclosure: (e.g. conference presentation, publication of paper, thesis submission, dissertation).

a) Has the invention been disclosed?

~~Yes:~~ ~~Date:~~

No:

b) Is any public disclosure planned?

Yes: Date: (Pending patent registration)
It will be made public once the MSc dissertation is submitted at the end of the year.

~~No:~~

c) Nature of Public Disclosures:

	Date Disclosed	Date Planned	Comments
Journal Articles			
Conference Papers			
Abstracts			

	Date Disclosed	Date Planned	Comments
Presentations			
Posters			
Grant/ Funding Proposals			
Potential Funder/ Commercial partner			
Academic Collaborator			
Thesis/ Dissertations		END OF AUGUST 2011	A SEMINAR MAY BE PLANNED TOO
Other			

Full Technical Description

Provide a FULL technical description of your invention (nature, purpose and operation) with sufficient detail that would enable a skilled person to replicate your invention. Experimental results, or details of prototypes, should be included where available. This section may be submitted as a separate document.

SEE DOCUMENT

Distinguishing Features

What are the advantages/differences of your invention over existing technology, i.e. what are the improvements? *Include a brief overview of existing, similar technology (ies).*

- Piezo-motor
- Electromagnetic transmission for power
- Feedback on extension
- The device is impervious to MRI exposure, hence sharp/clear images of surrounding tissue can be obtained

What possible extensions, variations or modifications are there? [*This assists with ensuring that ongoing and future work will be accommodated in the patent specification of possible*].

- Measurement of tissue tension
- Reduction of dimensions of motor/gearbox depending on manufacturers
- Location of control electronics inside the receiver unit, under the skin rather than inside the implant

In what way(s) is your invention 'inventive' or not obvious to people with your technical skills? *Describe any surprising effects or outcomes that could not have been predicted based on current understanding or theory.*

Existing devices use minimally invasive surgery to give access to the extending mechanism. Other devices use permanent magnets and an external rotating magnetic field as a driving mechanism.
The feedback on extension is by measuring the position of the devise at successive x-ray images.

Prior Art

Please submit a Prior Art Search Report with this Invention Disclosure Form, i.e. a review of patents and general literature to confirm the novelty of your invention. Separate information on the report requirements can be obtained from RCIPS.

STANMORE
IMPLANT CAST

Use of Biological (or other) Materials

Is the invention:

i) Based on, or derived from, a South African indigenous biological resource of a genetic resource?

Yes		No	X

ii) Based on, or derived from, traditional knowledge or use

Yes		No	X

iii) Co-owned with the local community or individual

Yes		No	X

Materials

a) Materials received from third parties under materials transfer agreement:

NONE

b) Sources:

N/A

c) Conditions of transfer including relevant agreements (RCIPS can assist here):

N/A

d) Do the conditions of transfer permit commercial exploitation and use of the material? If so, do any royalties need to be paid?

N/A

Confidentiality

Please list any relevant Confidential Disclosure/Non-Disclosure Agreements.

- UCT STAFF / STUDENT

Source of Research Funding

a) Funding sources:

Funder	Amount (R)
Materials funded by research entities	negligible

b) Relevant agreements (RCIPS can assist with this):

Funder / Party	Agreement Reference No.*	Date
NONE		

* UO (University Office) number or Fund number

c) Special terms:

Funder / Party	Comments
NONE	

Stage of Development

a) What is the current stage of development:

i) an idea	
ii) a proven concept	X

iii) a working prototype ☐

b) What is still to be done?

Next Developments	At UCT	External	Time Required	Projected Costs
Test the electronic components under gamma radiation and MRI exposure	X		June-July	MRI costs-negotiation with Sport Science Centre
Mechanical testing of prototype	X		June-July	minimal
Testing of hydraulic seals	X		June-July	minimal
Force response Temperature response	X		June-July	minimal
External transmitter/control unit	X		June-July	minimal

Potential Commercial Partners/Licensees

a) *Companies that may be interested in the invention:*

- Implant manufacturers of tumour prosthetics

b) *Existing links with potential commercial partners:*

- None yet

c) *Technical, marketing and investment contacts with knowledge relevant to the potential application that could assist with the commercial evaluation of the invention:*

- Yes. George Vicatos has and, also there are local and international companies that can promote the device.

d) *Information on the commercial viability of the invention, e.g. selling price, potential markets, or a business plan:*

- Selling price: about R250,000
- National and international market
- No business plan yet

G-2. Technical Description

Overview

The device is necessary to provide linear extension of Long bones in-vivo for skeletally immature patients, achieved through functional components, namely a piezo motor, gearbox and screw. The motor provides the necessary driving force, while the gearbox increases the torque and the screw provides further gearing as well as converting the rotational motion into linear, extended the length.

The motor is controlled and powered externally, via inductive coupling across the patient's skin. A cable delivers the power to the drive electronics (located immediately behind the piezo motor (dwg no. 002)) through a hole in the drive unit casing, sealed by means of biocompatible glue.

Given the operating environment for the device, biologically incompatible components (motor electronics, motor and gearbox) are to be completely sealed from the external environment (body fluids), while all components in contact with body fluids are of biocompatible materials, namely Titanium (Ti6Al4V) and Ultra High Molecular Weight Polyethylene (UHMWPE).

Description of Mechanical Extension Device.

List of mechanical components and corresponding drawings:

Component	Part No.
Piezo Motor	001
Adapter Plate	002
Transition Shaft	003
Gearbox	004
Drive Unit Casing	005
Spacing Plate	006
Drive Shaft	007
Seal	008
Cover Shaft	009
Extension Shaft	010

Drive Unit

The device drive unit consists of a Piezo Legs Rotary Motor (prt no. 001) connected to a Wittenstein Cyber Motor GCP 022 196:1 Gearbox (prt no. 004), sourced from separate suppliers. A fabricated transition shaft (prt no. 003) facilitates compatibility, connecting the motor output shaft and gearbox input, ensuring transfer of power between the motor and gearbox. The gearbox output shaft is further modified to a hexagonal shape, allowing transfer of power to the drive shaft (prt no. 007). The gearbox and motor are then rigidly

fixed to each other by means of an adapter plate (prt no. 002) and mounting screws, forming the complete drive unit.

The drive unit locates within the drive unit casing (prt no. 005), rigidly fixed in position by three machine screws. A polished spacing plate (prt no. 006) provides clearance between the screw heads and the drive shaft, as well as a low friction contact surface for the rotating drive shaft. The drive shaft (prt no. 007) locates within the drive unit casing on the gearbox output shaft and against the spacing plate. The contact surfaces between the spacing plate and drive shaft are polished to minimise frictional forces.

Sealing

A UHMWPE seal (prt no. 008) locates on the drive shaft, against a shoulder within the drive unit casing. The liquid seal with the drive shaft is produced by an interference fit. The cover shaft (prt no. 009) threads into the drive unit casing, compressing the UHMWPE seal against the locating shoulder of the drive unit casing. Additionally, a chamfer at the base of the cover shaft thread locks against a corresponding chamfer on the drive unit casing.

Rotation-linear Conversion

The extension shaft (prt no. 010) threads onto the drive shaft. Rotation of the extension shaft is prevented by screws in the over shaft locating within a groove on the extension shaft, causing rotary motion of the drive shaft to be converted into linear motion of the extension shaft.

Description of Electronic Circuits for Piezo Motor Drive System.

Background

The electronic system must perform the following functions under the following conditions:

1. Provide suitable signals to the piezo motor to make it step.

2. Allow monitoring of the amount of rotation executed by the motor.

3. Couple the motor drive energy through the skin of the patient.

4. Allow medical personnel to set up the amount of rotation (and hence extension) that will be executed in a given time period.

5. Optionally allow for force measurements to be performed and transmitted.

6. The implanted segment of the system must be tolerant of standard medical procedures such as sterilisation and MRI scanning

In order to achieve this, the system has been broken into three parts: viz one internal to the patient, one externally applied to the patient on a regular basis and one software program that allows configuration of the rest of the system.

Internal to the patient

Inside the patient are the motor, motor drive circuit and power-receiving coil and regulation circuit.

The motor requires four correctly phased electrical signals in order to make it rotate. These signals are shown here:

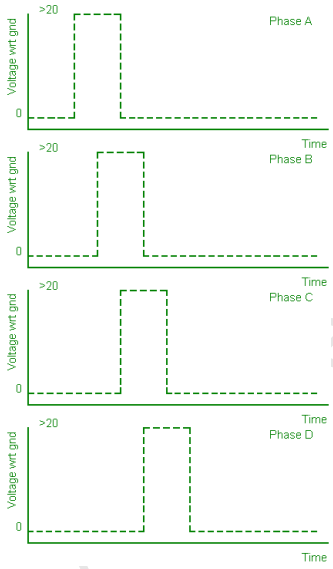

These waveforms are supplied repeatedly to the motor to rotate it. In addition, it is very useful to have feedback to measure the rotation of the motor. This is done by drawing a current impulse from the motor drives power supply. This impulse is phased as shown below:

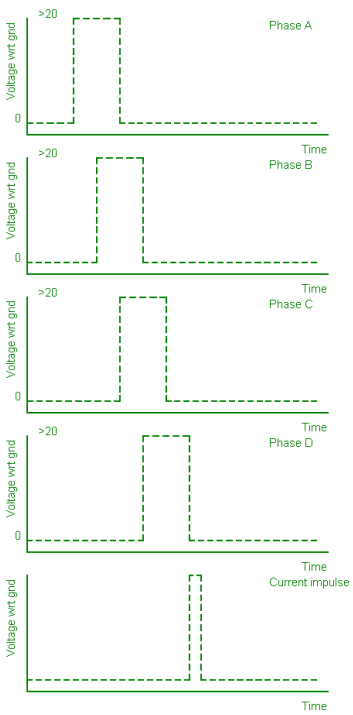

The energy to drive the system is supplied inductively from outside the body. According to the principles of electrical transformers, drawing a current impulse from the power supply within the body will cause a similar current impulse to be drawn from the unit outside the body. Thus, by monitoring the current consumption of the external unit, it is possible to determine when the motor has taken four 'steps' of rotation.

Given the need to withstand ionizing radiation during the sterilisation process, conventional microcontroller technology is not feasible as the radiation causes the contents of many memory types to be damaged. This includes the Flash and EEPROM used to store programs in the vast majority of microcontroller devices. For this reason, a different approach was taken. The circuit used is shown here:

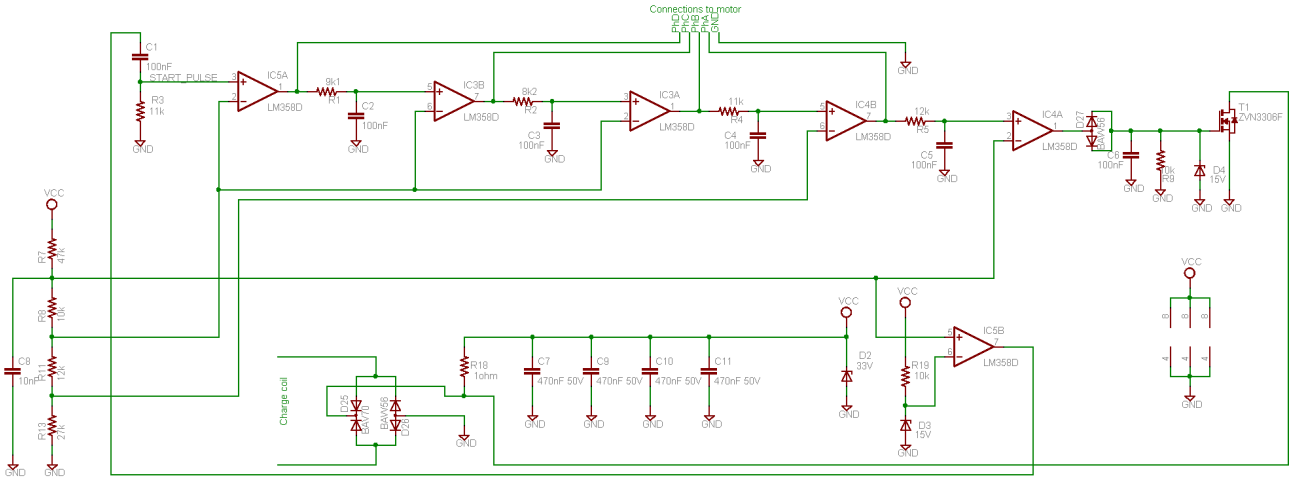

The charge coil is a coil of copper wire implanted just under the patient's skin. This coil connects to D25 and D26, which convert the alternating current from the coil to direct current. C7, C9, C10 and C11 store this energy briefly for use by the circuit. R18 and D2 regulate the voltage supplied to the rest of the circuit.

IC5B, R19 and D3 detect when the power supply has reached a high enough voltage to successfully turn the motor. When this happens a voltage pulse appears at the point labelled 'start pulse'.

The four cascaded circuits following the start pulse signal each serve as a time delay. Each time delay starts the following time delay and each time delay circuit's output drives one phase of the motor.

IC4A is a delay circuit which causes the transistor T1 to conduct, which draws a current impulse from the charge coil. In so doing, it discharges the voltage storage capacitors C7, C9, C10 and C11. When these capacitors recharge after the current impulse they cause the entire process to restart. Thus the waveforms above are reproduced for as long as the charge coil is exposed to a suitable alternating magnetic field.

By virtue of the fact that operation of this circuit is hard-wired rather than being controlled by a program, there is no need for radiation-intolerant memory devices.

Should in-vivo force measurements be required, this system could be enhanced by measuring the force experienced by the titanium components by attaching strain gages to a part which experiences extension force and measuring the strain (fractional compression) of that part. This information could be transmitted out through the skin either using conventional radio techniques (with power supplied through the charge coil) or by coded patterns of current impulses in an enhancement of the scheme shown above.

External to the patient

This unit is designed to strap on to the patient so that it can supply an alternating magnetic field to the internal charge coil. In addition, it will measure the number of steps taken by the motor and ensure that the motor rotates the correct number of times in a given period. Because this unit is not implanted in the patient there is no need for it to be radiation tolerant.

A flow chart of the device control is shown below:

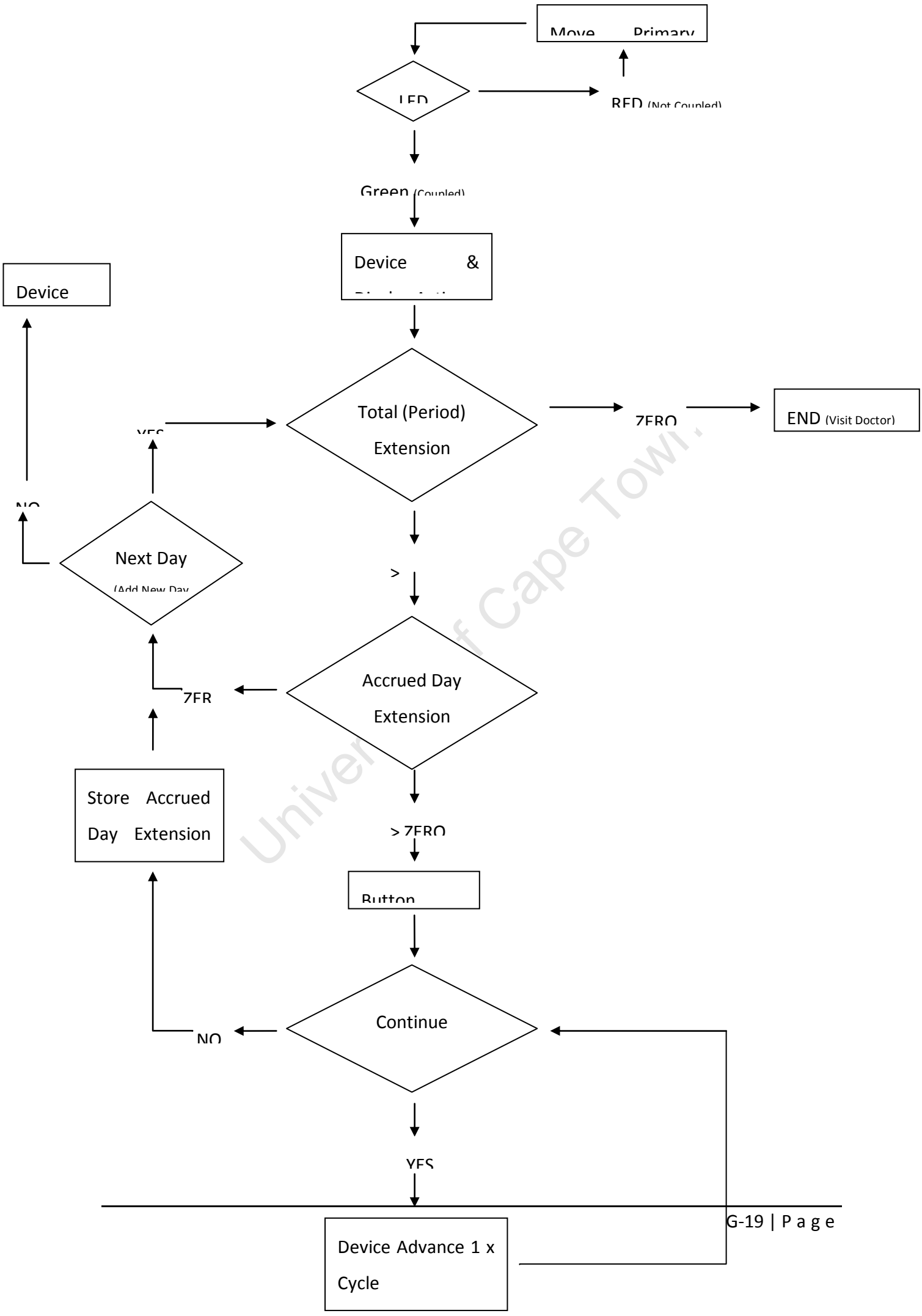

A block diagram of the external system is shown here:

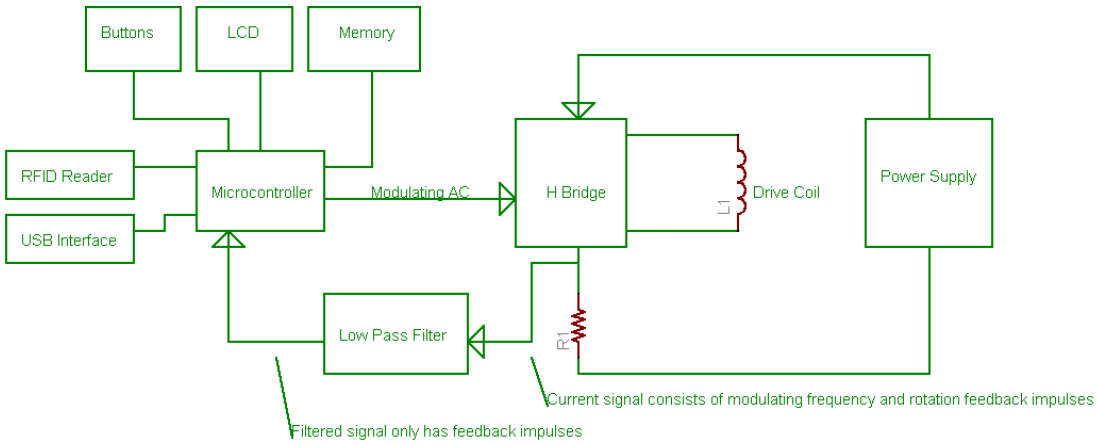

This system is controlled by a microcontroller. The microcontroller can be connected to a computer through some interface, typically USB. When the device is connected it will be informed, via the interface, of the required extension parameters and will store these in the memory device.

An RFID reader may optionally be present and this would be used to identify that the correct external device is being applied to the correct endoprosthetic device.

An LCD and buttons may be present for the user to start and stop extension (within the set extension parameters) and to inform the user of the progress of the extension.

The drive coil needs to be driven with an alternating current at high frequency. The charge coil produces an output proportional to rate of change of magnetic field strength, and thus the need for alternating current with higher coupling efficiencies obtained with increasing drive frequency. The H bride is a set of four power switches (typically transistors) which are controlled by the microcontroller to produce this waveform. The resistor, R1, is in series

with the power supply to the H bridge. Current drawn from the H bridge produces a proportional voltage across the resistor. This voltage has two main frequency components. The first of these is at the drive frequency (and its harmonics) and the second is the reflected current from the current impulses. These signals may be distinguished by their frequency. The reflected impulses will be below 1 kHz (as governed by the operation of the motor) whereas the drive frequency will typically be selected to be in the 100 kHz to 1 MHz region. The low pass filter removes higher frequencies and thus outputs a signal which the microcontroller can use to count the number of steps that the motor has taken. This is then controlled according to a flowchart (extra attachment) to produce the desired extension.

Software for Configuration

Medical personnel will need to instruct the external device as to the amount of extension required, and the time profile over which that extension is applied.

This is done through a computer application. An example of the user interface for such a program is shown here:

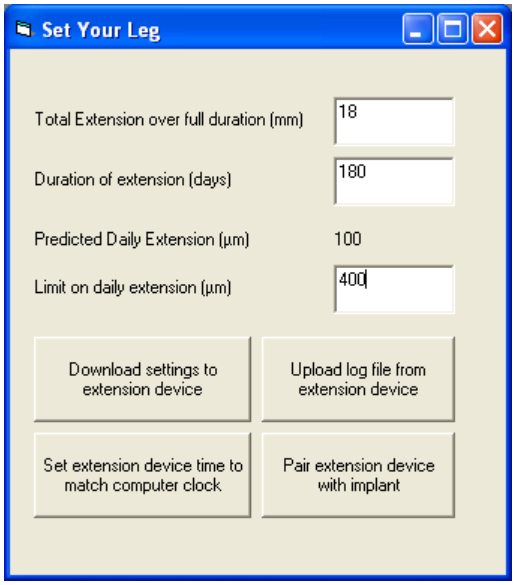

Once the extension information has been entered, the settings would be downloaded through USB or some similar interface into the external unit.

H-1. Irradiation Certificate

CERTIFICATE OF IRRADIATION No H 43880

Customer copy

HIGH ENERGY PROCESSING CAPE (PTY) LTD

HEPRO

P O Box 37195
7442 CHEMPET
Tel (021) 555-8880
Fax (021) 551-1766
e-mail info@hepro.co.za

6 Ferrule Avenue
Montague Gardens
Cape Town South Africa
Reg No 1985/004695/07

Established 1986

Radiation processing: Medical devices, foodstuffs, packaging, etc

We certify that the product itemised below has been irradiated at Hepro Cape gamma irradiation facility, 6 Ferrule Avenue, Montague Gardens, in accordance with conditions specified in a clearance granted for this product by the Department of Health and Welfare.

Company: University of Cape Town: Chemical Engineering

Date: 29 July 2011 Despatch Voucher: 47786

Ref	GRV	Batch	Quantity	Mass	Description	Dose kGy min
	57218	68126	1	0.5	Samples: 14x7.5x7cm: 0.5 kg	25

HP2.9 SF3 Rev 0

Operator: Production manager